Simple is beautiful.

Dare to think, dare to try.

Promoters:

Prof. dr. ir. Korneel Rabaey
Laboratory of Microbial Ecology and Technology, Ghent University, Ghent, Belgium

Dr. Stefano Freguia
Advanced Water Management Centre, The University of Queensland, Brisbane, Australia

Dr. Bogdan Donose
Advanced Water Management Centre, The University of Queensland, Brisbane, Australia

Prof. Jurg Keller
Advanced Water Management Centre, The University of Queensland, Brisbane, Australia

Members of the examination committee:

Prof. dr. ir. Peter Bossier (Chairman , UGent)
Laboratory of Aquaculture & Artemia Reference Center, Faculty of Bioscience Engineering, Ghent University, Ghent, Belgium

Dr. Phil Bond (Chairman ,UQ)
Advanced Water Management Centre, The University of Queensland, Brisbane, Australia

Prof. dr. ir. Arne Verliefde (Secretary)
Centre Environmental Science and Technology, Faculty of Bioscience Engineering, Ghent University, Ghent, Belgium

Prof. dr. ir. Pascal Boeckx
Department of Applied Analytical and Physical Chemistry, Faculty of Bioscience Engineering, Ghent University, Ghent, Belgium

Prof. Uwe Schroder
Institute of Environmental and Sustainable Chemistry, TU-Braunschweig, Braunschweig, Germany

Dr. Tom Sleutels
Wetsus, Centre of Excellence for Sustainable Water Technology, Leeuwarden, The Netherlands

Dean Faculty of Bioscience Engineering

Prof. dr. ir. Guido Van Huylenbroeck

Rector Ghent University

Prof. Dr. Anne De Paepe

The effects of electrode surface modifications on biofilm formation and electron transfer in bioelectrochemical systems

Kun Guo

Master of Science

A thesis submitted for the degree of Doctor of Philosophy at

The University of Queensland in 2014

School of Chemical Engineering/Advanced Water Management Centre

A thesis submitted for the degree of Doctor in Applied Biological Sciences at

Ghent University in 2014

Faculty of Bioscience Engineering

Titel van het doctoraat in het Nederlands:
De effecten van elektrode-oppervlak modificaties op biofilmformatie en elektronen transport in bio-elektrochemische systemen

Cover image (top-left) from http://rswater.phys.msu.ru/englishVersion/Science/water.html.

Please refer to his work as:
Guo K.(2014) The effects of electrode surface modifications on biofilm formation and electron transfer in bioelectrochemical systems. PhD thesis, Ghent University/The University of Queensland, Belgium/Australia.

ISBN: 978-90-5989-704-5

This work was supported by UQ International Postgraduate Research Scholarship (IPRS) , UQ TopUP Scholarship, and UGent Joint-PhD Cofunding (BOF) scholarship.

Table of Contents

Abstract

Bioelectrochemical systems (BESs) are bioreactors that use bacteria as catalysts to drive oxidation and/or reduction reactions at solid-state electrodes. They are considered as a promising technology for energy efficient wastewater treatment, power production, bioremediation, and the production of valuable chemicals. Currently, the practical application of this technology is limited by low current and power densities. Electrode surface modification has been proved an efficient way to enhance of the performance of BESs. However, there is still limited knowledge on the effects of surface chemistry on the biofilm formation and electron transfer. Moreover, most of the reported electrode modification methods are either complex, expensive or unscalable.

There is a need to fill in some of these knowledge gaps and to develop simple, effective, and scalable surface modification methods to enhance the bioanode current output of BESs. Therefore, the objectives of this work were: (i) to clarify the effects of surface chemistry of carbon electrode on anodic biofilm formation and current generation in BESs; (ii) to develop a quick approach to achieve desirable surface chemical properties on carbon electrode for faster anodic biofilm formation; (iii) to invent a novel strategy to graft electron transfer mediator to carbon electrode surface to enhance extracellular electron transfer (EET); (iv) to establish a simple method to make stainless steel (SS) surface biocompatible for scalable electrodes of BESs.

To investigate the effects of surface charge and surface hydrophobicity on anodic biofilm formation and current generation in BESs, glassy carbon electrodes were modified with –OH, $–CH_3$, $–SO_3^-$, or $–N^+(CH_3)_3$ functional groups and then tested as anode in BESs. The results demonstrated that: (i) positively charged and hydrophilic surfaces were more selective to electroactive microbes (*e.g. Geobacter*) and more conducive for electroactive biofilm formation; (ii) The effects of the surface hydrophilicity were more pronounced than surface charge; (iii) differences in the maximum current output between surface modifications were correlated with biomass quantity; and (iv) all biofilms were dominated by *Geobacter* populations, but the composition of $–CH_3$-associated biofilms differed from those formed on surfaces with different chemical modification.

Now that the mode of action of the surface charge was established with expensive aryl diazonium salts, the next step was to perform the modification in a more cost effective, realistic manner. To convert carbon the felt surface into hydrophilic and positively-charged surface, a cationic surfactant, cetyltrimethylammonium bromide (CTAB) based treatment method was developed. In an acetate-fed bioanode, the start-up time of current production and the time to reach stable current output at the CTAB-treated felt anodes were 36.1% and 49.4% shorter than the untreated anodes,

respectively. Moreover, the maximum current output with these treated electrodes was 23.8% higher than the untreated counterparts. Comparing to the routinely used electrode pretreatment methods such as high temperature ammonia, HNO_3/H_2SO_4 oxidation, NaOH/HCl soaking, and plasma treatment, surfactant treatment is quick, simple, cheap, and environmentally friendly way to make carbon felt surfaces hydrophilic and positively-charged. The use of this method will help researchers to save both time and chemicals involved in the electrode pretreatment procedure.

To accelerate EET, immobilization of neutral red onto carbon electrodes was achieved via spontaneous reduction of *in situ* generated NR diazonium salts. The current output of NR-modified graphite felt electrodes when used as bioanodes in BESs were 3.63 ± 0.36 times higher than the unmodified electrodes, which demonstrated the effectiveness of covalently bound NR as insoluble redox mediator during the microbial anodic oxidation of acetate. Comparing to the existing NR modification methods, no nitric/sulfuric acids and organic solvents were involved, and no expensive equipment were required in the new method. Most importantly, the whole procedure of this method only takes a couple of hours. Hence, spontaneous reduction of *in situ* generated NR diazonium salts is a simple, effective, and environmentally friendly method to graft NR molecules on carbon surface.

To enhance the biocompatibility of stainless steel felt (SS felt), iron oxide nanoparticles (IONPs) were *in situ* generated on SS felt by flame oxidation. Consequently, a robust anodic biofilm formation was achieved on SS felt surface in BESs. The current density of IONPs-coated SS felt electrodes were 14 times higher current than the untreated electrodes. The maximum current density achieved on the IONPs-coated SS felt (1.92 mA/cm^2) was one of the highest current densities reported. The flame oxidized SS felt reported here meets all requirements of the ideal anode materials for BESs:(1) high conductivity; (2) good biocompatibility; (3) strong chemical stability; (4) large specific surface area; (5) excellent mechanical strength; and (6) low cost. Attributed to these advantages, flame oxidized SS felt holds exciting opportunities for scaling-up of anode and for achieving high current densities in BESs.

Samenvatting

Bio-elektrochemische systemen (BES_S) zijn systemen die bacteriën gebruiken als katalysator voor het uitvoeren van oxidatie- en/of reductiereacties aan vaste elektroden, en worden beschouwd als een veelbelovende technologie voor energie-efficiënte afvalwaterzuivering, energieproductie, bioremediatie en de productie van waardevolle chemicaliën. Momenteel is de praktische toepassing van deze technologie beperkt door de lage stroom- en vermogensdichtheden. Elektrode-oppervlak modificatie is een bewezen efficiënte manier om de performantie van BESs te verbeteren. Er is echter weinig kennis over de gevolgen van oppervlakte chemie op biofilmvorming en elektronenoverdracht. Bovendien zijn de meeste van de gerapporteerde elektrode-modificatie methodes ofwel complex, duur of niet opschaalbaar.

Het doel van deze studie om een aantal van deze kennishiaten op te vullen en eenvoudige, effectieve en schaalbare oppervlaktemodificatie methodes te ontwikkelen om de bioanodische stroomproductie van BESs te verbeteren. De specifieke doelstellingen van dit werk zijn: (i) de effecten van de oppervlaktechemie van koolstofelektrodes op anodische biofilmvorming en stroomproductie in BESs in kaart brengen; (ii) een snelle manier ontwikkelen om de gewenste oppervlaktechemie van een koolstofelektrode te behalen voor een snellere anodische biofilmvorming, (iii) een nieuwe strategie ontwikkelen om een elektron transfer mediator te hechten aan het oppervlak van een koolstofelektrode zodoende de extracellulaire elektronenoverdracht (EET) te verbeteren; (iv) een eenvoudige methode ontwikkelen om het oppervlak van roestvrij staal (RVS) biocompatibel te maken en zo een opschaalbare elektrode te bekomen voor BESs.

Om de effecten van oppervlaktelading en oppervlaktehydrofobiciteit op anodische biofilmvorming en stroomproductie in BESs te onderzoeken werden glasachtige koolstof elektroden gemodificeerd met -OH , $-CH_3$, $-SO_3^-$, of $-N^+(CH_3)_3$ functionele groepen en vervolgens getest als anode in BESs. De resultaten tonen aan dat: (i) positief geladen en hydrofiele oppervlakken selectiever waren voor elektro-actieve micro-orgnaismen (bv. *Geobacter*) en bevorderlijk voor elektro-actieve biofilmvorming; (ii) Het effect van de oppervlaktehydrofobiciteit was meer uitgesproken dan het effect van de oppervlaktelading, (iii) verschillen in de maximale stroomproductie tussen verschillende oppervlaktemodificaties is gecorreleerd met de hoeveelheid biomassa; en (iv) alle biofilms werden gedomineerd door *Geobacter* populaties, maar de samenstelling van $-CH_3$-geassocieerde biofilms waren duidelijk verschillend van de biofilmsamenstelling gevormd op oppervlakken met andere een chemische modificatie.

Om koolstofviltoppervlak om te vormen tot een hydrofiel en positief geladen oppervlak werd een behandelingsmethode ontwikkeld met gebruik van een kationische oppervlakteactieve stof genaamd cetyltrimethylammoniumbromide (CTAB).. In een bioanode gevoed met acetaat was de start van stroomproductie en de tijd om een stabiele stroomproductie te bereiken met de CTAB-behandelde anodes respectievelijk 36.1 % en 49.4 % korter dan de onbehandelde anodes. Bovendien was de maximale stroomproductie met deze behandelde elektroden 23.8 % hoger dan de onbehandelde. In vergelijking met de huidige gebruikte elektrode voorbehandelingsmethoden zoals hoge temperatuur ammoniak, HNO_3/H_2SO_4 oxidatie, NaOH/HCl weken, en plasma behandeling , is oppervlakte-behandeling een snellere, eenvoudigere, goedkopere, en milieuvriendelijkere manier om koolstofvilt om te voorzien van een hydrofiel en positief geladen oppervlak. Het gebruik van deze methode zal onderzoekers helpen om zowel tijd als chemicaliën te sparen tijdens de voorbehandeling van elektrodes.

Ten einde te EET versnellen werd immobilisatie van neutraal rood op koolstofelektroden bereikt via spontane reductie van *in situ* gegenereerde NR diazonium zouten. De stroomproductie van NR-gemodificeerde grafietvilt elektroden toegepast als bioanodes in BESs was 3.63 ± 0.36 maal hoger dan de niet gemodificeerde elektroden. Dit toonde de effectiviteit aan van covalent gebonden NR als onoplosbare redoxmediator tijdens de microbiële anodische oxidatie van acetaat. In vergelijking met de bestaande NR modificatiewerkwijzen vereist deze methode geen gebruik van salpeterzuur / zwavelzuur en organische oplosmiddelen, alsook geen dure apparatuur. Belangrijker nog, de hele procedure van de deze methode duurt slechts enkele uren. Spontane reductie van *in situ* gegenereerde NR diazoniumzouten is dus een eenvoudige, effectieve en milieuvriendelijke methode om NR moleculen aan te brengen op een koolstofoppervlak.

Tot slot, om de biocompatibiliteit van roestvrij staalvilt te verbeteren (SS vilt), werden nanopartikeles van ijzeroxide (IONPs) *in situ* gegenereerd op SS vilt door vlam oxidatie. Bijgevolg werd een robuuste anodische biofilmvorming bereikt op SS vilt oppervlak in BESs. De stroomdensiteit van IONPs-gecoate SS vilt elektroden was 14 keer hoger stroom dan de onbehandelde elektroden. De maximale stroomdensiteit bereikt op IONPs geïmpregneerd SS vilt (1.92 mA/cm^2) was een van de hoogste stroomdichtheden die tot nu toe gerapporteerd zijn. De vlam geoxideerde SS vilt voldoet aan alle eisen voor anodematerialen in BESs: (1) hoge geleidbaarheid; (2) een goede biocompatibiliteit; (3) een sterke chemische stabiliteit, (4) groot specifiek oppervlak; (5) uitstekende mechanische sterkte; en (6) lage kosten. Vlam geoxideerde SS vilt heeft dus alle eigenschappen om een opschaalbaar anodemateriaal te worden voor hoge stroomdensiteit in BESs.

Declaration by author

This thesis *is composed of my original work, and contains* no material previously published or written by another person except where due reference has been made in the text. I have clearly stated the contribution by others to jointly-authored works that I have included in my thesis.

I have clearly stated the contribution of others to my thesis as a whole, including statistical assistance, survey design, data analysis, significant technical procedures, professional editorial advice, and any other original research work used or reported in my thesis. The content of my thesis is the result of work I have carried out since the commencement of my research higher degree candidature and does not include a substantial part of work that has been submitted *to qualify for the award of any* other degree or diploma in any university or other tertiary institution. I have clearly stated which parts of my thesis, if any, have been submitted to qualify for another award.

I acknowledge that an electronic copy of my thesis must be lodged with the University Library and, subject to the General Award Rules of The University of Queensland, immediately made available for research and study in accordance with the *Copyright Act 1968*.

I acknowledge that copyright of all material contained in my thesis resides with the copyright holder(s) of that material. Where appropriate I have obtained copyright permission from the copyright holder to reproduce material in this thesis.

Publications during candidature

Peer-reviewed journal papers

- **Kun Guo**, Bogdan C. Donose, Alexander H. Soeriyadi, Antonin Prevoteau, Sunil A.Patil, Stefano Freguia, J. Justin Gooding, Korneel Rabaey. Flame oxidation of stainless steel felt enhances anodic biofilm formation and current output in bioelectrochemical systems. Submitted to *Environmental Science & Technology*. 2014.
- **Kun Guo**, Alexander H. Soeriyadi, Sunil A. Patil, Antonin Prevoteau, Stefano Freguia, J. Justin Gooding, Korneel Rabaey. Surfactant treatment of carbon felt enhances anodic micorbial electrcatalysis in biolelectrochemical systems. *Electrochemistry Communication*. 2014, 39: 1-4.
- **Kun Guo**, Stefano Freguia, Paul G. Dennis, Xin Chen, Bogdan C. Donose, Jurg Keller, J. Justin Gooding, Korneel Rabaey. The effects of surface charge and hydrophobicity on anodic biofilm formation, community composition and current generation in bioelectrochemical systems. *Environmental Science & Technology*. 2013, 47: 7563-7570.
- **Kun Guo**, Xin Chen, Stefano Freguia, Bogdan Donose. Spontaneous modification of carbon surface with neutral red from its diazonium salts for bioelectrochemical systems. *Bisensors & Bioelectronics*. 2013, 47 (C):184-189.
- Paul G. Dennis, **Kun Guo**, Michael Imelfort, Paul Jensen, Gene W. Tyson, Korneel Rabaey. Spatial uniformity of microbial diversity in a continuous bioelectrochemical system. *Bioresource Technology*. 2013, 129: 599-605.

Conference presentations

- **Kun Guo**, Stefano Freguia, Bogdan Donose, Korneel Rabaey. Detergent soaking and neutral red modification of graphite felt enhance biofilm formation and current generation of BESs. The 4th International Microbial Fuel Cell Conference, Cairns, Australia.03/09/2013.
- **Kun Guo**, Stefano Freguia, Justin Gooding, Bogdan Donose, Jurg Keller, Korneel Rabaey. The effects of surface chemistry on biofilm formation and current generation in bioelectrochemical systems. The 63rd Annual Meeting of the ISE, Prague, Czech Republic. 21/08/2012.

Publications included in this thesis

- **Kun Guo**, Stefano Freguia, Paul G. Dennis, Xin Chen, Bogdan C. Donose, Jurg Keller, J. Justin Gooding, Korneel Rabaey. The effects of surface charge and hydrophobicity on anodic biofilm formation, community composition and current generation in bioelectrochemical systems. *Environmental Science & Technology*. 2013, 47: 7563-7570. – incorporated as Appendix A.

Contributor	Statement of contribution
Kun Guo (Candidate)	Designed experiments, conducted most the experiments, wrote the paper, and submitted the paper. (60%)
Stefano Freguia	Advised on experimental design and reviewed the paper. (10%)
Paul G. Dennis	Conducted the Pyrosequencing experiment and critically reviewed the paper. (5%)
Xin Chen	Taught me surface modification technique, conducted the XPS experiment, and critically reviewed the paper. (5%)
Bogdan C. Donose	Critically reviewed the paper. (2.5%)
Jurg Keller	Critically reviewed the paper. (2.5%)
J. Justin Gooding	Advised on experimental design and reviewed the paper. (5%)
Korneel Rabaey	Advised on experimental design, coordinated the study, and reviewed the paper. (10%)

- **Kun Guo**, Alexander H. Soeriyadi, Sunil A. Patil, Antonin Prevoteau, Stefano Freguia, J. Justin Gooding, Korneel Rabaey. Surfactant treatment of carbon felt enhances anodic micorbial electrcatalysis in biolelectrochemical systems. *Electrochemistry Communication*. 2014, 39: 1-4. – incorporated as Appendix B.

Contributor	Statement of contribution
Kun Guo (Candidate)	Designed experiments, conducted most the experiments, wrote the paper, and submitted the paper. (70%)
Alexander H. Soeriyadi	Conducted the XPS experiment and reviewed the paper. (10%)
Sunil A. Patil	Advised on experimental design and reviewed the paper. (5%)
Antonin Prevoteau	Conducted the CV experiment and reviewed the paper. (5%)
Stefano Freguia	Critically reviewed the paper. (2.5%)
J. Justin Gooding	Critically reviewed the paper. (2.5%)
Korneel Rabaey	Advised on experimental design and reviewed the paper. (5%)

- **Kun Guo**, Xin Chen, Stefano Freguia, Bogdan Donose. Spontaneous modification of carbon surface with neutral red from its diazonium salts for bioelectrochemical systems. *Bisensors & Bioelectronics*. 2013, 47 (C):184-189. – incorporated as Appendix C.

Contributor	Statement of contribution
Kun Guo (Candidate)	Designed experiments, conducted most the experiments, wrote the paper, and submitted the paper. (70%)
Xin Chen	Conducted the XPS experiment and reviewed the paper. (10%)
Stefano Freguia	Advised on experimental design and reviewed the paper. (10%)
Bogdan C. Donose	Conducted AFM experiment and reviewed the paper. (10%)

- **Kun Guo**, Bogdan C. Donose, Alexander H. Soeriyadi, Antonin Prevoteau, Sunil A.Patil, Stefano Freguia, J. Justin Gooding, Korneel Rabaey. Flame oxidation of stainless steel felt enhances anodic biofilm formation and current output in bioelectrochemical systems. Submitted to *Environmental Science & Technology*. 2014. – incorporated as Appendix D.

Contributor	Statement of contribution
Kun Guo (Candidate)	Designed experiments, conducted most the experiments, wrote the paper, and submitted the paper. (70%)
Bogdan C. Donose	Conducted the AFM and Raman experiments and critically reviewed the paper. (10%)
Alexander H. Soeriyadi	Conducted the XPS experiment and reviewed the paper. (5%)
Antonin Prevoteau	Conducted the CV experiment and reviewed the paper. (2.5%)
Sunil A. Patil	Critically reviewed the paper. (2.5%)
Stefano Freguia	Critically reviewed the paper. (2.5%)
J. Justin Gooding	Critically reviewed the paper. (2.5%)
Korneel Rabaey	Advised on experimental design and reviewed the paper. (5%)

Contributions by others to the thesis

- Mr Yang Lu from UQ contributed to the biofilm FISH and CLSM imaging in Appendix A.
- Mr Zhi Zhang from UQ contributed to the SEM imaging of SS felt in Appendix D.
- Mrs Hongli Ji and Chenjing Shang contributed to the biofilm microscope and CLSM imaging, respectively, in Appendix D.

Statement of parts of the thesis submitted to qualify for the award of another degree

None.

Acknowledgements

First of all, I would like to express my sincere gratitude to my advisors Prof. Korneel Rabaey, Dr. Stefano Freguia, Dr. Bogdan C. Donose, and Prof. Jurg Keller. Their priceless and untiring support has helped me overcome the inevitable difficulties that I have encountered during the course of my PhD. I have benefited from their expertise and knowledge in the fields of environmental microbiology, electrochemistry, surface chemistry and chemical engineering. They provided guidance and advise, but also constructive criticism and encouragement that helped this thesis to assume the present form.

Particularly, I would like to give special thanks to my two principal supervisors Korneel and Stefano. Without the help of Korneel, I might not be able to get the PhD position at UQ to fulfil my passions for science. Without the support of Korneel and Stefano, I would not be able to get this wonderful chance to conduct a joint-PhD between UQ and UGent. Thank you so much for all your efforts to make this possible. It was an amazing experience for me to conduct my PhD study in two leading labs in my research field and two top universities in the world. I really enjoyed it and benefited a lot from it.

Since this thesis is an interdisciplinary study, the job could not be done without our collaborators. I am very grateful to Prof. J. Justin Gooding and people from his group, especially Dr Xin Chen and Dr Alexander H. Soeriyadi, for the electrode surface modification training and the surface chemical analysis. It was always very nice and fruitful to visit your lab. I would also like to thank Dr. Paul G. Dennis for the training in the beginning of my PhD and the help for the biofilm community composition analysis. I am also very grateful to one of my advisors, Bogdan, for his help in the lab regarding the AFM and Confocal Raman analysis of my samples.

I would like to acknowledge the sources of funding for my PhD. In particular, the International Postgraduate Research Scholarship (IPRS) from the Australian government paid for my tuition fees and overseas student health cover. The UQ Centennial, AWMC Top-up, and UGent Joint-PhD Co-funding Scholarships paid for my living expenses, insurance, and travel cost. A special thank goes to CEMES and LabMET for the financial support to the scientific work during my PhD.

I am grateful to the AWMC and LabMET academics, technicians, administrative staffs, and students for their generous support and kindness what made my time at the Centre/Lab enjoyable. I

would also like to thank all the friends I met in Australia and Belgium who made my social life wonderful. There are too many people to thank so that I will not mention everybody here, but special thanks go to Yang Mu, Mi Zhou, Kenn Lu, Yingyu Law, Yuting Pan, Xufeng Zhang, Hang Wang, Dino, Tom, Ilje, Elena, Ludovic, Vivienne, Jessica, Stephen, Sylvia, Joachim, Jan, Sunil, Antonin, Christine, Regine, Mike. I miss the work we did together, the time we spent together, and the games we played together.

Finally, I would like to thank my parents and brother for their selfless love and generous financial support at different stages of my study. I attribute much of my achievements to them. Also, I want to thank my beautiful and considerate girlfriend Jianyun for accompanying me going through this journey with your love, understanding and support.

Keywords

bioelectrochemical systems, microbial fuel cells, surface chemistry, surface modification, extracellular electron transfer, biofilm formation, aryl diazonium salts, neutral red, surfactant, stainless steel felt

Australian and New Zealand Standard Research Classifications (ANZSRC)

ANZSRC code: 090703 Environmental Technologies, 50%
ANZSRC code: 030301 Chemical Characterisation of Materials, 30%
ANZSRC code: 030604 Electrochemistry, 20%

Fields of Research (FoR) Classification

FoR code: 0907 Environmental Engineering, 50%
FoR code: 0303 Macromolecular and Materials Chemistry, 30%
FoR code: 0306 Physical Chemistry (incl. Structural), 20%

List of Figures

List of Tables & Schemes

List of Abbreviations

AFM	Atomic force microscope
AQDS	Anthraquinone-1,6-disulfonic acid
BESs	Bioelectrochemical systems
CA	Chronoamperometry
CNTs	Carbon nanotubes
CE	Counter electrode
CEM	Cation exchange membrane
CLSM	Confocal laser scanning microscopy
CTAB	Cetyltrimethylammonium bromide
CV	Cyclic voltammetry
DET	Direct electron transfer
EAB	Electrochemically active bacteria
EET	Extracellular electron transfer
EPS	Extracellular polymeric substance
FISH	Fluorescence in situ hybridisation
GC	Glassy carbon
HER	Hydrogen evolution reaction
IONPs	Iron oxide nanoparticles
MB	Methylene blue
MEC	Microbial electrolysis cell
MES	Microbial electrosynthesis
MET	Mediated electron transfer
MFC	Microbial fuel cell
NHE	Normal hydrogen electrode

NQ	1,4-naphthoquinone
NR	Neutral red
ORR	Oxygen reduction reaction
PBS	Phosphate Buffer Solution
RE	Reference electrode
RMS	Root mean square
RVC	Reticulated vitreous carbon
SEM	Scanning electron microscope
WE	Working electrodes
XPS	X-ray photoelectron spectroscopy

Chapter 1 Introduction

1.1 Background

The world population is projected to increase from 6.1 billion in 2001 to 9.4 billion by 2050 (Lewis and Nocera, 2006). With the growth of economy and improving of living standard, the global energy consumption and fresh water demand are expected to increase at least by 100% and 55%, respectively in the same time frame (Leflaive, 2012; Lewis and Nocera, 2006). Meeting the fast growing demand will require not only energy/water-saving technologies but also sustainable energy and recyclable water.

A multitude of wastewaters are produced annually from municipal, industrial, and agricultural sources. Wastewaters contain organic matter that can be reused as energy source. It is estimated that the energy stored in the organic matter in domestic sewage could account for 10% of the residential electrical energy consumption (Freguia, 2010). Moreover, as wastewaters typically contain >99% water, they are potential sources of water for recycling and reuse. Therefore, it is of great significance to recover energy and water from wastewaters.

Traditionally, wastewater are treated in two main processes, namely aerobic activated sludge and anaerobic digestion. The aerobic activated sludge process oxidises the organics to carbon dioxide and yields purified water, but the energy consumption of this process is quite high due to the aeration (von Sperling, 2007). The anaerobic digestion converts wastewater organics to methane which can be burnt to produce heat and electricity, but the effluent of anaerobic reactors requires further aerobic treatment for the water reuse purpose (Taricska et al., 2007).

Bioelectrochemical systems (BESs), which use bacteria as the catalysts to drive oxidation and/or reduction reactions at solid-state electrodes, are considered as a promising technology for energy efficient wastewater treatment, power production, bioremediation, and the production of valuable chemicals (Rabaey et al., 2007; Rabaey and Rozendal, 2010). In the past decade, rapid progress has been made in BESs in terms of current density, electroactive bacteria (Logan, 2009), extracellular electron transfer (EET) (Huang et al., 2011; Schroder, 2007), electrode materials (Zhou et al., 2011), reactor configurations and process development (Du et al., 2007). At present, the practical

application of this technology is mainly limited by high capital cost and low current density (Rozendal et al., 2008).

In a BES, the electroactive biofilm on the electrode surface plays a key role in determining the current density. The biofilm formation is an extremely complicated process, which is affected by a series of factors including bacterial properties, material surface characteristics and environmental factors (Katsikogianni and Missirlis, 2004). Among them, the material surface properties can not only affect the bacterial initial attachment and biofilm development, but also influence the electron transfer between bacteria and the electrode. Hence, surface modifications of the electrode is an efficient way to improve performance of BESs.

In the past, many anode electrode surface modification studies, such as acid treatment (Zhu et al., 2011), ammonia treatment (Cheng and Logan, 2007), heat treatment (Wang et al., 2009), conductive polymer coating (Lai et al., 2011), carbon nanotube (CNT) coating (Nambiar et al., 2009), and mediator grafting (Park et al., 2000), have been successfully done to increase the current generation of BESs. They attributed the current increase to increase of specific surface area, improvement of biocompatibility, enhancement of surface conductivity, and facilitating electron transfer. However, there is still limited knowledge on the effects of surface chemistry on the biofilm formation and electron transfer. Moreover, most of the reported electrode modification methods are either complex, expensive, time-consuming or unscalable.

1.2 Objectives of the thesis

The aims of this study are to firstly gain fundamental knowledge on the effects of surface chemistry on anodic biofilm formation, bacterial community composition and current output in BESs, and then develop simple, effective, green, and scalable methods to modify carbon and stainless steel electrodes to enhance their performance as anode of BESs.

1.3 Organization of the thesis

This thesis is organized into three chapters and four appendices.

Chapter 1 gives a general introduction to the background, objectives, and organization of this thesis. Chapter 2 is a literature review section. Firstly, bioelectrochemical systems (BESs) are briefly reviewed in terms of principles, electron transfer mechanisms, challenges and applications. Secondly, biofilms on abiotic surfaces are discussed with particular focus on biofilm formation process, factors influencing biofilm formation, and biofilms in BESs. Thirdly, surface modification methods for carbon materials and surface modification studies in BESs are summarized. Chapter 3 consists of four sections, namely Research questions, Research methods, and Research outcomes, and Conclusions and perspectives. Chapter 4 describes the conclusions of this work and recommend future research opportunities in this direction.

The four appendices include detailed experimental studies for the distinctive research objectives. Appendix A investigates the effects of surface charge and hydrophobicity on anodic biofilm formation, community composition and current generation in bioelectrochemical systems; Appendix B shows that surfactant treatment of carbon felt enhances anodic micorbial electrcatalysis in biolelectrochemical systems; Appendix C reports spontaneous modification of carbon surface with neutral red from its diazonium salts for bioelectrochemical systems; Appendix D shows that flame oxidation of stainless steel felt enhances anodic bioelectrocatalysis in microbial electrochemical systems.

Chapter 2 Literature Review

2.1 An overview of bioelectrochemical systems

2.1.1 Principles of BESs

Bioelectrochemical systems (BESs) are bioreactors that use bacteria as catalysts to drive oxidation and/or reduction reactions at solid-state electrodes (Rabaey et al., 2007). Typically, the BES reactor consists of an anodic chamber and a cathodic chamber, sometimes separated by an ion exchange membrane. Both the anodic electrode and the cathodic electrode are normally immersed in respective electrolyte solutions, and they are connected via external circuit allowing the electrons to flow from the anode to the cathode.

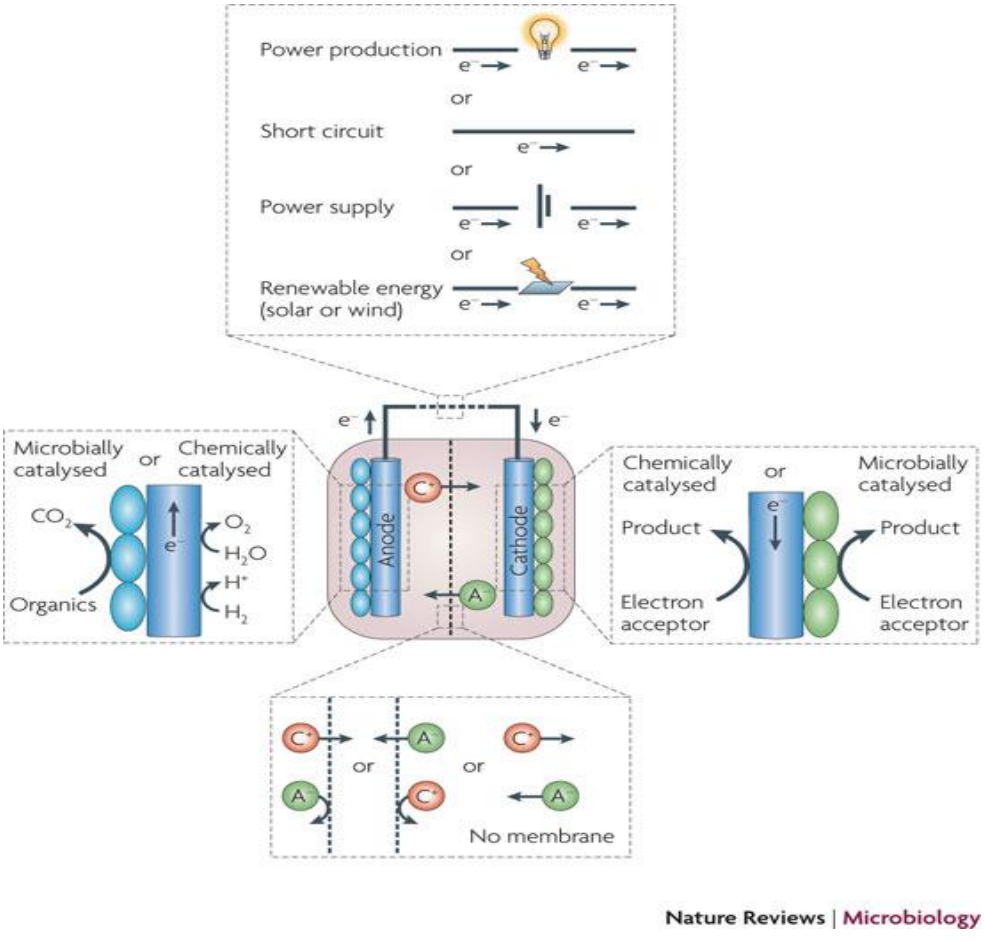

Figure 2.1 Schematics of typical bioelectrochemical systems. (Rabaey and Rozendal, 2010).

Depending on whether electrical power is extracted from or added to the systems, BESs can be divided into two modes, microbial fuel cell (MFC) and microbial electrolysis cell (MEC). When a BES is operated in MFC mode, the cathodic reaction (e.g. O_2 reduction reaction) happens spontaneously and the system is generating electrical power. If operated in MEC mode, extra electrical power is invested to drive thermodynamically unfavourable reactions (e.g. H_2 evolution reaction) at the cathode. In BESs, at least one of the two half-reactions is biocatalysed.

2.1.2 Electron transfer in BESs

2.1.2.1 Anode electron transfer–drawing electrons from microorganisms

Electrochemically active bacteria (EAB) are able to transfer electrons to an electrode from the inside of the cell via two different extracellular electron transfer mechanisms (Schroder, 2007). The first mechanism is mediated electron transfer (MET) that depends on redox cycling of mediators between the microbes and the electrode. The second mechanism is direct electron transfer (DET), which depends on the direct contact between microbes and the electrode surface.

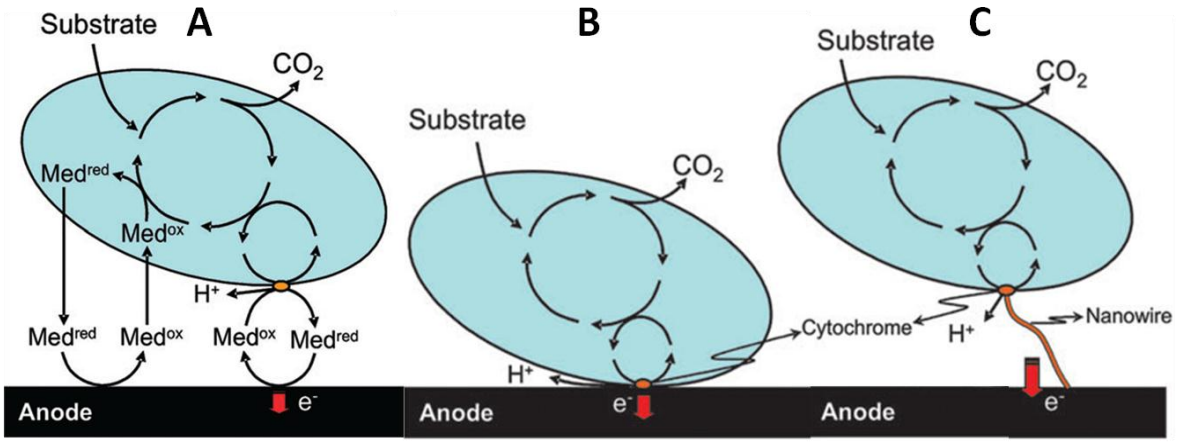

Figure 2.2 Mechanisms for electron transfer from microorganisms to electrodes. (Image modified from Schroder, 2007).

Figure 2.2A shows two different MET pathways. The only difference between them is where the mediators are reduced. The oxidized state mediators can either be reduced in the cytoplasm (Figure 2.2A left) or electron transport proteins (such as cytochrome) on outer cell membrane (Figure 2.2A right). Two proposed DET pathways are illustrated in Figure 2.2B and 2.2C. One is through the membrane bound electron transport proteins (Figure 2B), and the other one is through conductive pili (so-called nanowires) that are connected to the membrane bound electron transport compounds (Figure 2.2C).

2.1.2.2 Cathode electron transfer –pumping electrons into microorganisms

In the past, the focus of BESs was on the understanding and engineering of anode processes (Harnisch and Schroder 2010). Therefore, mechanistic information about anode electron transfer is abundant, while information about the reverse process, pumping electrons into microbes, is rather limited. In recent years, it has been found in a limited number of studies that cathodic bacterial communities exist and are highly diverse, but whether these communities are directly or indirectly involved in catalyzing the cathode reaction is still unclear (Rabaey and Rozendal, 2010).

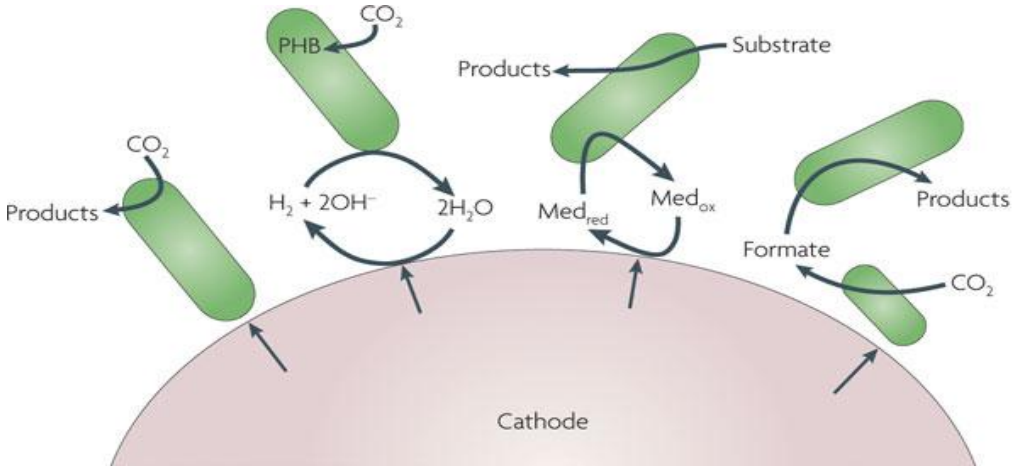

Figure 2.3 Proposed mechanisms for electron transfer from electrodes to microorganisms. (Image from Rabaey and Rozendal, 2010)

Figure 2.3 shows the possible cathodic electron transfer mechanisms in BESs. It has been proven that H_2 (Clauwaert et al., 2008) and electron shuttles, such as methyl viologen (Steinbusch et al., 2010), neutral red (Park et al., 1999), AQDS (Thrash et al., 2007), and iron (Ter Heijne et al., 2006), can be used for the cathodic EET. The direct electron transfer from electrode to microorganisms appears the most attractive means of cathodic EET. Several bacteria have been reported being able to obtain electrons directly from the electrodes, such as *Geobacter sulfurreducens* (Gregory et al., 2004), *Sporomusa ovate* (Nevin et al., 2010; Zhang et al., 2013), *Anaeromyxobacter dehalogenans* (Strycharz et al., 2010) and *Geobacter lovleyi* (Strycharz et al., 2010; Strycharz et al., 2008). Two or more bacterial species may work together to realize electron transfer from electrode to the final products.

2.1.3 Applications and challenges of BESs

2.1.3.1 Applications of BESs

Power supply

So far, the power produced by MFCs is still too low to be useful in most applications. It is likely that even with major advances in the future, MFCs will not contribute to the power grid. But MFCs are especially suitable for use as power supplies in small telemetry systems and wireless sensors that are not energy intensive in remote areas. For example, Ieropoulos et al. (2005) developed the robot EcoBot-II and used MFCs as the onboard energy supply. EcoBot-II fed (amongst other substrates) with flies was able to perform sensing, communication and actuation. An MFC consisting of a sacrificial anode combined with the reduction of biomineralized manganese oxides was used to power electrochemical sensors and small telemetry systems to transmit the acquired data to remote receivers (Shantaram et al., 2005). A Benthic Unattended Generator (BUG) MFC was also tested to power a data buoy that monitored air temperature, pressure, and humidity as well as water temperature. The system radioed data every 5 min to a shore-based receiver (Tender et al., 2008).

Removal of pollutants

BESs are attractive for the removal of pollutants that are recalcitrant under the anaerobic conditions that are typically found in sediments. Key advantages are in situ continued provision of oxidizing power as well as straightforward control of the bioremediation process. For instance, inorganic compounds, such as sulfides (Dutta et al., 2009), ammonium (Clauwaert et al., 2007; Virdis et al., 2008), and uranium (Gregory and Lovley, 2005) can be removed, and recovered using either anodic oxidation processes or cathodic reduction processes, or both of them. Moreover, BESs were also applied for the transformation of strongly oxidized functional groups in persistent chemicals, such as the nitro-group of nitrobenzene (Mu et al., 2009b) and the azo bond (–N=N–) of the widely used reactive azo-dyes (Mu et al., 2009a).

Production of fuels and chemicals

Bioelectrochemical systems can be applied for the production of fuels and chemicals. As synthesis of these fuels and chemicals are thermodynamically unfavourable reactions, power input rather than power generation is required. However, the products are potentially far more valuable than the power invested. Moreover, the energy content of the fuel in a BES stems partly from the organic

material oxidized at the anode and partly from the energy supplied via the applied voltage. Therefore, production of fuels and chemicals is likely the most promising application for BESs. Up till now, production of hydrogen (Rozendal et al., 2006), methane (Cheng et al., 2009), hydrogen peroxide (Rozendal et al., 2009), sodium hydroxide (Rabaey et al., 2010), ethanol (Steinbusch et al., 2010), acetate (Zhang et al., 2013), and 1,3- or 1,2-propanediol (Zhou et al., 2013) in BESs have been described.

2.2 Biofilms on abiotic surfaces

In the following section, the key parameters governing biofilm development and characteristics are discussed.

2.2.1 Biofilm formation process

The development of a biofilm can be divided into several stages. Four common steps are usually distinguished, even though they may overlap each other to some extent (Ploux et al., 2010). Figure 2.4 shows the schematic diagram of biofilm development based on a common 4-step representation, namely bacteria transport onto the surface, bacteria adhesion, biofilm matrix synthesis, and maturation and detachment.

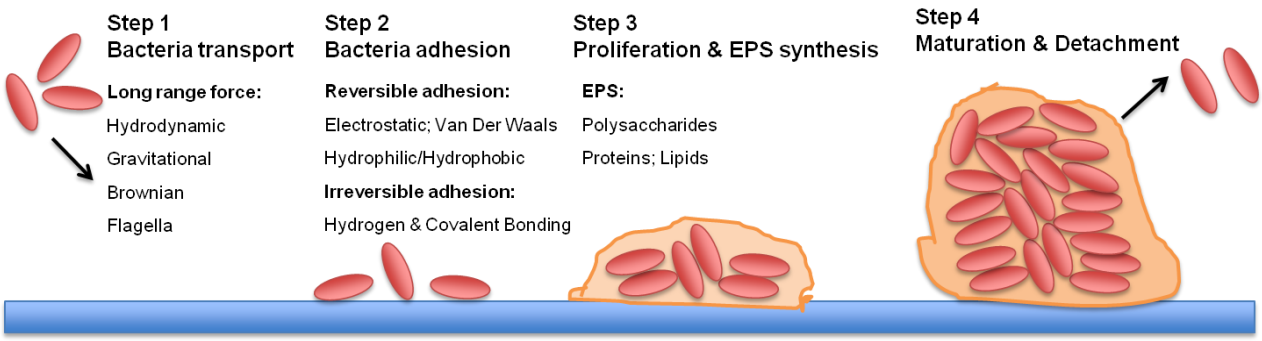

Figure 2.4 Schematic diagram of the biofilm development.

2.2.1.1 Transport of bacteria onto the surface

Bacteria can either be passively transported to the surfaces by long-range physical forces or actively swim to the surfaces using their flagella. The long range physical forces include gravitational forces, Brownian forces and hydrodynamic forces under flow conditions. It has to be noted that flagella are involved in the transport of bacteria species onto the surface, but do not influence the further biofilm development significantly (Ploux et al., 2010).

2.2.1.2 Adhesion of the bacteria to the surface

Generally speaking, bacterial adhesion can be further divided into two stages: the reversible adhesion and the irreversible adhesion (Katsikogianni and Missirlis 2004). The first stage refers to the short time period when bacteria are approaching the surface. In this stage, typically repulsive/attractive electrostatic, van der Waals and hydrophobic/hydrophilic interactions are thought to be involved. In the second stage, the bacterial anchorage on the surface is strengthened by short-range forces such as covalent and hydrogen bonding interactions. These interactions occur between bacterial outer cell wall and molecules present on the surface, which are much stronger than those involved in the reversible stage.

2.2.1.3 Proliferation and synthesis of the biofilm matrix

After adhesion on the material surface, bacteria start to proliferate to form bacterial colonies and synthesize extracellular polymeric substance (EPS) to form the biofilm matrix. It is very interesting that some adherent bacteria and microcolonies are able to move on the material surfaces, and their motions are called twitching and swarming, respectively. These movements accelerate the spreading of the bacteria over the material surface. Extracellular polymeric substance is comprised of polysaccharides, proteins and lipids coming from the bacterial metabolism. EPS plays an important role in the 3-dimensional structure and cohesion of the biofilm (Ploux et al., 2010).

2.2.1.4 Maturation and detachment

Mature biofilms are characterized by 3-dimensional architecture that possesses pores and channels allowing bacterial access to nutrients and oxygen and protection against hostile surroundings (Anderson and O'Toole, 2008). Another essential biofilm feature is that the modes of bacterial life differ considerably between biofilm-associated bacteria and planktonic bacteria. Bacteria in the biofilm are able to communicate each other using the so-called “Quorum Sensing” (QS) biochemical system (Bassler, 1999). QS is not only used by bacteria to regulate a variety of physiological functions, but is also thought to play an important role in the biofilm detachment occurring when biofilms become mature. Detachment of cells from the biofilm colony is an essential stage of the biofilm life cycle. Detachment enables bacteria to spread and colonize new surfaces.

2.2.2 Factors affecting biofilm formation

Biofilm formation is an extremely complicated process which is affected by a series of factors including bacterial properties, material surface characteristics and the environmental factors.

2.2.2.1 Surface hydrophobicity

It appears reasonable that bacteria with hydrophobic surfaces prefer hydrophobic materials while bacteria with hydrophilic surfaces prefer hydrophilic materials. However, several contradictory trends have been reported (Ploux et al., 2010). For example, Bakker et al. (2004) studied the adhesion of three marine bacteria on pre-conditioned polyurethane films (hydrophobic) and they found that bacteria with more hydrophobic surface character adhered better than hydrophilic bacteria. Cerca et al. (2005) tested the adhesion of nine *S. epidermidis* strains onto hydrophobic and hydrophilic surfaces. They found all of them attached better on hydrophobic surfaces and the bacterial cell hydrophobicity seemed to have much less influence on bacterial adhesion than material surface hydrophobicity did. It is also reported that the initial hydrophobic/hydrophilic character of the material surface can be modified by exogenous surfactants produced by bacteria (Leclere et al., 2006). Therefore, the relationships between bacterial adhesion and surface hydrophobicity are complex.

2.2.2.2 Surface charge

Except for a few bacterial species, bacterial surfaces in aqueous suspension are typically negatively charged. Therefore, attractive interactions are expected to occur between bacterial cells and positively charged surfaces, while repulsive interactions should occur when the surface is negatively charged. This trend was supported by a series of studies. For example, Roberts (2004) observed that a negatively charged mineral surface was unfavourable to bacterial adhesion. Terada et al. (2005) investigated the adhesion of five Gram-negative bacteria onto surface-modified polyethylene (PE) membrane sheets, and they found that electrostatic interaction is the most decisive factor for bacterial adhesion on positively charged surfaces. However, since the surface charge of bacteria varies according to bacterial species and is influenced by the environmental conditions such as pH and the ionic strength of the medium, the relative contribution of surface charge to bacterial adhesion has not been clearly elucidated. Bacterial behaviour on charged surfaces is not so easily interpreted.

2.2.2.3 Surface topography

Material surface topography influences bacterial adhesion to the surface significantly. It has been found that bacteria adhere and colonize preferably to the porous, grooved and braided surfaces (Flint et al., 2000; Whitehead and Verran, 2006). Obviously, rough surface is more conducive to bacterial attachment than smooth surface as a rough surface has a greater surface area and the valleys in the roughened surfaces provide more favourable sites for colonization. For example, McAllister et al. (1993) found that the irregularities of polymeric surfaces promote bacterial adhesion and biofilm deposition, and the ultrasmooth surface does not allow bacterial adhesion and biofilm deposition. However, the effect of surface roughness on bacterial adhesion is not linearly dependent. For example, an increase in surface roughness on stainless steel, from 0.04 μm for polished stainless steel to 0.30 μm for abraded, increased bacterial adhesion strength more than an even larger increase in surface roughness from 0.04 μm to 0.96 μm for unpolished stainless steel (Boyd et al., 2002). Besides roughness, Edwards and Rutenberg (2001) proposed and demonstrated theoretically that shape, profile and orientation of these features also play an important role in in bacterial adhesion and biofilm development. However, these topographical features are rarely taken into account. Therefore, so far mechanisms of bacterial response to topographical surface features have not yet been clearly elucidated. However, understanding the behaviour of bacteria on different topographical featured surfaces is essential for the design of surfaces that enhance or inhibit bacterial colonization.

2.2.2.4 Environmental conditions

Both bacterial and material surface physical–chemical properties are highly dependent on the environmental conditions. Therefore, certain factors in the environment, such as pH and ionic strength, nutrient abundance, and flow conditions greatly impact the bacterial adhesion and biofilm development (Katsikogianni and Missirlis, 2004). Flow conditions are considered dominant factors that strongly influence the number of attached bacteria as well as the biofilm structure and performance. It is generally considered that higher shear rates result in higher detachment forces that result in decreasing the number of attached bacteria, while they make the biofilm denser and thinner (Liu and Tay, 2002). Ionic strength and pH influence bacterial adhesion by changing surface hydrophobicity and charge of both the bacteria and the materials (Ploux et al., 2010). The biofilm formation is a nutrient-consuming process because of cell proliferation and synthesis of the biofilm matrix. Hence, nutrient-rich media is expected to be favourable for biofilm formation. This hypothesis was supported by several studies (Haznedaroglu et al., 2008; Walker, 2005).

2.2.3 Biofilms in BESs

2.2.3.1 Anodic biofilms

Certain electrochemical active bacteria could attach and form biofilms on the anode surface. The formation of biofilm plays an important role in the evolution of anodic potential in BESs. The anodic biofilms are essential for the transfer of electrons to the anode electrode. Ever since *Shewanella putrefaciens* was found to be capable of generating power in the absence of exogenous mediators (Kim et al., 1999b), studies that use pure cultures have now confirmed that many different bacterial species in anodic biofilms can transfer electrons directly to the anode via the cell membrane or special conductive pili (also known as nanowires) (Gorby et al., 2006). A list of anodic pure cultures used in MFCs is shown in Table 2.1.

Researchers found the bacterial species in mixed culture biofilms are much more diverse than the already known electrochemically active bacteria such as *Shewanella* and *Geobacter* species. The highest power densities in MFCs are almost always produced by inoculating the anode with a rich and diverse source of bacteria, such as a wastewater or sludge, while MFCs with pure cultures generated 2-3 orders of magnitude less power than MFCs with mixed cultures (Logan, 2009; Rabaey et al., 2004). The role of the electrochemical inactive species in the electron transfer is still unclear. It is possible that some of the electrochemically inactive bacteria secrete electron mediators that accelerate electron transfer of the electrochemically active bacteria. It is also possible that there are still undiscovered electrochemical mechanisms in synergistic biofilm communities that can be exploited to improve MFC performance. The structure and morphology of the biofilms is generally measured by SEM and CSLM. While SEM images provided higher levels of magnification, CSLM is able to image layers throughout the biofilm, providing spatial information such as thickness. The relationship between biofilm thickness and current density was also reported. Higher power densities were achieved using thicker biofilms due to the large number of bacteria that would contribute to current generation. In the case of *G. sulfurreducens* biofilms, the current density of the thicker and more heterogeneous biofilms was much higher than that of the initial and single layer of cells on the anode surface (Nevin et al., 2008).

Table 2.1 Anodic species capable of direct electron transfer

Microbe	Comment	Reference
Shewanella putrefaciens IR-1	Direct proof of electrical current generation in an MFC by a dissimilatory metal-reducing bacterium	(Kim et al., 1999a)
Desulfuromonas acetoxidans	Deltaproteobacteria identified from a sediment MFC	(Bond et al., 2002)
Geobacter metallireducens	Shown to generate electricity in a poised potential system	(Bond et al., 2002)
Geobacter sulfurreducens	generated current without poised electrode	(Bond and Lovley, 2003)
Rhodoferax ferrireducens	Betaproteobacteria used glucose as substrate	(Chaudhuri and Lovley, 2003)
Aeromonas hydrophila	Deltaproteobacteria	(Pham et al., 2003)
Desulfobulbus propionicus	Deltaproteobacteria	(Holmes et al., 2004))
Escherichia coli	Found to produce current after a long acclimation time	(Zhang et al., 2006))
Shewanella oneidensis DSP10	Achieved a high power density 2 W/m^2	(Ringeisen et al., 2007)
S. oneidensis MR-1	Various mutants identified that increase current or lose the ability for current generation	(Bretschger et al., 2007)
Pichia anomala	Current generation by yeast (kingdom Fungi).	(Prasad et al., 2007)
Rhodopseudomonas palustris DX-1	Produced high power densities of 2.72 W/m^2	(Xing et al., 2008)
Ochrobactrum anthropi YZ-1	An opportunistic pathogen	(Zuo et al., 2008)
Desulfovibrio desulfuricans	Reduced sulphate when growing on lactate	(Zhao et al., 2008)
Acidiphilium sp. 3.2 Sup5	Power production at low pH	(Borole et al., 2008)
Klebsiella pneumoniae L17	Produced current without a mediator for the first time	(Zhang et al., 2008)
Thermincola sp. strain JR	Phylum Firmicutes	(Wrighton et al., 2008)

2.2.3.2 Cathodic biofilms

The formation of biofilms on the cathode electrodes has been consistently observed by researchers, especially in membrane-free BESs. Rather than preventing their formation, investigators have used these biofilms as the biocatalysts to catalyse BES cathode reactions such as oxygen reduction reaction (ORR), hydrogen evolution reaction (HER), electrosynthesis of valuable chemicals. In recent years, there has been an increasing in the number of reports of bacterial species in cathodic biofilms. Table 2.2 shows a list of identified electrode-oxidizing microorganisms in biocathodes and their electron acceptors.

Besides these pure culture studies, there are many other studies using mixed cultures enriched from the natural environment. Similarly to the anode, the mixed culture biofilms are generally working better than the pure culture biofilms. Based on the comparison of power densities from a mixed culture and pure cultures biofilms using oxygen as electron acceptor, Rabaey et al. (2008) observed that the isolates produced low power relative to the mixed culture. Similarly, Erable et al. (2010) studied 30 pure cultures from a mixed culture biofilm, and they found only *Winogradskyella poriferorum* and *A. johsonii* gave current densities of respectively 7% and 3% of the current obtained with the mixed-culture biofilm. It is possible that synergetic effects occurred in the mixed-culture biofilms, or a more productive electroactive microorganism was present in the mixed culture. Other possible explanations are that pH change, surface modifications, or underdeveloped biofilm growth on the cathode electrode under pure-culture conditions may have contributed to the lower power generation.

Besides the positive effect of microbial consortia in the biofilms on cathodic potential, the role of biofilm thickness on the cathodic electrode was also recently reported. In the case of exoelectrogenic anode biofilms, higher power production was produced from thicker anodic biofilms of *G. sulfurreducens* (Nevin et al., 2008). However, cathodic biofilm thickness may affect power generation in a different manner, as power generation was observed to gradually decrease with an increase in cathode biofilm thickness on both graphite plate and stainless steel mesh (Behera et al., 2010).

Table 2.2 Types of electron acceptors and electrode-oxidizing microorganisms in biocathodes. (compiled from Huang et al., 2011)

Electron acceptor	Microbe	Mediator	Current density and/or poised potential	Reference
O_2	*Leptothrix discophora SP-6*	Mn(IV) and Mn(II)	+0.7 V	(Nguyen et al., 2007)
	Acinetobacter calcoaceticus	–	110 A/m3	(Rabaey et al., 2008)
	Sphingobacterium multivorum		49–103 A/m^3	
	Pseudomonas aeruginosa	–	−0.21 to +0.05 V	(Cournet et al., 2010)
	Pseudomonas fluorescens	–	−0.21to + 0.06 V	
	Brevundimonas diminuta	–	−0.09 to + 0.11 V	
	Burkholderia cepacia	–	−0.12 to + 0.10 V	
	Branhamella catarrhalis	–	−0.20 to + 0.06 V	
	Enterobacter cloacae	–	−0.24 to +0.05 V	
	Escherichia coli	–	−0.25 to +0.03 V	
	Shigella flexneri	–	−0.27 to +0.03 V	
	Acinetobacter sp.	–	−0.17 to +0.08 V	
	Kingella kingae	–	−0.25 to + 0.02 V	
	Kingella denitrificans	–	−0.25 to +0.03 V	
	Micrococcus luteus	–	−0.22 to +0.05 V	
	Bacillus subtilis	–	−0.25 to +0.06 V	
	Staphylococcus carnosus	–	−0.28 to +0.02 V	

To be continued on next page.

Table 2.2 Types of electron acceptors and electrode-oxidizing microorganisms in biocathodes. (Continue to previous page)

Electron acceptor	Microbe	Mediator	Current density and/or poised potential	Reference
O_2	*Winogradskyella poriferorum*	–	0.04 A/m^3, +0.00 V	(Erable et al., 2010)
	Acinetobacter johsonii	–	0.02 A/m^3, +0.00 V	
	Acinetobacter calcoaceticus	Pyrroloquinoline quinone	1.3 A/m^3, +0.10 V	(Freguia et al., 2010)
	Shewanella putrefaciens	–	0.7 A/m^3, ±0.20 V	
U(VI)	*Geobacter sulfurreducens*	–	−0.30 V	(Gregory and Lovley, 2005)
Perchlorate	*Dechloromonas sp.*	AQDS	−0.30 V	(Thrash et al., 2007)
	Azospira sp.			
Fumarate	*Geobacter sulfurreducens*	–	2.4–12 A/m^3, −0.40 V	(Dumas et al., 2008)
	Geobacter lovleyi	–	4.8 A/m^3, −0.30 V	(Strycharz et al., 2008)
Nitrate	*Geobacter metallireducens*	–	−0.30 V	(Gregory et al., 2004)
H_2O	*Desulfovibrio vulgaris*	Methyl viologen	−0.30 V	(Lojou et al., 2002)
CO_2	*Methanobacterium palustre*		0.07 A/m^3, −0.80 to −0.50 V	(Cheng et al., 2009)
	Chlorella vulgaris	Methylene blue	0.3 A/m^3	(Powell et al., 2009)
	Sporomusa species	–	−0.40 V	(Nevin et al., 2011)
	Clostridium aceticum	–		
	Clostridium ljungdahlii	–		
	Moorella thermoacetica	–		

2.3 Surface modifications of carbon materials

Carbon materials are the most widely used electrode materials in BESs studies due to their excellent electrical conductivity and chemical stability. As the biofilm carrier and reaction interface, the carbon surface properties can not only affect the bacteria initial attachment and biofilm development, but also influence the electron transfer between bacteria and electrode. Therefore, changing the surface properties of carbon electrodes may be an efficient way to improve biofilm formation and electron transfer in BESs. In this section, the most commonly used carbon surface modification methods were firstly summarized, then the carbon surface modification works in the BES field were reviewed.

2.3.1 Surface modification methods

2.3.1.1 Thin-film coating

Deposition of a thin film coating on the external surface provides a means to impart additional properties and functionality to carbon material. Various surface coating techniques have been investigated to improve the physical properties and handling of carbon nanomaterials, including physical vapour deposition (PVD), chemical vapour deposition (CVD), and electrochemical deposition. A diverse set of material coatings has been deposited successfully on carbon substrates including dielectrics, metals, and polymers.

Different metallic coatings have been deposited on individual carbon nanotubes (CNT) for improved contact electrical properties by PVD such as electro-beam evaporation (Star et al., 2006; Zhang et al., 2000). Silicon oxide coatings were deposited on carbon nanofibers (CNF) surfaces by plasma-enhanced CVD to prevent high temperature oxidation and thermal degradation (Moon et al., 2006) and improve mechanical strength and electrically insulate (Baker et al., 2006). CVD was also used to coat CNTs with polymer thin films such as carbonflourine polymer (He et al., 2005). Electrochemical deposition is another widely used method for metal deposition and polymerization, and the process can be controlled by various electrodeposition parameters. Electrochemical deposition of Ni has been demonstrated on the surface of herringbone-type carbon material to produce a vertical nanotube heterojunction (Cassell et al., 2004). Chen, et al. (2001) demonstrated that polypyrrole (PPy) could be electropolymerized from an acidic monomer solution as a conformal, electronically conductive film over the entire length of vertically aligned carbon material for potential use as high performance electrode in rechargeable batteries.

2.3.1.2 Chemical functionalization

The surface functional groups were found to be responsible for the physicochemical and catalytic properties (towards a plethora of reactions) of the carbon matters. The nature and concentration of carbon surface functional groups might be modified by suitable thermal or chemical treatments to improve or extend their practical applications. Table 2.3 shows the methods commonly used to chemically functionalize the carbon surfaces. (Shen et al., 2008).

Table 2.3 Methods of chemical functionalization of carbon electrodes (Information from Shen et al., 2008)

Treatment	Reagent and method	Effects of treatment
Acid	Nitric/sulphuric acid	Increase the concentration of oxygen groups such as: -OH, -COOH, carbonyl, phenol, quinone, lactone.
Ammonia	Dry ammonia (500 to 800℃)	Introduce nitrogen-containing groups such as: C=N, -NH_2, cyclic amides, nitrile groups, pyrrole-like structure
Thermal	Heating under Inert atmosphere	Remove some of surface oxygen groups
	Heating oxidation	Increase the concentration of oxygen groups
Plasma	O_2	Increase –COOH and C=O concentration, decrease -C-OH and C-O-C concentration
	N_2	Increase –C-OH, C-O-C, O=C-O, pyridine and quaternary nitrogen concentration, decrease –C=O (aromatic ring) concentration
	NH_3	Increase –N-H concentration
	CO_2	Increase –COOH and C=O concentration
	H_2O	Increase –COOH and C=O concentration

2.3.1.3 Electrochemically assisted covalent modification

Modification via oxidation of amines

Primary and secondary amines may be coupled to glassy carbon (GC) and carbon fiber surfaces via oxidation of the amine in anhydrous ethanol or acetonitrile electrolyte solutions. Either cyclic voltammetric (CV) scans to potentials over the irreversible amine oxidation peaks or controlled potential electrolysis at sufficiently positive potentials can be used to achieve surface modification. The modification process can be divided into two steps, electrochemical generation of solution

radicals and formation of covalent bonds between carbon surface and the modifier (Scheme 2.1). Table 4 lists some amines which have been grafted to carbon surfaces by the electrochemically oxidation method.

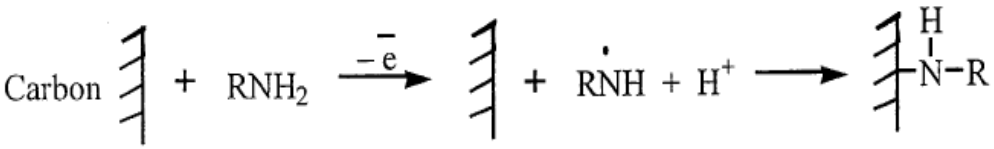

Scheme 2.1 Electrochemical oxidation of amines (Downard 2000)

Table 2.4 Amines which have been electrochemically bonded to carbon electrode (Information from Downard, 2000)

Amine	References
Etlhylene diamine, Triethylene tetramine, 4-Nitrobenzylamine, 2-Amino-4-methylthiazole, Aminomethyl-9-anthracene, Isobutylamine, N-(2-Aminoethyl)-4-fluorobenzamide	(Barbier et al., 1990)
N-(5-Aminopentyl) biotinamide, Butylamine, N-Ethylbutylamine, N-Acetylethylenediamine, N-Methylbutylamine, Dopamine	(Deinhammer et al., 1994)
Tetraethylene glycol diamine	(Downard and bin Mohamed, 1999)
Cysteine	(Yan et al., 1999)
Imidazole, 4-Aminopyridine, 4-Aminoethylpyridine	(Tanaka and Aramata, 1997)
6-Amino-1-hexanol, Octadecylamine, Decylamine	(Hoekstra and Bein, 1996)

Modification via reduction of aryl diazonium salts

Electrochemical reduction of aryl diazonium salts is a versatile technique for the covalent modification of carbon substrates. The mechanism of modification of surfaces by electrochemical reduction of diazonium salts can be summarized in Scheme 2.2. Diazonium salts ($^{+}N_2$-Ar-R) are easily and rapidly prepared in one step from a wide range of aromatic amines many of which are commercially available. Reduction of the diazonium can be carried out by CV or controlled potential reduction. It is well documented that aryl diazonium reduction at carbon electrodes yields a covalently bound modifier layer of the polyphenylene type, with thicknesses up to ca. 10 nm (Ceccato et al., 2011).

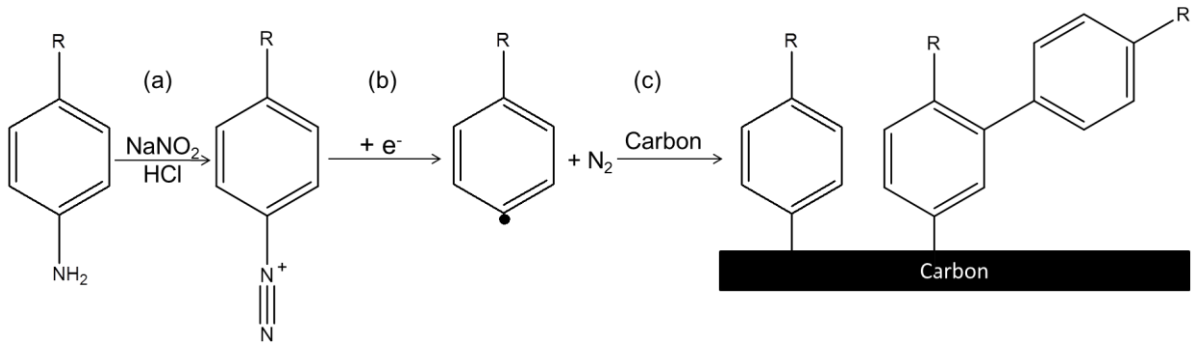

Scheme 2.2 Electrochemical reduction of aryl diazonium salts.

As a number of different groups can be attached to the aromatic ring, it is possible to obtain surfaces bearing a wide variety of functions (alkyl, halogenoalkyl, perfluoroalkyl, carboxylic, ester, cyanide, halides, nitro, alcohols, thiols, and more complicated structures including polyaromatics and compounds with triple bond) (Pinson and Podvorica, 2005). Hence, the grafting on carbon electrodes of a large range of groups with different chemical and physical properties can be readily achieved (Gooding, 2008; Mahouche-Chergui et al., 2011). In addition, the modification of carbon surfaces with an electrochemical approach (through CV sweeps or potentiostatic techniques) allows the fine tuning of the amount of modifier (i.e. thickness) grafted at the electrode surface by simply controlling the coulombic charge consumed in the modification process (Brooksby and Downard, 2004). A large variety of carbon materials have been modified by this method such as glassy carbon (Gui et al., 2010; Liu et al., 2010), HOPG (Allongue et al., 1997; Kariuki and McDermott 2001), carbon fibers (Delamar et al., 1997), carbon nanotubes (Dyke and Tour, 2003), diamond (Jian et al., 2004).

2.3.2 Surface modifications in BESs

It has been suggested that surface modification may be an efficient way to enhance the performance of BESs. In BESs, electrodes were initially usually made of carbon-based materials, such as graphite granules, carbon paper, carbon cloth, carbon fibre, and graphite felt, due to their chemical stability and conductivity. However, the conductivity and biocompatibility of these materials still have room to improvement. Moreover, as the biofilm carrier and reaction interface, it is better for the electrode to have high specific surface area and great ability to facilitate the electron transfer. Several chemical, electrochemical, and physical modification of anode surfaces have successfully been done to improve the performance of BESs. Table 2.5 summarized the strategies and methods used to modify the anode surfaces.

Ammonia treatment is suitable for many carbon electrode materials and it has been regarded as one of the most effective ways to improve electrode performance. The first report using ammonia to treat carbon cloth was completed by Cheng and Logan (2007). Treatment of carbon cloth using 5% NH_3 gas in a helium carrier gas at 700°C (for 60 minutes) increased the positive surface charge of the cloth from 0.38 to 3.99 meq/m^2. This reduced acclimation time needed for a wastewater culture to produce power by 50%, and it increased power to 1970 mW/m^2, compared to (a) 1640 mW/m^2 without the ammonia treatment in the same high ionic strength phosphate buffer and (b) 1330 mW/m^2 in a lower ionic strength solution. They attributed the result to the fact that the treated carbon cloth can improve the amount of positive surface charge and thus is more conductive to microbial electron transport.

Wang et al. (2009) heated carbon mesh in a muffle furnace at 450 °C for 30 min, which resulted in a maximum power density of 922mW/m^2 (46W/m^3); this was 3% more than that produced using a mesh anode that was cleaned with acetone (893mW/m^2; 45W/m^3). They attributed such a change in the power density to the facts that the heating method could modify the electrochemical activity by increasing the electrochemically active surface area and decreasing the O/C ratio, which led to the active surface area increasing by 190% and the charge transfer coefficients increasing by 44% compared to the untreated one.

Nitric acid is widely used for surface modification of carbon materials. Scott et al. (2007) increased power generation by depositing nitric acid-treated carbon on graphite felt as support. However, no information about the treated graphite surface was mentioned in the report. Erable et al. (2009) activated graphite granules as electrodes (both anode and cathode) with nitric acid, and achieved an improvement of +400 mV in open circuit potential. They ascribed the reason of performance improvement to the increase of specific surface area of the activated material and the emergence of nitrogen superficial groups. Zhu et al. (2011) treated activated carbon fibre felt (ACF) with nitric acid, and they found that the start-up time was shorten by 45% and the power density increased by 58%. They attributed the power enhancement to the changes of surface functional groups.

Table 2.5 Anodic surface modifications in BESs

Modification method	Anode	Major change of surface	Improvement of performance	Ref.
NH_3 (700°C)	Carbon cloth	Increase positive charge Introduce nitrogen groups	Shorten start-up time by 50% Increase current density by 20%	(Cheng and Logan, 2007)
Heat (450°C for 30 min)	Carbon brush	Increase N/C ration	Increase power density by 25%	(Feng et al., 2010b)
N_2/O_2/Air Plasma	Glassy carbon	Improve hydrophilicity	Fasten biofilm formation	(Flexer et al., 2013b)
Flame (ethylene/air)	SS mesh	Generate CNTs	60-fold increase in power density	(Lamp et al., 2011)
Acid (HNO_3)	Carbon felt	Introduce nitrogen groups	Shorten start-up time by 45% Increase current density by 58%	(Zhu et al., 2011)
Amidation reaction (NR)	Carbon fiber	Covalently immobilize NR	Increase power output	(Wang et al., 2011)
Electrochemical oxidation	Graphite felt	Generate –COOH groups	Increase current density by 39.5%	(Tang et al., 2011)
Iron oxide coating	Graphite felt	Introduce iron oxide	Increase power density by 72%	(Wang et al., 2013)
CNTs coating	Carbon paper	Introduce CNTs nanostructure	Increase power density by 20%	(Sun et al., 2010)
CVD of CNTs	RVC	Generate CNTs nanostructure	3-fold increase in current density	(Flexer et al., 2013a)
Polyaniline	Carbon cloth	Generate polyaniline film	Shorten start-up time by 33% 3-fold increase in power density	(Lai et al., 2011)
Reduction of aryl diazonium salts	Graphite disk	Change surface charge by grafting functional groups	Positively charged surface performed better than negatively charged surface	(Picot et al., 2011)

Park and Zeikus (2000) bound a known mediator, neutral red (NR), to a woven graphite electrode and increased power to 9.1 mW/m^2 compared to only 0.02 mW/m^2 with the same electrode lacking NR, using a pure culture of *Shewanella putrefaciens* and lactate as substrate. In an improved system lacking a CEM, they achieved 845 mW/m^2 with complex medium (lactate, peptone and yeast extract) and a sewage sludge inoculum compared to 0.65 mW/m^2 using the plain electrode (Park and Zeikus, 2003). The addition of bound mediators has also been tested in sediment fuel cells. Lowy et al. (2006a) found that AQDS- and 1,4-naphthoquinone (NQ)-modified anodes produced 1.7 and 1.5 times as much current as plain graphite electrodes. The AQDS-modified electrode produced up to 98 mW/m^2 in field tests, which was much better than the plain graphite electrodes (20 mW/m^2) and only slightly less than the 105 mW/m^2 produced using Mn^{2+} and Ni^{2+}-modified electrodes.

Conductive polymers, due to their special properties such as environmental stability, ease of synthesis, and conductivity at room temperature, have been used as electrode modifier for the improvement of MFCs. Yuan and Kim (2008) modified reticulated vitreous carbon (RVC) with electropolymerized polypyrrole (Ppy). They obtained a maximum power density of 1.2 mW/cm^3 which is the highest value among the reported ones for the similar system. Lai et al. (2011) synthesized a conductive polyaniline modified carbon cloth anode. By comparison with fresh carbon cloth anode in MFC reactors, they detected that the MFC maximum power density was 5.16 W/m^3 anode chamber volume, which was increased by 2.66 times compared to the control experiment, and the internal resistance and start-up time was decreased 65.5% and 33.3% respectively.

CNTs can improve the performance of MFCs because they have very high surface areas (usually a few hundred to 1300m^2/g), and the groove openings that are formed between CNTs bundles and the outside surface area of CNT bundles are thought to be accessible by bacteria (Donaldson et al., 2006). Sharma et al. (2008) developed an MFC using an anode made of carbon paper that was coated with multi-walled CNTs. The power density was found to be approximately six times greater than with the pure graphite electrode. They confirmed that the carboxyl groups on the surface of multi-walled CNTs could increase the chemical reactivity of metal nanoparticles. Tsai et al. (2009) investigated the performance of CNT modified carbon cloth electrodes in single-chamber MFCs. when compared to the unmodified electrode, the power density and cell voltage increased by approximately 148% and 147%, respectively.

Recently, conductive polymer/CNTs composites have received significant interest because the incorporation of CNTs in conductive polymers can lead to a synergistic effect. Qiao et al. (2007) reported the feasibility of an MFC that used CNTs/polyaniline composite as the anode material. They believed that CNTs could enhance the electrode surface area and electron transfer capability. Additionally, polyaniline, as a conductive polymer, could not only provide a protective effect for the microorganisms but also improve the electro-catalytic activity of the catalyst. Zou et al. (2008) used polypyrrole (PPy)/CNTs as the anode material, and the results showed that the modified carbon paper had better electrochemical properties, and the power output of the MFC increased along with the increase of the composite loading.

Electrochemical reduction of aryl diazonium salts is a versatile technique for the covalent modification of carbon substrates. A large range of functional groups with different chemical and physical properties can be readily grafted on carbon electrodes. Saito et al. (2011) introduced 4-(N,N-dimethylamino) aryl groups at carbon cloth anodes through diazonium reduction to increase nitrogen-containing functional groups. They concluded on the basis of X-ray photoelectron spectroscopy studies that a small amount of nitrogen functionalization on the carbon cloth material is sufficient to enhance MFC performance, likely as a result of promoting bacterial adhesion to the surface without adversely affecting microbial viability or electron transfer to the surface. The effect of the introduction of charged groups at the surface by electrochemical reduction of aryl diazonium salts was investigated by Picot et al. (2011). It was found that negatively charged groups at the surface (carboxylate) decreased microbial fuel cell power output while the introduction of positively charged groups doubled the power output. Scanning electron microscopy revealed that the microbial anode modified with positively charged groups was covered by a dense and homogeneous biofilm.

2.4 Knowledge gaps

Limited knowledge on cell-electrode interface

The cell-electrode interfaces plays a crucial role in BESs as the extracellular electron transfer occurs at this interface. Since the electrode is not only the biofilm carrier but also the electron donor or acceptor, the material surface properties can not only affect the bacteria initial attachment and biofilm development, but also influence the electron transfer ability of mature biofilms. However, thus far, the effects of the electrode surface chemical and physical properties on the biofilm formation and electron transfer in BESs are still unclear. Hence, more work needs to be done to find effective electrode surfaces that are not only able to sustain microbial attachment but also facilitate electron transfer.

Lack of simple and effective methods for electrode surface modifications

Thus far, the current densities of BESs are still too low for most envisioned applications. Electrode surface modification is considered as an effective pathway to enhance the current densities of BESs. Although many surface modification works have been successfully done to increase the current densities of BESs, most of the reported surface modification methods are either expensive, complex, time-consuming, or energy/chemical-extensive. Thus, novel surface modification methods are required to be developed and they should meet the following requirements: (1) cheap; (2) simple; (3) quick; (4) effective; (5) environmentally friendly; and (6) scalable. Only when all of these conditions are satisfied, the novel surface modification method can be used for the medication of large scale electrodes.

Lack of scalable electrode materials

The ideal electrode for BESs should possess following features: (1) high conductivity; (2) good biocompatibility; (3) strong chemical stability; (4) large specific surface area; (5) excellent mechanical strength; and (6) low cost (Logan et al., 2006; Zhou et al., 2011). Carbon materials have been widely used as electrodes in MESs because of their biocompatible, corrosion-resistant and inexpensive properties. However, scale-up of carbon-based electrodes is limited by relatively high resistivity and low mechanical strength (Zhou et al., 2011). Metal-based electrodes such as stainless steel (SS) materials are commonly used in industries, due to their good corrosion resistance, great mechanical strength, high conductivity and easily up-scalable characteristics. However, the major limitation in their use as anodes in MESs is poor biocompatibility (Dumas et al., 2008).

Chapter 3 Thesis overview

This chapter provides an overview of the research work undertaken in this thesis. First, the research objectives are discussed. Then the key research methods and analytical techniques are briefly described. Finally, the major outcomes and key results are outlined.

3.1 Research objectives

Objective 1: To clarify the effects of surface charge and surface hydrophobicity on anodic biofilm formation and current generation in BESs

The impact of surface chemistry (e.g. surface charge, surface hydrophobicity) on the biofilm formation and current production is still unclear. Some of the published results are even controversial. For example, some investigators claimed that adding positive charged groups such as amino groups would decrease the start-up time and enhance power density of MFCs (Cheng and Logan, 2007; Feng et al., 2010a), while others argued the negative charged groups like carboxyl groups were also able to enhance current generation due to their strong hydrogen bonding with peptide bonds in bacterial cytochromes (Crittenden et al., 2006; Tang et al., 2011). The controversial results are likely due to the fact their surface modification methods are not well-controlled so that other surface properties other than surface charge are also changed. Therefore, the first objective of this thesis was to modify carbon electrodes using a well-controlled method and then clarify the effects of surface charge and surface hydrophobicity on biofilm formation and current output in BESs.

Objective 2: To develop a simple and effective method to optimise chemical surface characteristics for faster electroactive biofilm formation

From research objective 1, we have learned that hydrophilic and positively-charged surfaces are more attractive for electroactive bacterial. Previously, several pre-treatment methods such as the use of ammonia (Cheng and Logan, 2007), heat (Wang et al., 2009), acid (Zhu et al., 2011), and electrochemical oxidation (Tang et al., 2011) have been reported to improve the surface wettability of carbon surfaces and enhance current outputs of BESs. However, either strong acids, harsh conditions or expensive equipment are used in these methods, and most of them are quite time-consuming. Hence, the third research objective was to develop a simple and effective technique to

make carbon surface hydrophilic and positively-charged, thereby speeding up the biofilm formation process in BESs.

Objective 3: To devise and optimise a simple method to graft an effective electron transfer mediator to the electrode surface to enhance extracellular electron transfer

It has been previously shown that immobilization of electron transfer mediators, such as neutral red (NR) (Park and Zeikus, 2000; Wang et al., 2011), methylene blue (MB) (Popov et al., 2012), anthraquinone-1,6-disulfonic acid (AQDS) (Lowy and Tender, 2008; Lowy et al., 2006b), and 1,4-naphthoquinone (NQ) (Lowy and Tender, 2008), onto electrode surface is an efficient way to facilitate electron transfer from bacteria to electrode. However, the reported mediator immobilization methods usually consume large amount of nitric/sulphuric acids and organic solvents. Moreover, most of the methods are quite time-consuming. Therefore, the second objective of this thesis was to develop new, simple, and environmentally friendly methods to graft electron transfer mediators onto electrode surface to enhance extracellular electron transfer.

Objective 4: To develop scalable electrode materials for BESs

Currently, carbon are the most commonly used electrode material in BESs. However, Attempts to the scaled-up BESs demonstrated that the high electrical resistivity of carbon electrodes (1375 μΩ/cm for graphite) causes very high electrode ohmic losses. Thus, carbon materials are not suitable for scaled-up BESs. Sintered SS fibre felt (SS felt) is a commercially available and cheap filter material for gas and liquid filtration. It has an open 3D macroporous structure with great conductivity, large specific surface area, high corrosion resistance, excellent mechanical strength and easily up-scalable characteristics. However, the poor biocompatibility of this material limits its application as anodes in BESs. Hence, the fourth research objective was to find a simple and effective method to make SS felt electrode biocompatible.

3.2 Research methods

In this paragraph the electrode materials and surface modification methods, surface characterizations, BES reactor setup and operation, electrochemical cell and operation, biofilm analysis techniques are described. A detailed description of the experiments can be found in the appendices A-D.

3.2.1 Electrode materials and surface modifications

3.2.1.1 Electrodes

Three types of electrode materials were used for the thesis study, namely glassy carbon plate (GC plate, 20 mm × 20mm × 2mm, HTW, Germany), carbon felt (20 mm × 10 mm × 3.2 mm, Alfa Aesar, Belgium), and stainless steel felt (SS felt, 20 mm × 10 mm × 0.7 mm, Lier Filter, China). Figure 3.1 shows the connections of the electrodes. Copper wires were glued on the backside of the GC plates by silver paint to make the external connection. Then the back and side of the plates were insulated by water proof epoxy glue, leaving an exposed (effective) surface area of 4 cm^2. Carbon felt and SS felt were connected to titanium wires as current collectors.

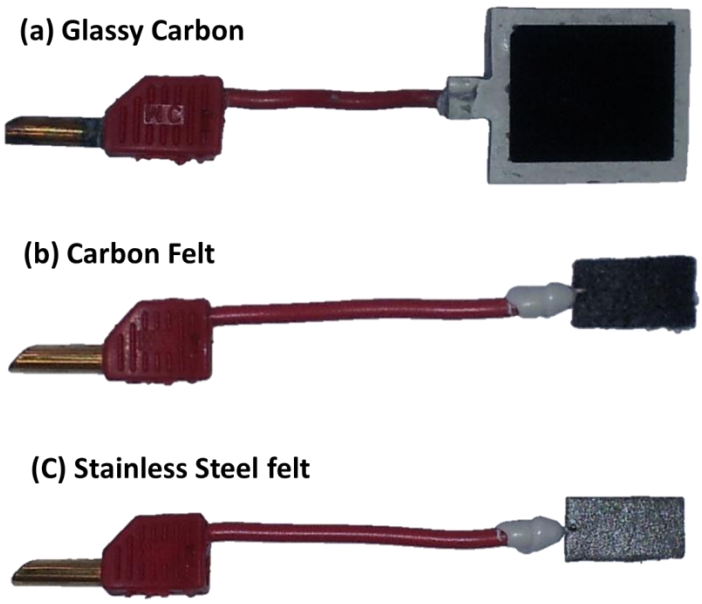

Figure 3.1 Electrical connections of the electrodes

3.2.1.2 Electrode surface modifications

Functionalization of glassy carbon: Electrochemical reduction of *in situ* generated aryl diazonium salts were used to graft various functional groups to the glassy carbon (GC) surfaces (Scheme 3.1). Electrochemical reduction of the diazonium salts was carried out either by chronoamperometry (CA) or cyclic voltammetry (CV).

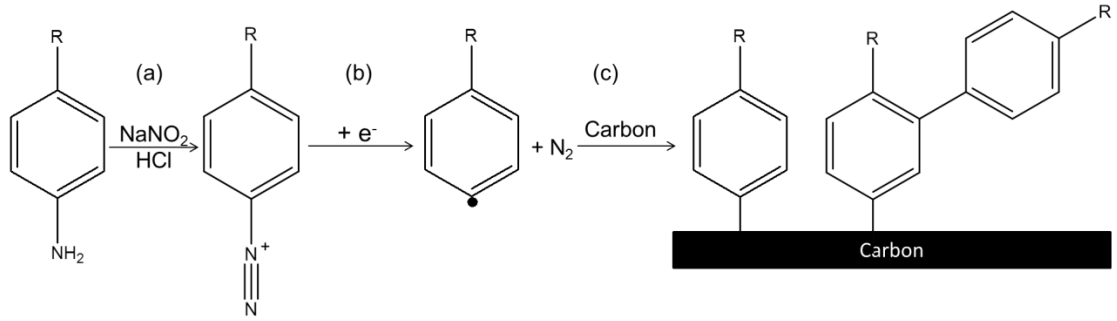

Scheme 3.1 Procedure for electrochemical reduction of aryl diazonium salts: a) in situ generation of diazonium salts, b) electrochemical reduction of aryl diazonium salts and c) C–C bond formation. Candidate R groups: $–CH_3$, –OH, $–SO_3^-$, $–N^+(CH_3)_3$.

Neutral red modification of glassy carbon and carbon felt: Electron transfer mediator neutral red (NR) was grafted to carbon felt surface by electrochemical or spontaneous reduction of in *in situ* generated NR diazonium salts. To prove that the formation of NR diazonium salts is essential for the NR immobilization, GC electrodes were also immersed in NR (1mM)-$NaNO_2$ (1 mM) solution and NR (1mM)-HCl (0.5M) solution for 3h at room temperature as controls. At the end of modification, all the electrodes were successively sonicated in ethanol, acetonitrile, DI water for 5 min each to thoroughly remove the physically adsorbed species.

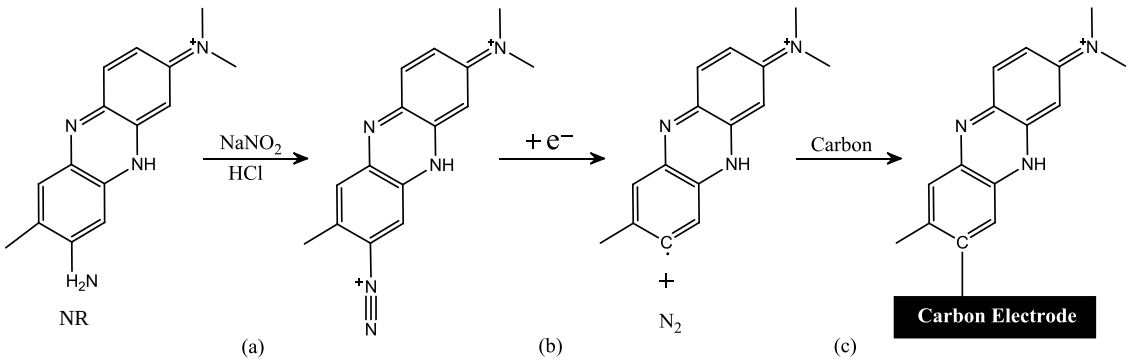

Scheme 3.2 Modification of carbon surface with neutral red via electrochemical and spontaneous reduction of its diazonium salts

Surfactant treatment of carbon felt: Surfactant cetyltrimethylammonium bromide (CTAB) was immobilized on carbon felt surface by soaking the electrode in 2 mM CTAB solution. The electrodes were firstly soaked in 500 mL vigorously stirred (1000 rpm) CTAB (Sigma-Aldrich) solution (2 mM) for 5 min and then rinsed three times in 500 mL vigorously stirred (1000 rpm) deionized water for 5 min. The untreated electrodes were only rinsed in deionized water with the same protocol.

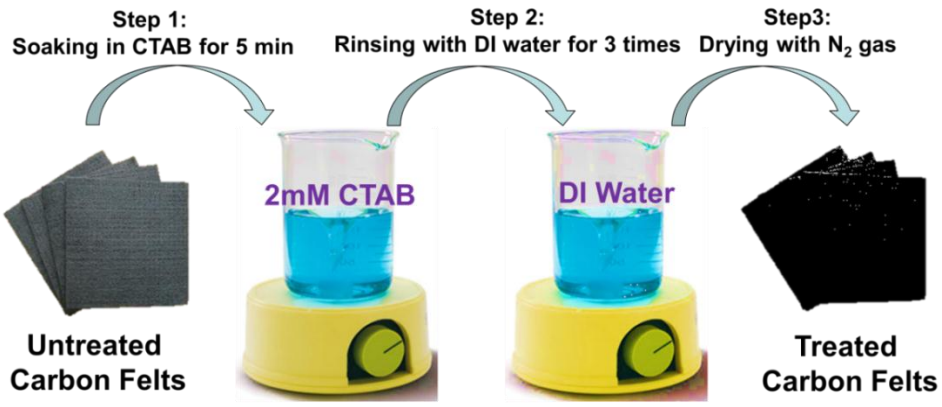

Figure 3.2 Procedure of surfactant treatment of carbon felt electrode

Flame treatment of stainless felt: SS felt was oxidized by burning in the flame of Burnsen burner employing natural gas as fuel. In order to yield a strong oxidizing flame, the air hole was completely open to generate a 13 cm long "roaring" blue flame. Before insertion into the flame, the SS felt was thoroughly cleaned in acetone and dried by a stream of nitrogen gas. Then, the SS felt was perpendicularly inserted into the tip of the inner flame (~1200 °C) that was 5 cm above the nozzle of burner. After 60 s, the SS felt was removed from the flame and allowed to cool to ambient temperature.

Figure 3.3 Flame oxidation of the SS felt. (~1200°C, 1 min)

3.2.2 Electrode surface characterizations

3.2.2.1 Surface elemental compositions

X-ray photoelectron spectroscopy (XPS) is a spectroscopic technique that measures the material surface atomic composition and chemical bonding information. In this study, XPS was used to analyse the surface atomic compositions before and after surface modification. The results allowed us to confirm whether certain functional groups are grafted to the surfaces and how much of them are there on the surfaces.

3.2.2.2 Surface hydrophobicity

The water contact angle is the angle between the outline tangent of a water drop deposited on a solid and the surface of this solid. The contact angle is linked to the surface hydrophobicity. The higher the contact angle, the more hydrophobic the surface. In this study, water contact angle was used to measure the surface hydrophobicity change of glassy carbon and carbon felt electrodes before and after modifications.

3.2.2.3 Surface electrochemical properties

Cyclic voltammetry (CV) is generally used to study the electrochemical properties of the electrode surface. CV can be conducted either with or without redox probes. In this study, it was used to analyse electrode surface charge, electrochemically active surface area, surface electron transfer mechanisms, and surface elemental composition.

3.2.2.4 Surface topography

The surface morphological structure and topography of the electrode samples were visualized by light microscope, scanning electron microscope (SEM) and atomic force microsope (AFM). Light microscope images gave an overview of the electrode surface at relatively large scale. SEM and AFM images gave information of the electrode surface at micro/nano scales.

3.2.3 Reactor setup and operation

3.2.3.1 Reactor setup

In order to test all the electrodes in one reactor, two high-throughput BES reactors were designed and fabricated (Figure 3.4). The first one is a single-chamber reactor (Figure 3.4 a,b) which has a

total volume of 700 mL. To avoid the effects of the hydrogen produced at the cathode on the anode, the single-chamber reactor was modified into a double-chamber reactor (Figure 3.4 c,d). The double-chamber reactor has an 550 mL anodic chamber and an 150 mL cathodic chamber which are separated by a cation exchange membrane (CEM, Ultrex CMI7000, Membranes International Inc., USA). This high-throughput BES reactors allowed within an identical geometry simultaneous testing of eight working electrodes (WE, SS felt anodes) with the use of one counter electrode (CE, SS mesh cathode), and one reference electrode (RE, Ag/AgCl 3 M KCl). All electrochemical experiments were conducted with a CHI 1000C Multi-Potentiostat (CH Instruments, Austin, TX, USA).

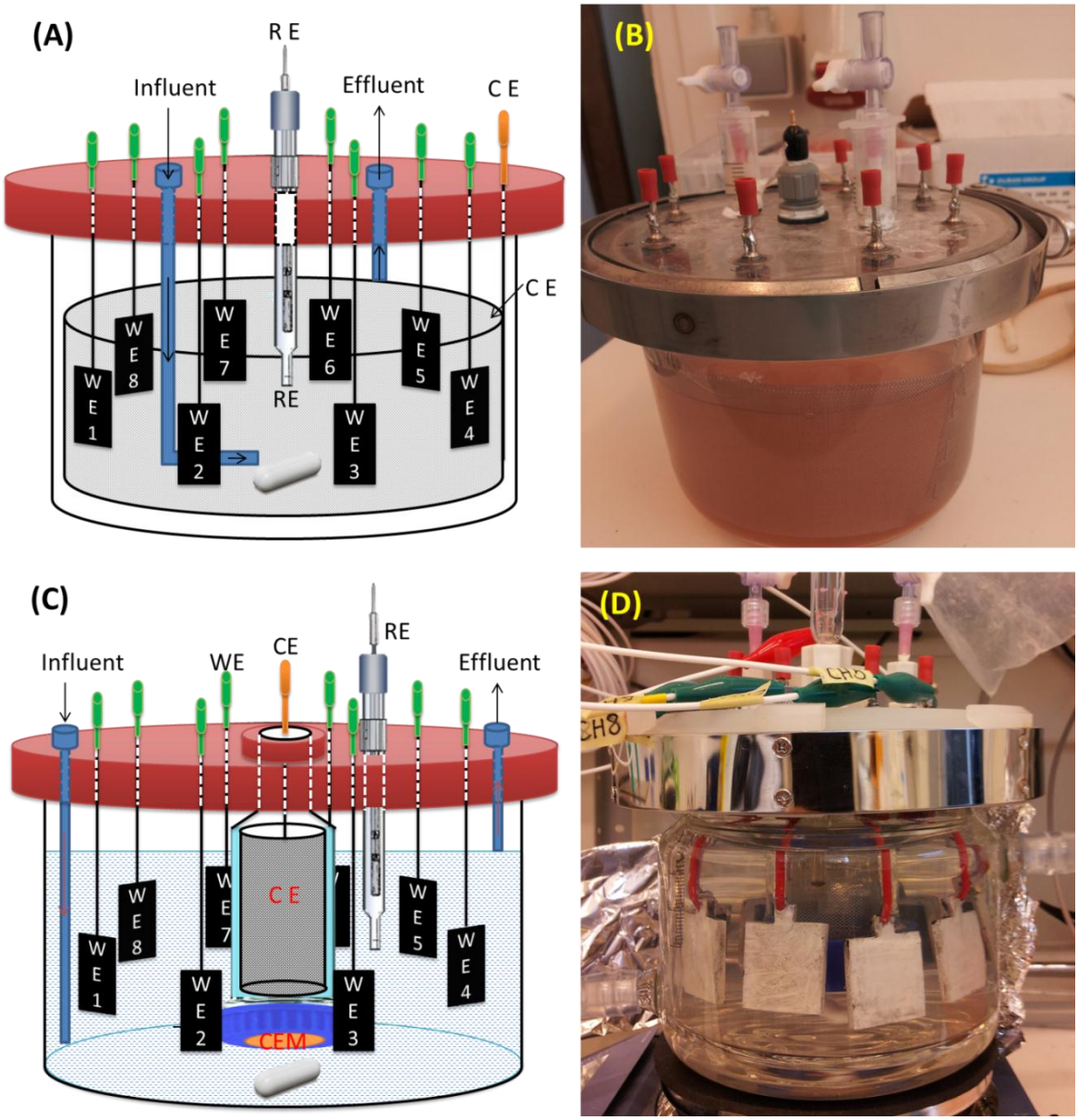

Figure 3.4 Schematics and photos of the multi-WE BES reactors: single-chamber(a and b) and double-chamber (c and d).

3.2.3.2 Medium

The anodic medium is the modified M9 medium with 2 g/L (24 mM) sodium acetate as the electron donor. The recipe of the modified M9 medium is shown in Table 3.1. The medium except vitamins was firstly autoclaved at 120ºC for 20 min. When the medium was cooled down to room temperature, the vitamin solution was added in through a sterile filter. The catholye was either 1 g/L of NaCl solution or M9 medium without sodium acetate.

Table 3.1 Recipe of the modified M9 medium

Modified M9 medium		Vitamin solution		Trace solution	
Chemical	Amount	Chemical	Amount (g/L)	Chemical	Amount (g/L)
Na_2HPO_4	6 g/L	Biotin	0.002	$FeCl_3 \cdot 6H_2O$	1.5
KH_2PO_4	3 g/L	Folic acid	0.002	H_3BO_3	0.15
NaCl	0.5 g/L	Pyridoxine-HCl	0.01	$CuSO_4 \cdot 5H_2O$	0.03
NH_4Cl	0.5 g/L	Riboflavin	0.05	KI	0.18
$MgSO_4 \cdot 7H_2O$	0.1 g/L	Thiamine	0.05	$MnCl_2 \cdot 4H_2O$	0.12
$CaCl_2 \cdot 2H_20$	14.6 mg/L	Nicotinic acid	0.05	$Na_2MoO_4 \cdot 2H_2O$	0.06
Sodium Acetate	2 g/L	Pantothenic acid	0.05	$ZnSO_4 \cdot 7H_2O$	0.12
Trace solution	1 mL/L	Vitamin B12	0.0001	$CoCl_2 \cdot 6H_2O$	0.15
Vitamin solution	1 mL/L	p-Aminobenzoic acid	0.05	EDTA (acid form)	10
		Thioctic acid	0.05	NaOH	adjust pH to 7
				$NiCl_2 \cdot 6H_2O$	0.023

3.2.3.3 Reactor operation

The anodic chamber was filled with 400 mL of modified M9 medium .The cathodic chamber (if present) was filled with 100 mL of 1 g/L of NaCl solution or M9 medium without sodium acetate. The anodic chamber was sparged with nitrogen for 30 min to ensure anaerobic conditions, and then inoculated with fresh anodic effluent from an existing acetate-fed BES reactor. The potential of each anode was set at -0.2 V vs. Ag/AgCl and current generation was recorded using chronoamperometry (CA). A magnetic stirrer was used to mix the solution continuously in the BES at a speed of 200 rpm unless stated otherwise. The reactor was normally firstly run in a fed-batch mode to allow the bacteria to attach on the electrode surface, and then switched to continuous mode to achieve a stable current output. These experiments were conducted in the dark in a temperature-controlled room (T = 25 ± 3°C).

3.2.4 Biofilm characterizations

3.2.4.1 Biofilm electrochemical activity

Cyclic voltammetry (CV) is a powerful technique for the study of the extracellular electron transfer between the electrode and bacteria. The electrochemical activity of the biofilms in this study was analysed with CV under either turnover (with electron donor) or non-turnover (without electron donor) conditions at very slow scan rates (1-10 mV/s).

3.2.4.2 Biofilm morphology

After completion of electrochemical experiments, biofilms on the electrodes were observed directly by light microscope which gave an overview of the biofilm. After that, the biofilm samples were subjected to Live/Dead staining or fluorescence in situ hybridisation (FISH) for confocal laser scanning microscopy (CLSM). The CLSM gave a 3D view of the biofilm and also provided the thickness information of biofilm. If FISH was used, the CLSM images also provided the information of bacterial community spatial distribution in the biofilm.

3.2.4.3 Biofilm community composition

The community composition of the biofilm was analysed by 16s rRNA Pyrosequencing. Firstly, the biofilm was scraped from the surface of the electrode. Then, DNA was extracted using a DNA Isolation Kit (MO BIO PowerBiofilm™) according to the manufacturer's instructions. After that, the universal 16S rRNA genes were amplified by PCR and sequenced by 454 Pyrosequencing. Finally, the sequencing data was analysed by a series of bioinformatics softwares to give out the community compositions of biofilms.

3.2.4.4 Statistical analysis of the biofilm

The effect of surface modification on the composition of microbial communities was assessed using Redundancy analysis (RDA) with subsequent Monte-Carlo permutation tests (999 permutations). Differences were investigated using Hellinger-transformed OTU abundances. Generalized linear modeling (GLM) was used to determine whether variation in the maximum current output between samples could be attributed to community composition and/or biomass. All analyses were implemented using R 2.12.0 (R Development Core Team).

3.3 Research outcomes

3.3.1 The effects of surface chemistry on current output, biofilm formation and community composition

3.3.1.1 Impact on current output

In this study, the startup time of current ($t_{startup}$) and time needed to reach a stable current (t_{stable}) were defined as the time taken to the point when current exceeded 0.01 mA/cm^2 (the yellow line in the new Figure 3) and when current stopped logarithmic increase, respectively. The average startup times and final current densities for the $–N^+(CH_3)_3$, –OH, $–SO_3^-$, and $–CH_3$, electrodes were (23 d, 0.204 mA/cm^2), (25.4 d, 0.149 mA/cm^2), (25.9 d, 0.114 mA/cm^2), and (37.2 d, 0.048 mA/cm^2).

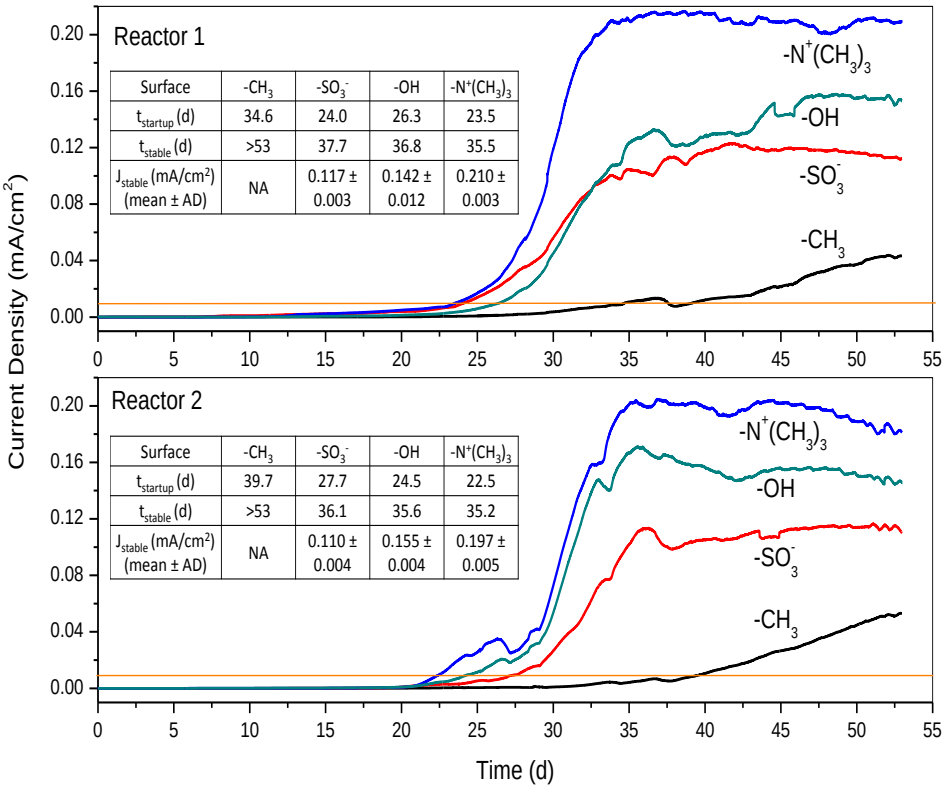

Figure 3.5 Current output over time of BE cells with different modified electrodes. The inset table compares the startup time of current ($t_{startup}$), time needed to reach a stable current (t_{stable}), and average current density at the stable stage (J_{stable}) of each electrode. E_{we} = -0.2 V vs Ag/AgCl, 24 mM of acetate as substrate.

3.3.1.2 Impact on biofilm formation

Figure 3.6 shows the representative CLSM 3D images of biofilms on different modified GC electrodes. It can been seen from the FISH images indicate that *Geobacter* populations dominated the biofilms irrespective of surface functionalization. Biofilms covered 100% of the surface area of $–N^+(CH_3)_3$, –OH, and $–SO_3^-$ functionalized electrodes but only around 30% of the surface area on $–CH_3$ functionalized electrodes. The maximum biofilm thicknesses followed the order $–CH_3$ > $–N^+(CH_3)_3$ > –OH > $–SO_3$. The amount of biomass associated with each electrode modification was calculated based on biofilm coverage and thickness data and followed the order $–N^+(CH_3)_3$ > –OH > $–SO_3^-$ > $–CH_3$. The results demonstrate that: 1) positively charged and hydrophilic surfaces were more conducive for electroactive biofilm formation; 2) the effects of the surface hydrophilicity was more pronounced than surface charge; 3) the differences in the maximum current output between surface modifications was correlated with biomass quantity.

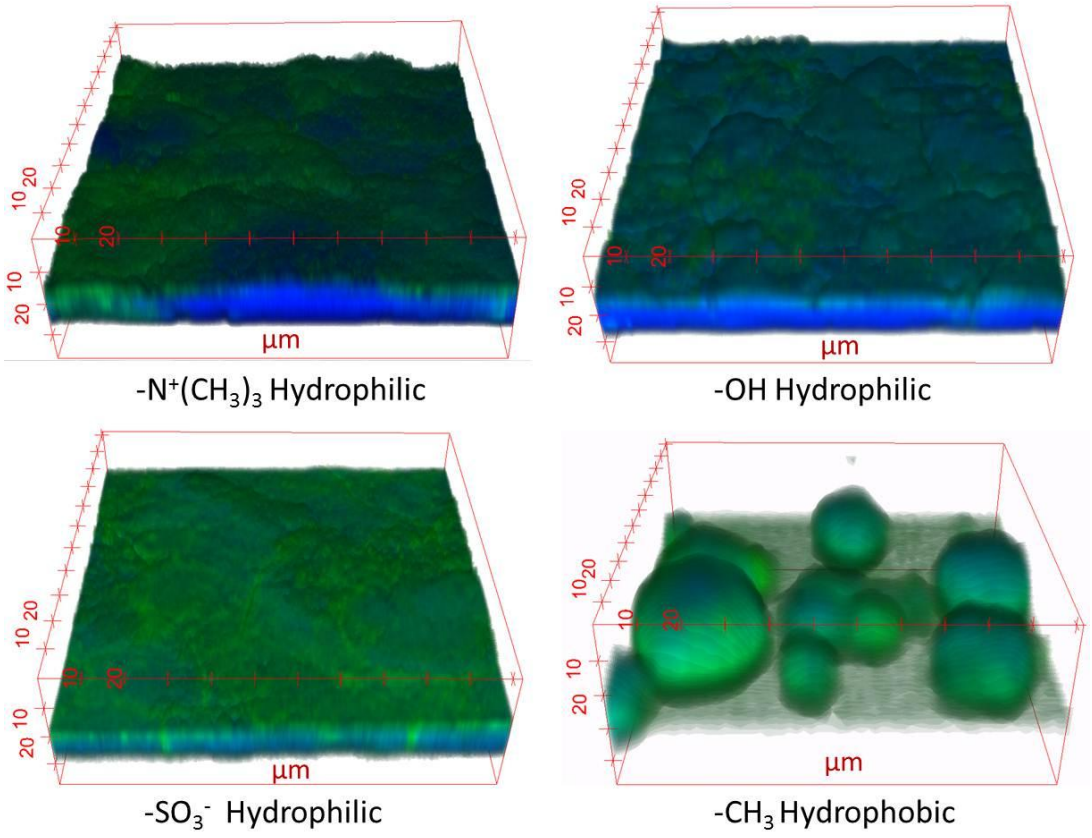

Figure 3.6 CLSM 3D images of biofilms on different modified GC electrodes. The biofilms were stained with EUB338mix-FITC (All bacteria, Green) and Geo1A-Cy5 (*Geobacter*, Blue).

3.3.1.3 Impact on bacterial community composition

Pyrosequencing of 16S rRNA gene amplicons revealed that the biofilms were dominated by *Geobacter* populations (Figure 3.7). The most similar *Geobacter* sp. to the most dominant of these populations, *Geobacter* 1, was *G. psychrophilus*, and the less dominant of these populations, *Geobacter* 2, was most similar to *G. sulfurreducens*. Most of the other populations present at more than 1% relative abundance (i.e. *Chlorobaculum*, *Clostridiales*, and *Bacteroidales* populations) were also observed in other mixed-culture anodic biofilm studies, but their specific roles in the functioning of BESs are yet to be determined. The composition of microbial communities associated with the $–CH_3$ terminated surface was significantly different to that of those associated with other surface modification chemistries. Methyl-group functionalized anodes were associated with larger abundances of *Chlorobaculum* and *Geobacter* 2 and a smaller abundance of *Geobacter* 1 when compared with other communities.

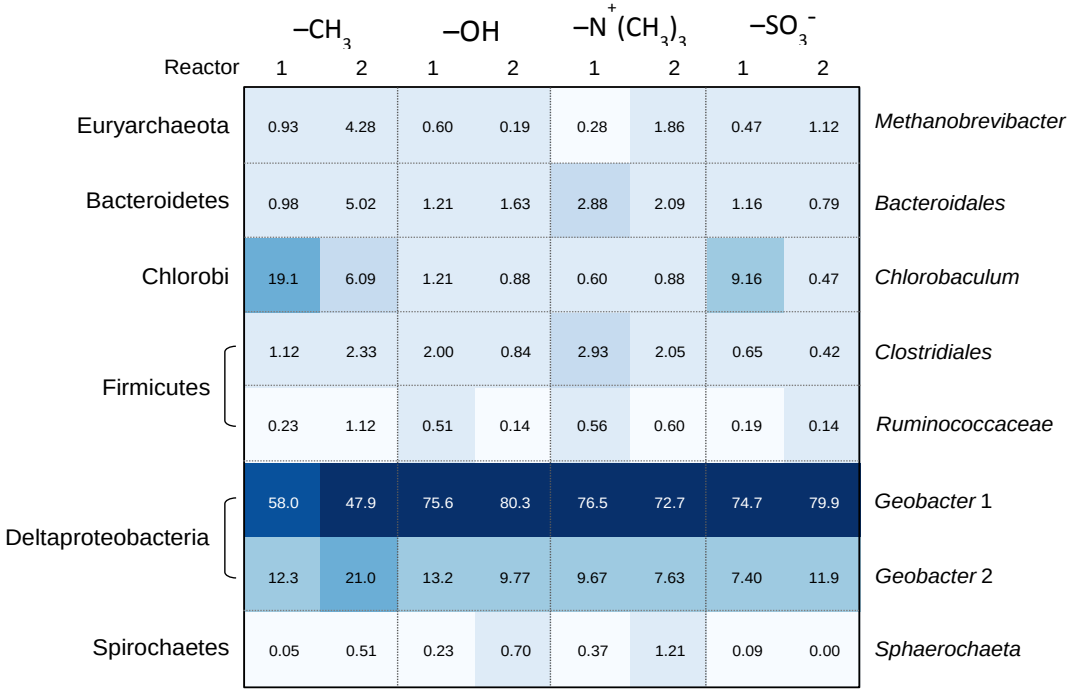

Figure 3.7 Percent relative abundances of microbial populations present at greater than 1% in any community.

3.3.2 Surfactant treatment of carbon felt surface

3.3.2.1 Surface hydrophilicity and wettability

The effect of the detergent treatment on hydrophobicity was assessed by water contact angle measurements and water absorption observations. The water contact angles of the untreated, control electrodes were greater than 120°. Comparatively, with CTAB-treated electrodes the water droplet would immediately penetrate the felt that resulted in a contact angle lower than 10° (Figure 3.8a). It was also noticed in the water absorption experiment that the treated felt sunk to the bottom of Milli-Q water quickly, whereas the untreated felt remained floating at the top of the water level (Figure 3.8b). These results demonstrated that the hydrophobic carbon felt surface could be transformed into hydrophilic in a couple of minutes only by 2mM CTAB soaking.

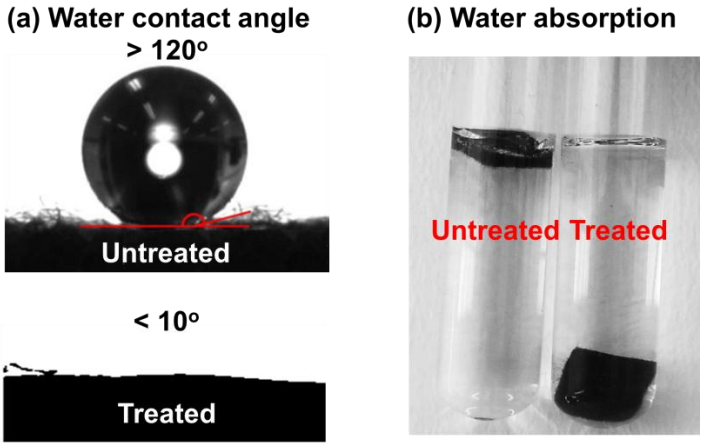

Figure 3.8 Water contact angle (a) and water absorption (b) images of untreated and CTAB-treated carbon felts showing surface hydrophobicity.

3.3.2.2 Surface elemental composition

The atomic composition of the electrode surfaces were determined by XPS and reported in Figure 3.9. These analyses revealed that: 1) the nitrogen content of CTAB-treated surfaces (0.96%) was higher than that of the untreated surfaces (0.3%); 2) 24% of the nitrogen content of CTAB-treated surfaces could be attributed to $-N^{+}(CH_3)_3$; 3) bromine was not present in either surface, but the oxygen content of the CTAB-treated surface increased from 5.6% to 6.9% with respect to the untreated surface. Since $-N^{+}(CH_3)_3$ is the characteristic functional group of the CTAB molecule, these results indicate that detergent molecules were adsorbed on the carbon felt surface. The absence of bromine on CTAB-treated surface is likely due to the fact that the bromine ion could be

easily washed away by water during rising and replaced by some oxygen-containing anions (e.g. OH^-).

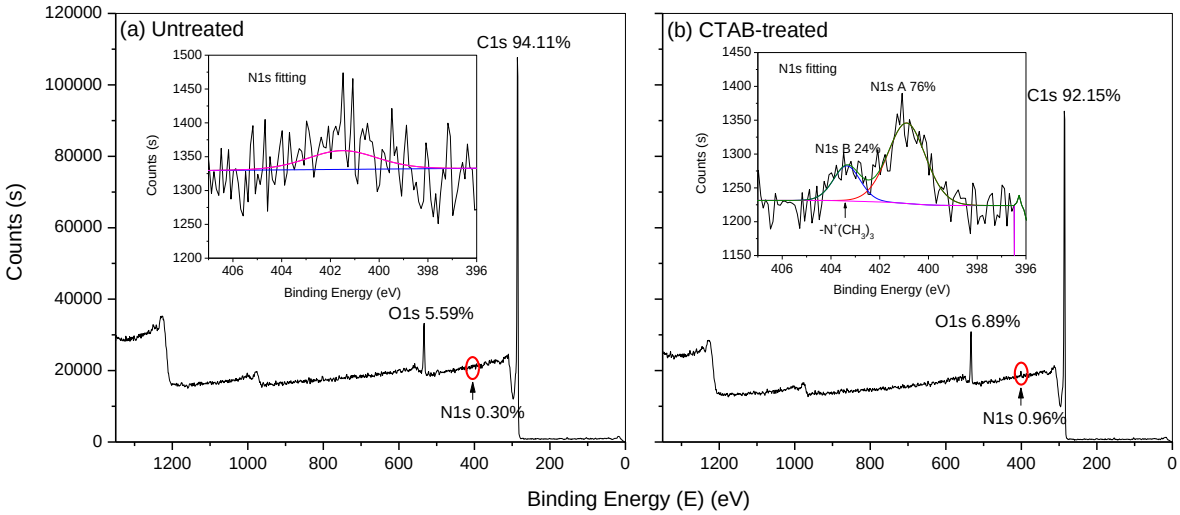

Figure 3.9 XPS spectra of (a) untreated and (b) CTAB-treated carbon felt surfaces showing elemental composition. Inset figures show N1s peak fitting and assignment.

3.3.2.3 Proposed mechanism of surfactant treatment

It has been reported that cationic surfactants such as HDTMA, DTAB, TTAB, and most importantly CTAB could form a film on the substrate surface via hydrophobic bonding. As the carbon felt surface is quite hydrophobic, it is very likely that detergent formed a film on the electrode surface via hydrophobic interaction between electrode surface and the non-polar tail of detergent, and left the polar head of the detergent ($-N^+(CH_3)_3$) exposed to the outside. As a result, the detergent modified carbon felt surface became hydrophilic. Figure 3.10 shows the proposed mechanism of surfactant treatment of carbon felt.

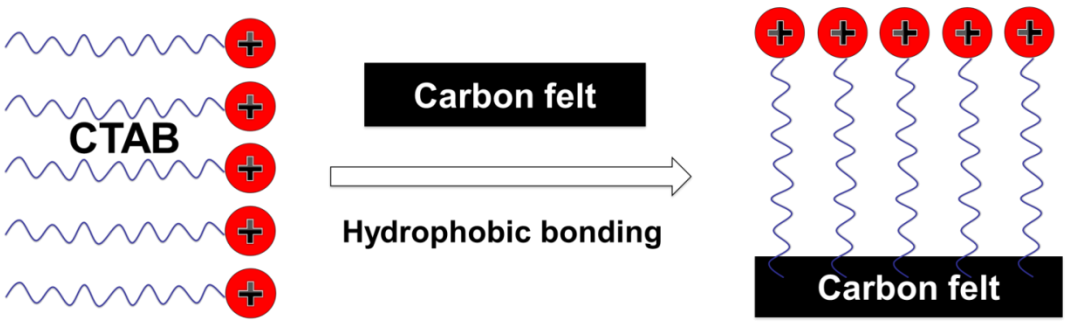

Figure 3.10 Proposed mechanism of CTAB treatment of carbon felt.

3.3.2.4 Effect of surfactant treatment on current output

Figure 3.11 shows the bioelectrocatalytic current generation over time at the untreated and CTAB-treated electrodes. The reactor was firstly run in a fed-batch mode to allow the bacteria to attach to the electrodes. After two batch cycles, the reactor was switched to a continuous flow mode to maintain the maximum current output. The medium feed rate was changed from 30 to 40 mL/h on day 6 because it was noticed that the former rate was not able to maintain the maximum current output of the treated electrodes. The start-up time ($t_{startup}$) of current generation of the untreated and CTAB-treated electrodes were 36 h and 23 h, respectively. The CTAB-treated electrodes reached a stable stage current densities (j_{stable}) of 1.56 ± 0.11 mA/cm^2 (mean ± SD) within 3.32 days, while the current outputs of the untreated electrodes stopped increase and stabilized around 1.26 ± 0.04 mA/cm^2 (mean ± SD) after 6.56 days. The experiments were continued for up to 30 days revealing consistently higher currents for the CTAB treated electrodes.

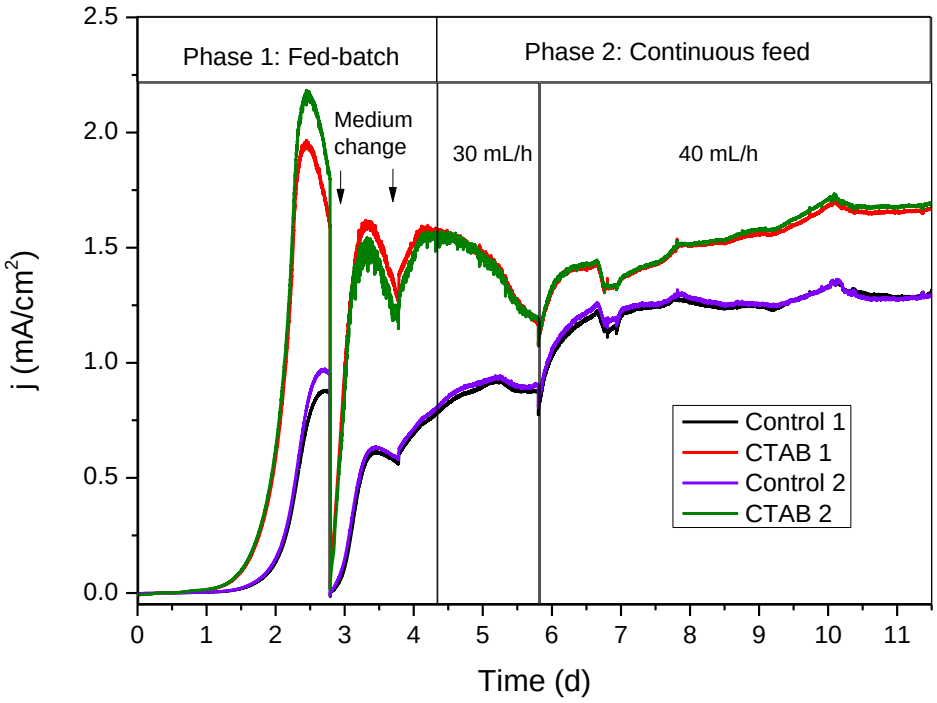

Figure 3.11 Bioelectrocatalytic current generation with untreated and CTAB-treated carbon felts. E_{we} = -0.2 V vs Ag/AgCl, 24 mM of acetate as substrate.

3.3.2.5 Pros and cons of surfactant treatment

Figure 3.12 summarizes the advantages of surfactant treatment over other anode surface functionalization methods. Compared to the routinely used electrode pre-treatment methods (high temperature ammonia, HNO_3/H_2SO_4 oxidation, NaOH/HCl soaking, plasma treatment, *etc.*), surfactant treatment is quick, simple, cheap, and environmentally friendly way to make carbon felt surfaces hydrophilic and positively-charged. The only chemical reagent used in this method is CTAB and it is used in very low concentration (2 mM). Furthermore, the whole treatment protocol takes only 15 min. Assume 1 L of 2 mM CTAB solution is needed for 1 m^2 of carbon felt, the cost of the chemical is only ~0.5 EUR (based on the price of CTAB retrieved from http://www.sigmaaldrich.com/). If ordered in bulk, it is estimated that the cost of CTAB will be reduced to half of the original price. Attributed to all these advantages, this method has potential to help researchers to save both time and chemicals involved in the electrode pretreatment procedure.

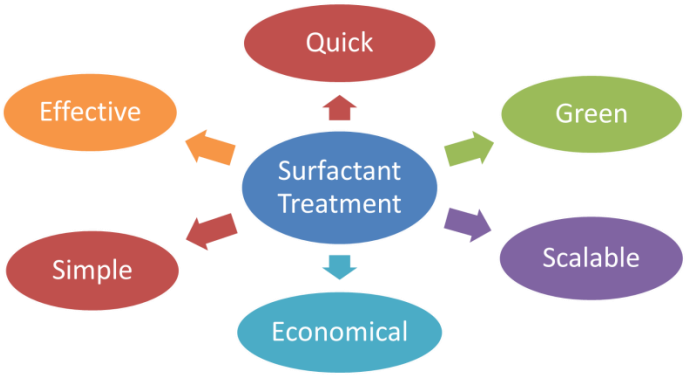

Figure 3.12 Advantages of surfactant treatment over other electrode surface functionalization methods

On the other hand, two disadvantages of surfactant treatment can be foreseen. First, it may not be applicable to other carbon materials whose surfaces are not hydrophobic enough. This is because surfactant molecules attach to the electrode surface via hydrophobic bonding. Second drawback of this method is the hydrophobic bonding, which is normally weaker than covalent bonding. However, the BES experiments suggest that the CTAB-modified surfaces are quite stable in reactors.

3.3.3 Simple method for grafting neutral red onto carbon surface

3.3.3.1 Surface modification of GC with neutral red

To check whether NR was covalently bound to the GC surface, GC plates with different modification methods were tested by CV in oxygen free PBS solution. As can be seen from Figure 3.13, bare electrodes and electrodes immersed in NR-HCl solutions did not show any obvious reversible redox peaks, while electrodes immersed in NR-$NaNO_2$ and NR-$NaNO_2$-HCl solutions all showed an obvious pair of symmetric peaks with a midpoint redox potential around -0.55V (vs Ag/AgCl). The peak current of NR-$NaNO_2$ treated electrode is much smaller than that for NR-$NaNO_2$-HCl treated ones. This result indicated that the addition of $NaNO_2$ is essential for the NR immobilization and that the acid environment enhances this process, which is likely due to fact that the *in situ* generated diazonium salts are not stable at pH > 2. For the electrodes immersed in NR-$NaNO_2$-HCl solution, both electrochemical reduction method and spontaneous reduction method were applied. The electrodes modified via electrochemical reduction and spontaneous reduction showed similar CV curves with comparable peak height and peak location. This result corroborates our hypothesis that NR could be covalently bound to carbon surface via spontaneous reduction of its diazonium salt. It is likely that NR diazonium salts could be reduced by the redox active groups on the carbon surface such as quinones under acidic condition.

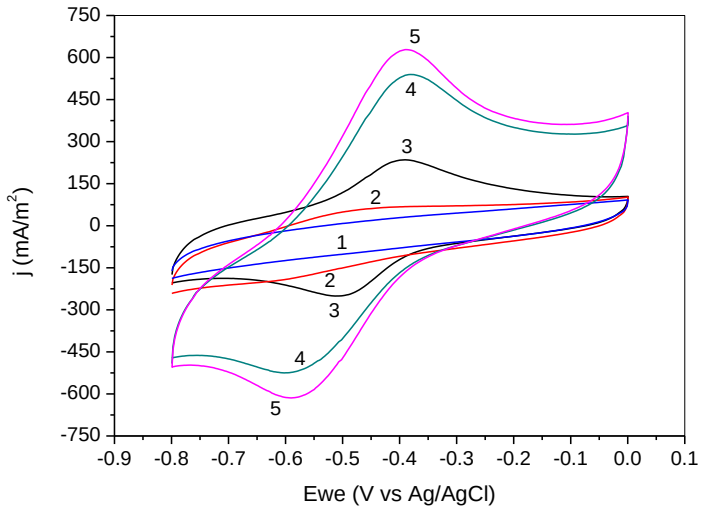

Figure 3.13 Cyclic voltammograms of GC plates with different treatments in oxygen-free PBS (0.1M, pH 7.0) at a scan rate of 50 mV/s. Curves: (1) bare; (2) NR-HCl treated; (3) NR-$NaNO_2$ treated; (4) NR-$NaNO_2$-HCl electrochemically modified; (5) NR-$NaNO_2$-HCl spontaneously modified surface.

3.3.3.2 Surface elemental composition

Table 3.2 displays the XPS results of the bare and NR-coated glassy carbon surfaces. It can be seen that, in comparison to the bare GC, the nitrogen content of NR-coated surfaces increased significantly. Also, chlorine is present in the NR-coated surfaces. The additional nitrogen and the chlorine are characteristic to NR hydrochloride. To distinguish between different nitrogen elements, the high resolution N1s peaks of the NR-coated surfaces were fitted using Avantage 4.54 software. Hereby, a surface that was physically coated with NR by simple adsorption is compared with the spontaneously modified surface described above. The N1s peak of physically coated surface was split into two peaks, one at 399.1 eV (N1sA) and the other one at 400.0 eV (N1sB). According to the literature, N1sA may be attributed to the imine (-N=) and amine (-NH- and $–NH_2$) nitrogens, while N1sB is likely from the positively-charged nitrogen atom in $=N^+(CH_3)_2$. The N1sA/ N1sB ratio (2.95:1) is very close to the theoretical value for NR (3:1).

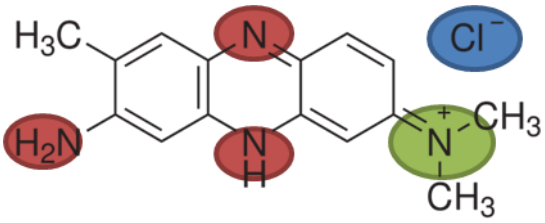

Scheme 3.3 Structure of neutral red molecule

For the spontaneously modified surfaces, besides the previous two peaks, another peak can be fitted at 401.5 eV, very close to the binding energy of nitrogen in NO_2^- group. The NO_2^- group comes originally from the unreacted $NaNO_2$ and is electrostatically attracted to the electrode surface by the positively-charged $=N^+(CH_3)_2$ group in the NR molecule. The N1sA/ N1sB ratios of the electrochemically modified surfaces was 2.04:1 which is very close to the theoretical value 2:1 for covalently bound NR, if we assume that the $–NH_2$ group in NR was lost during reduction of its diazonium salt (see Figure 1), while the N1sA/ N1sB ratios of the spontaneously modified surfaces is 1.80:1 which is slightly lower than the theoretical value. As a possible explanation for the missing N, it was previously shown that some diazonium groups ($-N^+\equiv N$) can also be transformed to azo groups (-N=N-) and then bound to the electrode surface via N-C bond, and the binding energy for the azo group is around 400 eV (Doppelt et al., 2007). In other words, some $–NH_2$ groups from NR molecules were not transformed to nitrogen gas but ended up with -N=N- groups during spontaneous reduction, which makes the N1sA/ N1sB ratio of the spontaneously modified surfaces less than 2:1.

Table 3.2 Elemental contents and atomic ratios of bare and NR-coated glassy carbon

Peak/Peak ratio	Bare GC	NR-coated GC			Binding Energy (eV)	Peak assignment
		Physically absorbed	Spontaneously modified	Electrochemically modified		
C1s (%)	88.99	86.24	88.33	89.63	---	---
O1s (%)	9.96	7.71	6.68	6.07	---	---
Cl2p (%)	**0**	**0.87**	**0.63**	**0.55**	---	---
N1s (%)	**1.06**	**5.17**	**4.36**	**3.76**	---	---
N1s A(%)	0.88	3.86	2.24	2.31	399.1	C-N*=C; -N*H_2
N1s B (%)	0	1.31	1.25	1.13	400.0	=N*$^{+}$$(CH_3)_2$; -N*=N*-
N1s C (%)	0.18	0	0.88	0.32	401.5	-N*O_2
N1s A/ N1s B	---	**2.95:1**	**1.80:1**	**2.04:1**	---	---

3.3.3.3 Effect of NR modification on current output

Both electrodes showed a fast start-up as the current started to increase 12 hours after the inoculation (Figure 3.14). On day 2, the current hit a peak value and started to drop, which was very likely due to the depletion of substrate in the BE reactor because of bacteria growth, biofilm formation and current generation. Thereafter, from day 2.5, the BE reactor was switched to a continuous mode with a feed flow rate of 30 mL/h. After that, the current recovered gradually and then increased significantly in the following few days. The current density of the bare and NR-modified electrodes stopped increasing and started to fluctuate around 0.1089 ± 0.002 mA/cm^2 and 0.4100 ± 0.008 mA/cm^2 from day 7 and day 7.5, respectively. Thus, the current output of the modified electrode was about 3.7 times higher than the unmodified electrode.

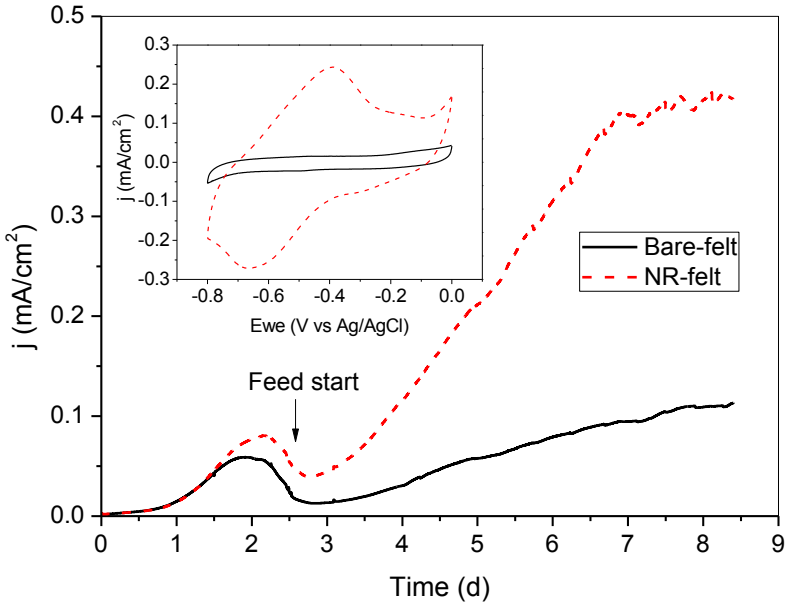

Figure 3.14 Current generation of acetate-oxidising BES reactor with bare and NR-modified graphite felts. Inset: cyclic voltammograms (50 mV/s) of bare and NR-modified graphite felts in oxygen-free 0.1 M PBS (pH 7.0).

3.3.3.4 Comparison of different NR modification methods

Figure 3.15 presents two existing methods of covalent modification of carbon surface with NR. As can be seen from the figure, both methods require several organic solvents and are quite time-consuming (Wang et al., 2011). In our study, spontaneous reduction of NR diazonium salts was investigated and verified that could covalently graft of NR onto carbon surfaces. This novel method involves soaking of carbon electrodes in NR-$NaNO_2$-HCl solution for 2h. Assume 1 L of 1mM NR diazonium salt solution is needed for 1 m^2 of carbon felt, the cost of the chemical is only ~0.5 EUR (based on the price of CTAB retrieved from http://www.sigmaaldrich.com/). If ordered in bulk, it is estimated that the cost of CTAB will be reduced to half of the original price.

Consequently, it is obvious that the new method is more time-saving and environmentally-friendly than the aforementioned methods. Moreover, this simple and quick method can be used for large scale electrode surface modifications. It is also anticipated that this method might be applicable to other electron transfer mediators with an amino group such as 1-Aminoanthraquinone (AQ) and 3-aminonaphthoquinone (NQ).

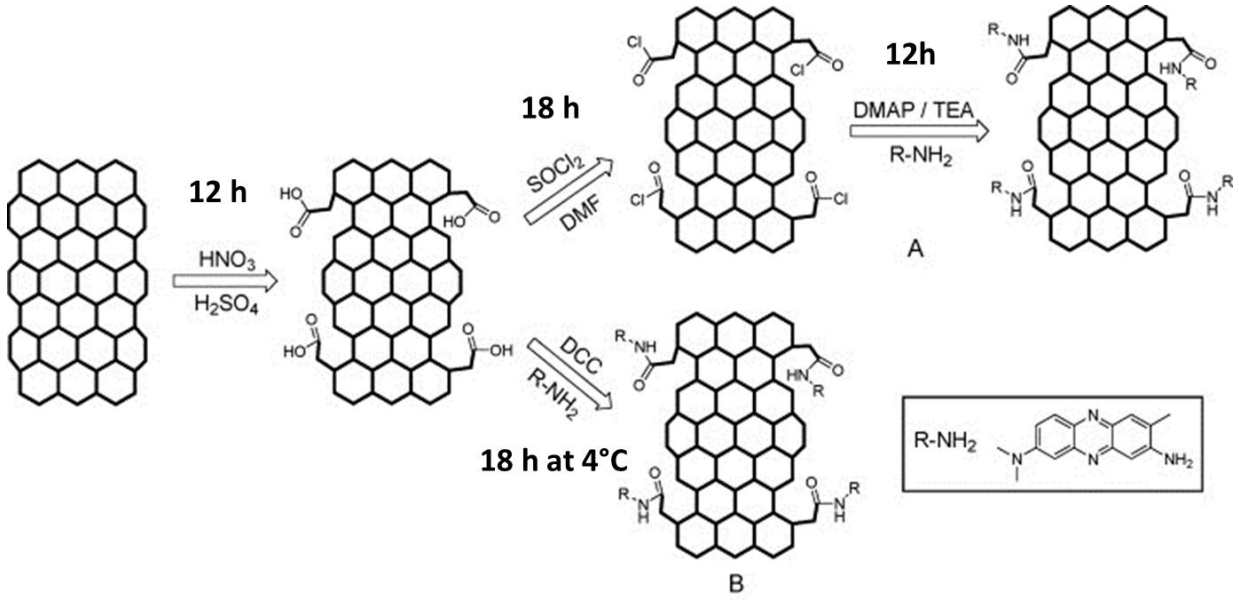

Figure 3.15 The schematic illustration for two methods of covalent modification of carbon surface with NR. (A) The stepwise amidation procedure. (B) The one-step condensation amidation procedure. DCC (N,N'-dicyclohexylcarbodiimide), DMF(N,N-dimethylformamide), $SOCl_2$ (thionyl chloride), DMAP (4-dimethylaminopyridine), TEA (triethylamine). (Image modified from Wang et al., 2011)

In order to avoid unrealistic comparisons, it has to be stressed here that the current densities achieved with the reactor used in this study were much lower than the reactor used in another study discussed in section 3.3.2. It was because of the use of different materials and conditions as listed henceforth: (1) microbial inoculum sources (UQ vs. UGent); (2) reactor designs (single chamber vs. double chamber); (3) brands of carbon felt (Morgan Australia vs. Alfa Aesar); (4) operational temperature (20°C vs 28°C); (5) electrode size (40mm × 30 mm × 2 mm vs. 20mm × 10 mm × 3.2 mm); (6) calculation methods for surface area (double sides vs. single side).

3.3.4 Flame oxidation of stainless steel felt

3.3.4.1 Electrode surface topography

After flame oxidation, the weight of the electrodes increased by 3.24 ± 0.65% (Average ± SD, n = 3), and the BET surface area increased from 461 to 719 m^2/m^2. Figure 3.16 shows the surface topography of the untreated and flame oxidized SS felts. Stereo microscope images provide a macro-scale view of the materials and clearly show the 3D, fibrous and porous structure of the SS felts. The diameter of the SS fiber is about 25 μm. The oxidized SS surface became darker and less shining than the untreated SS surface. SEM images of single SS fibres reveal that the oxidized SS electrodes were uniformly covered with nanoparticles of diameter ranging from 100 to 400 nm. AFM images show the 3D structure of the electrode surface. AFM results also reveal that the surface average roughness (Ra) of the untreated and oxidized surfaces were 75 and 151 nm, respectively. These results demonstrate that flame oxidation of the SS felt uniformly generated nanoparticles on the SS felt surface.

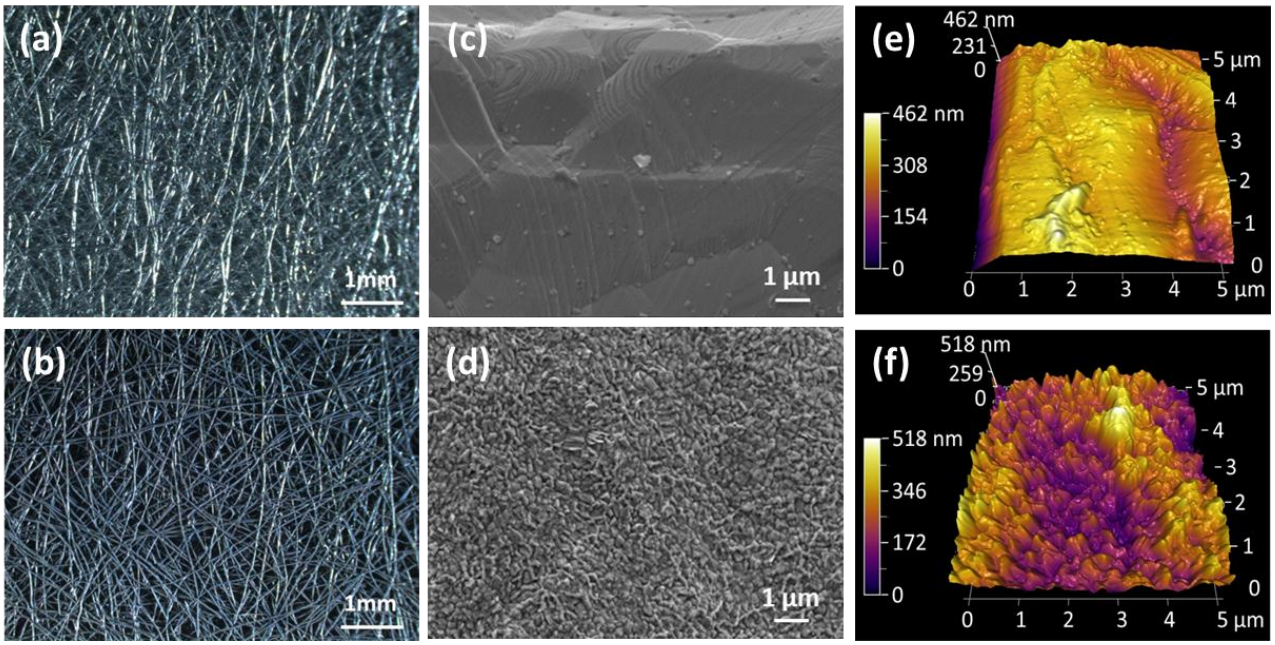

Figure 3.16 Representative light microscope images (a, b), SEM images (c, d), and AFM micrographs (e, f) of untreated (left column) and flame oxidized (right column) SS felt electrodes.

3.3.4.2 Electrode surface elemental composition

In order to understand the surface chemical composition and the electrochemical properties of the untreated and SS felts, XPS and Raman microscopy were conducted (Figure 3.17). As can be seen from XPS spectra, after flame oxidation, the surface iron and oxygen content increased from 4.76% and 42.24% to 13.25% and 54.61% respectively, while the carbon and chromium content decreased from 45.59% and 1.76% to 28.37 to 0%, respectively. Raman spectra indicate that the surface of the untreated SS felt was mainly composed of γ-FeOOH, $MnCr_2O_4$, and $FeCr_2O_4$, while the flame oxidized SS felt surface was dominated by α-Fe_2O_3. These results indicate that the nanoparticles generated on SS felt surface by flame oxidation are iron oxide nanoparticles (IONPs).

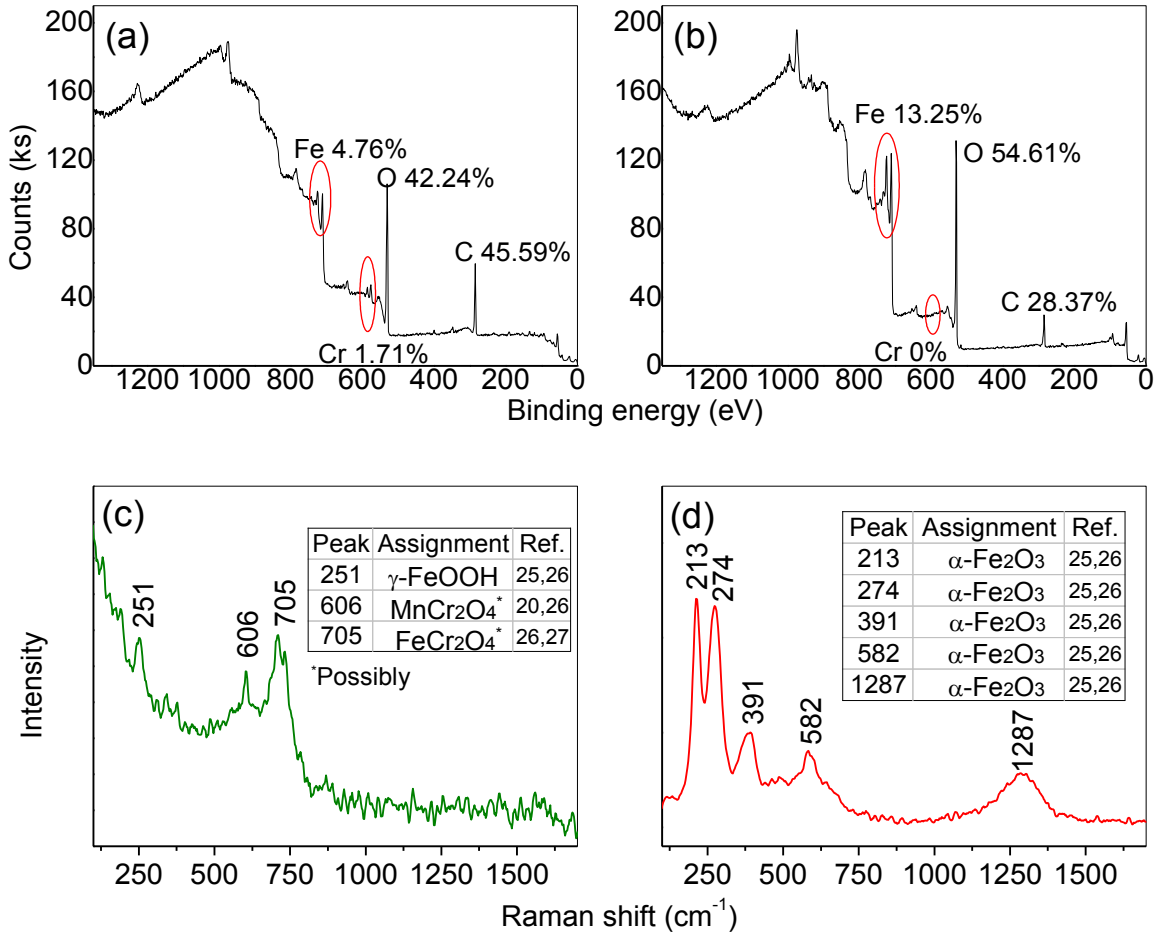

Figure 3.17 Representative XPS spectra (a, b) and Raman spectra (c, d) of untreated (left column) and flame oxidized (right column) SS felt electrodes.

3.3.4.3 Bioelectrocatalytic performance

It can be seen from Figure 3.18 that the bioelectrocatalytic current at the oxidized electrodes increased very quickly during the batch mode operation and reached a maximum current density (j_{max}) of 1.92 ± 0.08 mA/cm^2 in the third batch cycle, whereas the current at the untreated electrodes increased slowly and attained a j_{max} of 0.06 ± 0.01 mA/cm^2 during the same experimental period. The current density at the oxidized electrodes stabilized at around 1.51± 0.10 mA/cm^2, while the current density at the untreated electrodes gradually increased and stabilized at around 0.11 ± 0.01 mA/cm^2. In order to test the effect of mass transfer on the current density, the stirring rate was increased from 350 rpm to 500 rpm on day 11, and then to 650 rpm on day 12. The current density of the oxidized electrodes sharply increased by 7% and 5% on each step of the stirring rate increase, while the current density of the untreated electrodes gradually increased by 14% and 7% accordingly. On day 13, the stirring rate was switched back to 350 rpm. The current density of the untreated and treated electrodes both dropped sharply and stabilized at their original values. These observations demonstrate that the current density of the electrodes could be enhanced by improving the mass transfer.

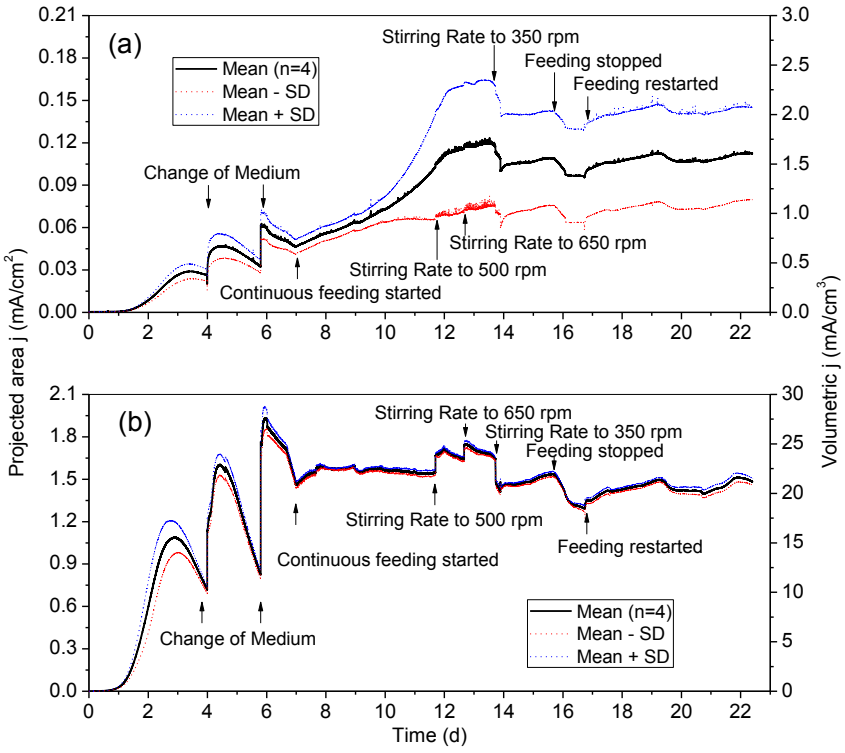

Figure 3.18 Bioelectrocatalytic current generation at untreated (a) and flame oxidized (b) SS felt electrodes. E_{we} = -0.2 V vs Ag/AgCl, 24 mM of acetate as substrate.

3.3.4.3 Characterization of electroactive Biofilm

The turnover CVs at both untreated and flame oxidized electrodes exhibited the classic sigmoidal shape for anodic biofilms under turnover conditions. At both untreated and flame oxidized electrodes, the acetate oxidation current started around -0.45 V *vs.* Ag/AgCl and reached a plateau from -0.2 V (Figure 3.19a and b). These plateau current densities are logically similar to the current densities recorded at the end of the respective CA experiments. These results indicate the biofilm-associated extracellular electron transfer to electrodes and thus the generation of current. Stereo microscopy images clearly show that a thick and reddish biofilm uniformly covered the whole surface area of the oxidized SS felt electrode, while almost no biofilm was observed on the untreated SS felt electrode (Figure 3.19c and d). It can be seen from CLSM biofilm images (Figure 3.19e and f) that bacteria only attached to certain points on the untreated SS felt, but covered the entire electrode surface of oxidized SS felt and formed a thick (~40 µm) biofilm. These results clearly reveal that flame oxidation considerably enhances the biocompatibility of SS felt electrodes and the maximum current output is positively correlated with the biofilm coverage on these electrodes.

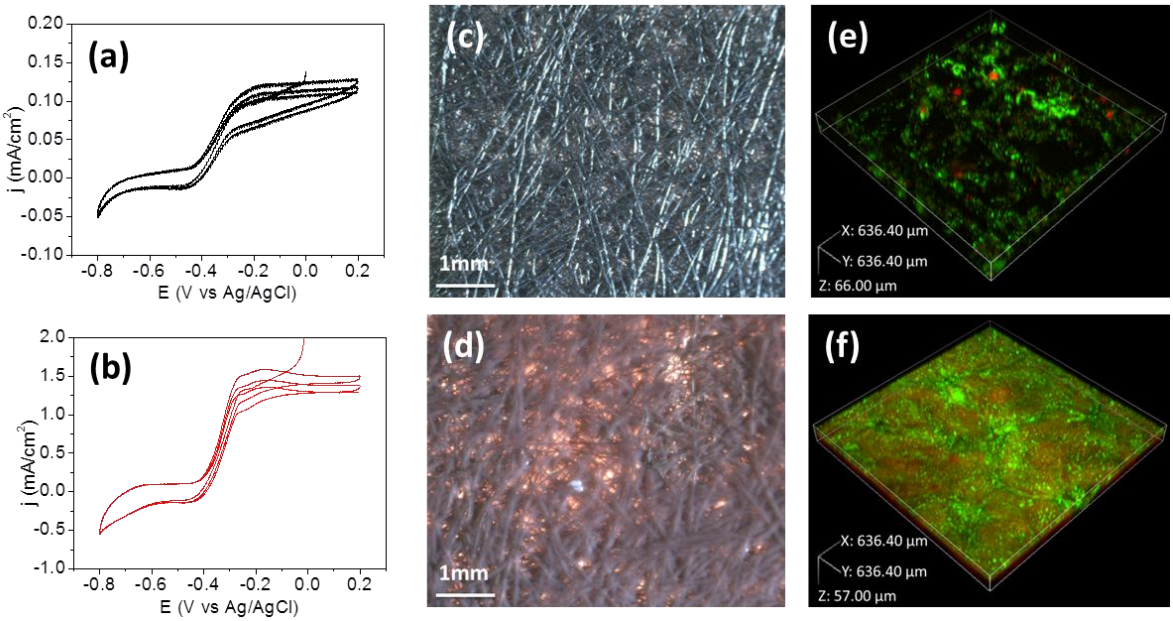

Figure 3.19 Representative turnover CVs (a, b), light microscope images (c, d), and CLSM images (e, f) of biofilms on untreated (top row) and flame oxidized (bottom row) SS felt electrodes.

3.3.4.4 Scalability of flame oxidized of SS felt

As stated earlier, the advantages of SS felt over carbon materials include high conductivity, excellent mechanical strength, scale-up possibility and low capital cost. A comparative analyses of resistivity, price and recyclability for carbon cloth, carbon felt, and SS felt materials is provided in Table 3.3. The resistivity of SS felt is at least hundred times lower than the carbon materials, which significantly reduces the electrode ohmic losses in full-scale BESs. The price of the SS felt is also lower than the carbon felt, which makes them more favourable for scaling up. More importantly, the weak mechanical strength of carbon-based materials limits their reuse. The used SS felt can be regenerated by burning the biofilm on the surface using flame. The possibility of reusing the SS felt can dramatically reduce the capital cost of full-scale BESs.

Table 3.3 Comparison of stainless steel felt with carbon materials

Electrode materials	Resistivity (Ω/m)	Bulk Price[a] ($/m^2)	Recyclability (Yes/No)	Reference
Carbon cloth	~100	10-30	No	(Cheng and Logan 2007)
Carbon felt	~200	50-150	No	This study
Stainless steel felt	~1	30-100	Yes	This study

[a] 2014 values from http://www.alibaba.com/.

In this study, Bunsen burner loaded with natural gas was used to generate iron oxide nanoparticles (IONPs) on SS felt surface to make its surface biocompatible. The natural gas flow rate is around 1L/min, it takes one min to treat one piece of SS felt (2 cm^2). Extending this on a large scale, 5 m^3 of natural gas is needed for the treatment of 1 m^2 of SS felt. The price of natural gas in Europe is around 0.55 EUR/m^3 (Source from Http://ec.europa.eu/eurostat/). Hence, the cost for flame treatment of SS felt is about 2.75 EUR/m^2. Based on trial experiments, it has to be mentioned that the flame treatment for 20 s also achieves the similar treatment effects. With this, the treatment cost can be reduced to 0.92 EUR/m^2. Even after combining both the material cost and the treatment cost, the price of flame oxidized SS felt remains cheaper than carbon felt electrode. More importantly, large scale flame sprayers are also available. If larger flame sprayer rather than Bunsen burner is used, the time needed for treatment of per square metre of SS felt will be dramatically reduced. In summary, attributed to the aforementioned advantages, flame oxidized SS felt holds exciting opportunities for scaling-up of anode in BESs.

Chapter 4 Conclusions and perspectives

4.1 Main conclusions of the thesis

Firstly, the effects of surface charge and surface hydrophobicity on anodic electroactive biofilm formation, bacterial community composition, and current generation in BESs were clarified. The findings suggested that positively-charged and hydrophilic surfaces were more selective to electroactive microbes (e.g. *Geobacter* sp.) and more conducive for electroactive biofilm formation. Moreover, the effect of the surface hydrophilicity on biofilm formation was more pronounced than the surface charge. The more the biofilm colonized on the electrode surface, the higher the current densities achieved.

Secondly, cationic surfactant (i.e. CTAB) treatment was demonstrated to be a simple and effective method to make carbon felt surface hydrophilic and positively-charged. The CTAB molecules could self-assemble a surfactant layer on carbon felt surface via hydrophobic bonding and leave the surface hydrophilic and positively-charged heads ($–N^{+}(CH_3)_3$) exposing outwardly. The study indicated that the CTAB treatment of carbon felt dramatically accelerates the anodic biofilm formation process and enhances current output of BESs. These results are consistent with the findings of first objective.

Thirdly, we hypothesized and proved that the electron transfer mediator, neutral red, could be bound to the carbon surface via electrochemical reduction of NR diazonium salts. We found out that the reduction of NR diazonium salt can happen spontaneously on carbon surfaces. Moreover, when tested as anode in BESs, the current output of NR-modified graphite felt electrodes were 3.63 ± 0.36 times higher than the unmodified electrodes. Thus, spontaneous reduction of *in situ* generated NR diazonium salts proved to be a simple method to graft NR molecules on carbon surface and an effective way to enhance the performance of anode in BESs. This study demonstrated the effectiveness of covalently bound NR as insoluble redox mediator during the microbial anodic oxidation of acetate.

Finally, flame oxidation was shown to be a quick and efficient method to break down the chromium-rich passive film and generate iron oxide nanoparticles (IONPs) at the SS felt surface. The results revealed that the IONPs-coating dramatically enhances the anodic biofilm formation and thus the current density at the SS felt electrode in BES. The maximum current density achieved with the flame oxidized SS felt (1.92 mA/cm^2) in this study is one of the highest reported for

acetate-fed MESs. The flame oxidized SS felt meets almost all requirements of the ideal anode materials for BESs and can be therefore considered as acpromising and scalable electrode material for BES.

In summary, surface chemistry of carbon and SS electrode surfaces significantly affects the electroactive biofilm formation and the current generation of BESs.

4.2 Recommendations for future research

Surface chemistry on cathodic biofilm formation

So far most of the surface modification studies were focused on improving the performance of anodic microbial biofilms. Recently, cathodic microbial processes have attracted increasing interest as they are essential for the bioelectrosynthesis of valuable chemicals. Unlike the anode case, bacteria do not adhere well to the cathode surface. It is still unclear how electrons are transported to the inside of bacteria. Modification of the cathode surface characteristics is probably going to be one of the effective strategies to promote cathodic biofilm formation and electron transfer. Consequently, it is of great significance to use the knowledge we gained on the anode surface chemical modifications to enhance the cathodic biofilm formation and the cathodic extracellular electron transfer with different types of bacteria.

Surface topography on biofilm formation

It is well known in other biofilm research fields that the surface topography not only impacts bacteria attachment and biofilm formation, but also influences the structure and function of the biofilm (Ploux et al., 2010). Hence, the topographic features at macro, micro, and nano scales most probably influence the biofilms in BESs as well. However, in the BES field, the only proven fact thus far is that increasing the specific surface area of electrode increases current generation (Ye et al., 2012). The impact of surface topography on the bacterial adhesion and biofilm formation in BESs is still unknown. Moreover, the effects of the size, configuration, and density of topographic features on the performance of BESs have not been investigated. Therefore, a great potential is foreseen to increase bacterial adhesion, biofilm formation via optimizing the material surface topography properties.

Scale-up of the SS felt anode

The flame oxidized SS felt has showed exciting potential and possibilities for scale-up. Thus, it is suggested to test the performance of this material at larger scale in BES. To further increase the specific surface area, different configurations of this material such as pleated stainless steel felt can be used. In order to enhance the mass transfer of nutrients and ions, holes of millimetre scale can be generated on the electrode. Recently, a high-performance air-cathode based on activated carbon was reported (Dong et al., 2012; Zhang et al., 2014). Hence, it would be very interesting to investigate whether combining SS felt anode with activated carbon based air-cathode could results in a high power density production in microbial fuel cells (MFCs). Moreover, the high current produced at the SS felt anode can also be used for CO_2 fixation and H_2O_2 production at the cathode of BES reactors.

SS felt as cathode for BESs

In addition to the great mechanical strength and excellent conductivity, SS material is also proven to be a better catalyst for hydrogen evolution reaction (HER) than carbon-based materials. The SS felt used in this study possesses a high specific surface area. Thus, it holds exciting opportunity for scaled-up cathode for microbial electrolysis cells (MECs). It would be interesting to evaluate the performance of the MECs with flame oxidized SS felt as anode and unmodified SS felt as cathode. SS felt can also be used as cathode for microbial electrosynthesis (MES). The suitability of flame oxidized SS felt for MES needs to be checked because the surface iron oxide nanoparticles might get reduced at low potential. To improve the biocompatibility of SS felt, new surface modifications are required. It has been reported that CNTs can be *in situ* synthesised on SS surface by flame treatment and chemical vapour deposition (CVD). These two CNTs synthesis methods are both inexpensive and scalable. Therefore, the CNTs-coated SS felt is recommended for the use of MES in the future.

4.3 Perspectives

The present thesis firstly elucidated the impact of the surface chemistry on the anodic biofilm formation and current generation in BESs, and then developed simple and effective methods to modify the surfaces of carbon and SS electrodes to obtain desired properties. The fundamental knowledge gained on anodic surface modifications can also be useful for other material science engineers for biofilm control and management. The novel surface modification methods presented in this study can also be applicable for other material surface modifications. The SS felt electrodes

reported in this study can be used in scaled-up BESs not only as anode but also as cathode for several BES applications.

Engineered surface for biofilm control

The aim of this study was to enhance the bacterial attachment and biofilm formation by surface chemical modification. Our results demonstrated that hydrophilic surface and positively-charged surfaces are more conducive to bacterial adhesion. We also found that surface elemental composition and surface roughness dramatically affect the biocompatibility of SS felt. These findings can be extended in designing materials that are unfavourable for biofilm formation. For example, biofilm formation is a major problem in biomedical materials such as artificial teeth, and in sewer pipes as it causes corrosion. In the field of MFCs, biofouling on the membrane such as nafion greatly increases the internal resistance. Also, in single-chamber MFCs, the biofilm growth on the cathode significantly reduces the catalytic activity and longevity of the electrodes (Logan 2008). Thus, changing the surface chemistry and topography might be a good strategy to prevent the biofilm growth on the material surfaces in different fields.

Surface modifications for other applications

Two new and efficient carbon surface modification methods namely surfactant treatment and spontaneous reduction of NR diazonium salts were described in the present thesis.. Surfactant treatment provides a simple and effective method to change surface charge and hydrophobicity. Besides CTAB, many other surfactants can be used to change the functional groups on material surfaces. This method can be applied to other surfaces with high hydrophobicity such as activated carbon and zeolite. Surfactant-modified activated carbon and zeolite will make the surface area in their tiny hole structures available for chemical or electrochemical reactions. Spontaneous reduction of NR diazonium salts as demonstrated in this thesis, is a quick and efficient method to graft NR onto carbon surface. Using the same method, electrode transfer mediators such as anthraquinone (AQ) can also be grafted onto the carbon surfaces. Such mediator-modified surfaces can be used to catalyse specific electrochemical reactions. For example, AQ-modified carbon surface is more favourable for reduction of oxygen to peroxide. The use of AQ-modified carbon electrode as the cathode of MFCs might be able to increase the peroxide production rate.

Scale-up of BESs for the production valuable chemicals

In this study, record-high current density was achieved on flame oxidized SS felt. Due to its high mechanical strength and excellent conductivity, SS felt can be easily scaled up for large scale BESs.

Nowadays, electrical power can be produced in a sustainable and efficient way using photovoltaics or wind turbines. Hence, production of electrical power from BESs becomes less attractive. However, the high oxidation current can be used to produce high value chemicals. For example, H_2O_2 can be produced at the cathode of MFCs, and the produced H_2O_2 can be further used to disinfect wastewater. Also, H_2 and caustic production can be carried out at the cathode of MECs. The H_2 gas can be used as fuel directly and the caustic solution could be used to adjust the pH of anaerobic digesters. Moreover, CO_2 can be electrochemically reduced into formate and CO at the cathode.

New BES-based approach for organic wastewater treatment

Over the past two decades, the current/power density of BESs has significantly improved. However, the high capital cost of BESs makes them less competitive with other traditional wastewater treatment techniques such as anaerobic digestion. In order to transit this technology into market, it is of high importance to raise the value of the products from BESs. In the past decade, the H_2 production rate form MECs has dramatically increased and several pilot-scale MEC reactors were reported. However, most of them only focused on improving the production of H_2, and the value of the CO_2 produced at the anode got ignored. It has been reported that H_2/CO_2 mixed gas can be converted into specific products using microorganisms or chemical catalysts. For example, homoacetogenic bacteria can use H_2 to reduce CO_2 into acetate and acetate can be further converted into longer chain fatty acids which have higher value (Grootscholten et al., 2013). Moreover, under high pressure, H_2/CO_2 can also be converted into formic and methanol on copper-based and rhodium-based catalysts, respectively (Sakakura et al., 2007). Therefore, a combination of these two approaches with a H_2/CO2 producing BES might significantly improve the value of organic waste.

References

Allongue, P., Delamar, M., Desbat, B., Fagebaume, O., Hitmi, R., Pinson, J., Saveant, J.M., 1997. Covalent modification of carbon surfaces by aryl radicals generated from the electrochemical reduction of diazonium salts. Journal of the American Chemical Society 119(1), 201-207.

Anderson, G.G., O'Toole, G.A., 2008. Innate and induced resistance mechanisms of bacterial biofilms. Current Topics in Microbiology and Immunology 322, 85-105.

Baker, S.E., Colavita, P.E., Tse, K.Y., Hamers, R.J., 2006. Functionalized vertically aligned carbon nanofibers as scaffolds for immobilization and electrochemical detection of redox-active proteins. Chemistry of Materials 18(18), 4415-4422.

Bakker, D.P., Busscher, H.J., van Zanten, J., de Vries, J., Klijnstra, J.W., van der Mei, H.C., 2004. Multiple linear regression analysis of bacterial deposition to polyurethane coatings after conditioning film formation in the marine environment. Microbiology 150(6), 1779-1784.

Barbier, B., Pinson, J., Desarmot, G., Sanchez, M., 1990. Electrochemical Bonding of Amines to Carbon-Fiber Surfaces toward Improved Carbon-Epoxy Composites. Journal of The Electrochemical Society 137(6), 1757-1764.

Bassler, B.L., 1999. How bacteria talk to each other: regulation of gene expression by quorum sensing. Current Opinion in Microbiology 2(6), 582-587.

Behera, M., Jana, P.S., Ghangrekar, M.M., 2010. Performance evaluation of low cost microbial fuel cell fabricated using earthen pot with biotic and abiotic cathode. Bioresource technology 101(4), 1183-1189.

Bond, D.R., Holmes, D.E., Tender, L.M., Lovley, D.R., 2002. Electrode-reducing microorganisms that harvest energy from marine sediments. Science 295(5554), 483-485.

Bond, D.R., Lovley, D.R., 2003. Electricity production by Geobacter sulfurreducens attached to electrodes. Applied and Environmental Microbiology 69(3), 1548-1555.

Borole, A.P., O'Neill, H., Tsouris, C., Cesar, S., 2008. A microbial fuel cell operating at low pH using the acidophile Acidiphilium cryptum. Biotechnology Letters 30(8), 1367-1372.

Boyd, R.D., Verran, J., Jones, M.V., Bhakoo, M., 2002. Use of the atomic force microscope to determine the effect of substratum surface topography on bacterial adhesion. Langmuir 18(6), 2343-2346.

Bretschger, O., Obraztsova, A., Sturm, C.A., Chang, I.S., Gorby, Y.A., Reed, S.B., Culley, D.E., Reardon, C.L., Barua, S., Romine, M.F., Zhou, J., Beliaev, A.S., Bouhenni, R., Saffarini, D., Mansfeld, F., Kim, B.H., Fredrickson, J.K., Nealson, K.H., 2007. Current production and metal oxide reduction by Shewanella oneidensis MR-1 wild type and mutants. Applied and Environmental Microbiology 73(21), 7003-7012.

Brooksby, P.A., Downard, A.J., 2004. Electrochemical and atomic force microscopy study of carbon surface modification via diazonium reduction in aqueous and acetonitrile solutions. Langmuir 20(12), 5038-5045.

Cassell, A.M., Li, J., Stevens, R.M.D., Koehne, J.E., Delzeit, L., Ng, H.T., Ye, Q., Han, J., Meyyappan, M., 2004. Vertically aligned carbon nanotube heterojunctions. Applied Physics Letters 85(12), 2364-2366.

Ceccato, M., Bousquet, A., Hinge, M., Pedersen, S.U., Daasbjerg, K., 2011. Using a Mediating Effect in the Electroreduction of Aryldiazonium Salts To Prepare Conducting Organic Films of High Thickness. Chemistry of Materials 23(6), 1551-1557.

Cerca, N., Pier, G.B., Vilanova, M., Oliveira, R., Azeredo, J., 2005. Quantitative analysis of adhesion and biofilm formation on hydrophilic and hydrophobic surfaces of clinical isolates of Staphylococcus epidermidis. Research in Microbiology 156(4), 506-514.

Chaudhuri, S.K., Lovley, D.R., 2003. Electricity generation by direct oxidation of glucose in mediatorless microbial fuel cells. Nature Biotechnology 21(10), 1229-1232.

Chen, J.H., Huang, Z.P., Wang, D.Z., Yang, S.X., Li, W.Z., Wen, J.G., Ren, Z.F., 2001. Electrochemical synthesis of polypyrrole films over each of well-aligned carbon nanotubes. Synthetic Metals 125(3), 289-294.

Cheng, S.A., Logan, B.E., 2007. Ammonia treatment of carbon cloth anodes to enhance power generation of microbial fuel cells. Electrochemistry Communications 9(3), 492-496.

Cheng, S.A., Xing, D.F., Call, D.F., Logan, B.E., 2009. Direct Biological Conversion of Electrical Current into Methane by Electromethanogenesis. Environmental Science & Technology 43(10), 3953-3958.

Clauwaert, P., Rabaey, K., Aelterman, P., De Schamphelaire, L., Ham, T.H., Boeckx, P., Boon, N., Verstraete, W., 2007. Biological denitrification in microbial fuel cells. Environmental Science & Technology 41(9), 3354-3360.

Clauwaert, P., Toledo, R., Van der Ha, D., Crab, R., Verstraete, W., Hu, H., Udert, K.M., Rabaey, K., 2008. Combining biocatalyzed electrolysis with anaerobic digestion. Water Science and Technology 57(4), 575-579.

Cournet, A., Delia, M.L., Bergel, A., Roques, C., Berge, M., 2010. Electrochemical reduction of oxygen catalyzed by a wide range of bacteria including Gram-positive. Electrochemistry Communications 12(4), 505-508.

Crittenden, S.R., Sund, C.J., Sumner, J.J., 2006. Mediating electron transfer from bacteria to a gold electrode via a self-assembled monolayer. Langmuir 22(23), 9473-9476.

Deinhammer, R.S., Ho, M., Anderegg, J.W., Porter, M.D., 1994. Electrochemical Oxidation of Amine-Containing Compounds - a Route to the Surface Modification of Glassy-Carbon Electrodes. Langmuir 10(4), 1306-1313.

Delamar, M., Desarmot, G., Fagebaume, O., Hitmi, R., Pinson, J., Saveant, J.M., 1997. Modification of carbon fiber surfaces by electrochemical reduction of aryl diazonium salts: Application to carbon epoxy composites. Carbon 35(6), 801-807.

Donaldson, K., Aitken, R., Tran, L., Stone, V., Duffin, R., Forrest, G., Alexander, A., 2006. Carbon nanotubes: A review of their properties in relation to pulmonary toxicology and workplace safety. Toxicological Sciences 92(1), 5-22.

Dong, H., Yu, H.B., Wang, X., 2012. Catalysis Kinetics and Porous Analysis of Rolling Activated Carbon-PTFE Air-Cathode in Microbial Fuel Cells. Environmental Science & Technology 46(23), 13009-13015.

Downard, A.J., 2000. Electrochemically assisted covalent modification of carbon electrodes. Electroanalysis 12(14), 1085-1096.

Downard, A.J., bin Mohamed, A., 1999. Suppression of protein adsorption at glassy carbon electrodes covalently modified with tetraethylene glycol diamine. Electroanalysis 11(6), 418-423.

Du, Z.W., Li, H.R., Gu, T.Y., 2007. A state of the art review on microbial fuel cells: A promising technology for wastewater treatment and bioenergy. Biotechnology Advances 25(5), 464-482.

Dumas, C., Basseguy, R., Bergel, A., 2008. Microbial electrocatalysis with Geobacter sulfurreducens biofilm on stainless steel cathodes. Electrochimica Acta 53(5), 2494-2500.

Dutta, P.K., Keller, J., Yuan, Z.G., Rozendal, R.A., Rabaey, K., 2009. Role of Sulfur during Acetate Oxidation in Biological Anodes. Environmental Science & Technology 43(10), 3839-3845.

Dyke, C.A., Tour, J.M., 2003. Unbundled and highly functionalized carbon nanotubes from aqueous reactions. Nano Letters 3(9), 1215-1218.

Edwards, K.J., Rutenberg, A.D., 2001. Microbial response to surface microtopography: the role of metabolism in localized mineral dissolution. Chemical Geology 180(1-4), 19-32.

Erable, B., Duteanu, N., Kumar, S.M.S., Feng, Y.J., Ghangrekar, M.M., Scott, K., 2009. Nitric acid activation of graphite granules to increase the performance of the non-catalyzed oxygen reduction reaction (ORR) for MFC applications. Electrochemistry Communications 11(7), 1547-1549.

Erable, B., Vandecandelaere, I., Faimali, M., Delia, M.L., Etcheverry, L., Vandamme, P., Bergel, A., 2010. Marine aerobic biofilm as biocathode catalyst. Bioelectrochemistry 78(1), 51-56.

Feng, Y.J., Lee, H., Wang, X., Liu, Y.L., He, W.H., 2010a. Continuous electricity generation by a graphite granule baffled air-cathode microbial fuel cell. Bioresource technology 101(2), 632-638.

Feng, Y.J., Yang, Q., Wang, X., Logan, B.E., 2010b. Treatment of carbon fiber brush anodes for improving power generation in air-cathode microbial fuel cells. Journal of Power Sources 195(7), 1841-1844.

Flexer, V., Chen, J., Donose, B.C., Sherrell, P., Wallace, G.G., Keller, J., 2013a. The nanostructure of three-dimensional scaffolds enhances the current density of microbial bioelectrochemical systems. Energy & Environmental Science 6(4), 1291-1298.

Flexer, V., Marque, M., Donose, B.C., Virdis, B., Keller, J., 2013b. Plasma treatment of electrodes significantly enhances the development of anodic electrochemically active biofilms. Electrochimica Acta 108, 566-574.

Flint, S.H., Brooks, J.D., Bremer, P.J., 2000. Properties of the stainless steel substrate, influencing the adhesion of thermo-resistant streptococci. Journal of Food Engineering 43(4), 235-242.

Freguia, S., 2010. Organics oxidation. In: Rabaey, K., Angenent, L., Schroder, U., Keller, J. (Eds.), Bioelectrochemical systems : From extracellular electron transfer to biotechnological application. IWA Publishing, London, Engalnd, U.K.

Freguia, S., Tsujimura, S., Kano, K., 2010. Electron transfer pathways in microbial oxygen biocathodes. Electrochimica Acta 55(3), 813-818.

Gooding, J.J., 2008. Advances in interfacial design sensors: Aryl diazonium salts for electrochemical biosensors and for modifying carbon and metal electrodes. Electroanalysis 20(6), 573-582.

Gorby, Y.A., Yanina, S., McLean, J.S., Rosso, K.M., Moyles, D., Dohnalkova, A., Beveridge, T.J., Chang, I.S., Kim, B.H., Kim, K.S., Culley, D.E., Reed, S.B., Romine, M.F., Saffarini, D.A., Hill, E.A., Shi, L., Elias, D.A., Kennedy, D.W., Pinchuk, G., Watanabe, K., Ishii, S., Logan, B., Nealson, K.H., Fredrickson, J.K., 2006. Electrically conductive bacterial nanowires produced by Shewanella oneidensis strain MR-1 and other microorganisms. Proceedings of the National Academy of Sciences 103(30), 11358-11363.

Gregory, K.B., Bond, D.R., Lovley, D.R., 2004. Graphite electrodes as electron donors for anaerobic respiration. Environmental Microbiology 6(6), 596-604.

Gregory, K.B., Lovley, D.R., 2005. Remediation and recovery of uranium from contaminated subsurface environments with electrodes. Environmental Science & Technology 39(22), 8943-8947.

Grootscholten, T.I.M., Steinbusch, K.J.J., Hamelers, H.V.M., Buisman, C.J.N., 2013. Chain elongation of acetate and ethanol in an upflow anaerobic filter for high rate MCFA production. Bioresource technology 135, 440-445.

Gui, A.L., Liu, G.Z., Chockalingam, M., Le Saux, G., Luais, E., Harper, J.B., Gooding, J.J., 2010. A Comparative Study of Electrochemical Reduction of 4-Nitrophenyl Covalently Grafted on Gold and Carbon. Electroanalysis 22(16), 1824-1830.

Haznedaroglu, B.Z., Bolster, C.H., Walker, S.L., 2008. The role of starvation on Escherichia coli adhesion and transport in saturated porous media. Water Research 42(6-7), 1547-1554.

He, P., Shi, D.L., Lian, J., Wang, L.M., Ewing, R.C., van Ooij, W., Li, W.Z., Ren, Z.F., 2005. Plasma deposition of thin carbonfluorine films on aligned carbon nanotube. Applied Physics Letters 86(4).

Hoekstra, K.J., Bein, T., 1996. Adsorption of zirconium-phosphonate multilayers onto phosphate-derivatized glassy carbon substrates. Chemistry of Materials 8(8), 1865-1870.

Holmes, D.E., Bond, D.R., Lovley, D.R., 2004. Electron transfer by Desulfobulbus propionicus to Fe(III) and graphite electrodes. Applied and Environmental Microbiology 70(2), 1234-1237.

Huang, L.P., Regan, J.M., Quan, X., 2011. Electron transfer mechanisms, new applications, and performance of biocathode microbial fuel cells. Bioresource technology 102(1), 316-323.

Ieropoulos, I., Melhuish, C., Greenman, J., Horsfield, I., 2005. EcoBot-II: An artificial agent with a natural metabolism. pp. 295-300, 4 ed. Vienna University of Technology.

Jian, W., Firestone, M.A., Auciello, O., Carlisle, J.A., 2004. Surface functionalization of ultrananocrystalline diamond films by electrochemical reduction of aryldiazonium salts. Langmuir 20(26), 11450-11456.

Kariuki, J.K., McDermott, M.T., 2001. Formation of multilayers on glassy carbon electrodes via the reduction of diazonium salts. Langmuir 17(19), 5947-5951.

Katsikogianni, M., Missirlis, Y.F., 2004. Concise review of mechanisms of bacterial adhesion to biomaterials and of techniques used in estimating bacteria-material interactions. European cells & materials 8, 37-57.

Kim, B.H., Ikeda, T., Park, H.S., Kim, H.J., Hyun, M.S., Kano, K., Takagi, K., Tatsumi, H., 1999a. Electrochemical activity of an Fe(III)-reducing bacterium, Shewanella putrefaciens IR-1, in the presence of alternative electron acceptors. Biotechnology Techniques 13(7), 475-478.

Kim, H.J., Hyun, M.S., Chang, I.S., Kim, B.H., 1999b. A microbial fuel cell type lactate biosensor using a metal-reducing bacterium, Shewanella putrefaciens. Journal of Microbiology and Biotechnology 9(3), 365-367.

Lai, B., Tang, X.H., Li, H.R., Du, Z.W., Liu, X.W., Zhang, Q., 2011. Power production enhancement with a polyaniline modified anode in microbial fuel cells. Biosensors and Bioelectronics 28(1), 373-377.

Lamp, J.L., Guest, J.S., Naha, S., Radavich, K.A., Love, N.G., Ellis, M.W., Puri, I.K., 2011. Flame synthesis of carbon nanostructures on stainless steel anodes for use in microbial fuel cells. Journal of Power Sources 196(14), 5829-5834.

Leclere, V., Marti, R., Bechet, M., Fickers, P., Jacques, P., 2006. The lipopeptides mycosubtilin and surfactin enhance spreading of Bacillus subtilis strains by their surface-active properties. Archives of Microbiology 186(6), 475-483.

Leflaive, X., 2012. Water Outlook to 2050: The OECD calls for early and strategic action. OECD. OECD Publishing, Paris.

Lewis, N.S., Nocera, D.G., 2006. Powering the planet: Chemical challenges in solar energy utilization. Proceedings of the National Academy of Sciences 103(43), 15729-15735.

Liu, G.Z., Chockalingham, M., Khor, S.M., Gui, A.L., Gooding, J.J., 2010. A Comparative Study of the Modification of Gold and Glassy Carbon Surfaces with Mixed Layers of In Situ Generated Aryl Diazonium Compounds. Electroanalysis 22(9), 918-926.

Liu, Y., Tay, J.H., 2002. The essential role of hydrodynamic shear force in the formation of biofilm and granular sludge. Water Research 36(7), 1653-1665.

Logan, B.E., 2008. Microbial Fuel Cells. Wiley.

Logan, B.E., 2009. Exoelectrogenic bacteria that power microbial fuel cells. Nature Reviews Microbiology 7(5), 375-381.

Logan, B.E., Hamelers, B., Rozendal, R.A., Schrorder, U., Keller, J., Freguia, S., Aelterman, P., Verstraete, W., Rabaey, K., 2006. Microbial fuel cells: Methodology and technology. Environmental Science & Technology 40(17), 5181-5192.

Lojou, E., Durand, M.C., Dolla, A., Bianco, P., 2002. Hydrogenase activity control at Desulfovibrio vulgaris cell-coated carbon electrodes: Biochemical and chemical factors influencing the mediated bioelectrocatalysis. Electroanalysis 14(13), 913-922.

Lowy, D.A., Jhaveri, S.D., Foos, E.E., Tender, L.M., Ancona, M.G., Snow, A.W., 2006a. Effects of ion-pairing on rate of electron transfer between immobilized gold nanoclusters and soluble redox probes. Electrochemistry Communications 8(12), 1821-1824.

Lowy, D.A., Tender, L.M., 2008. Harvesting energy from the marine sediment-water interface III. Kinetic activity of quinone- and antimony-based anode materials. Journal of Power Sources 185(1), 70-75.

Lowy, D.A., Tender, L.M., Zeikus, J.G., Park, D.H., Lovley, D.R., 2006b. Harvesting energy from the marine sediment-water interface II - Kinetic activity of anode materials. Biosensors and Bioelectronics 21(11), 2058-2063.

Mahouche-Chergui, S., Gam-Derouich, S., Mangeney, C., Chehimi, M.M., 2011. Aryl diazonium salts: a new class of coupling agents for bonding polymers, biomacromolecules and nanoparticles to surfaces. Chemical Society Reviews 40(7), 4143-4166.

Mcallister, E.W., Carey, L.C., Brady, P.G., Heller, R., Kovacs, S.G., 1993. The Role of Polymeric Surface Smoothness of Biliary Stents in Bacterial Adherence, Biofilm Deposition, and Stent Occlusion. Gastrointestinal Endoscopy 39(3), 422-425.

Moon, J.S., Alegaonkar, P.S., Han, J.H., Lee, T.Y., Yoo, J.B., Kim, J.M., 2006. Enhanced field emission properties of thin-multiwalled carbon nanotubes: Role of SiOx coating. Journal of Applied Physics 100(10).

Mu, Y., Rabaey, K., Rozendal, R.A., Yuan, Z.G., Keller, J., 2009a. Decolorization of Azo Dyes in Bioelectrochemical Systems. Environmental Science & Technology 43(13), 5137-5143.

Mu, Y., Rozendal, R.A., Rabaey, K., Keller, J., 2009b. Nitrobenzene Removal in Bioelectrochemical Systems. Environmental Science & Technology 43(22), 8690-8695.

Nambiar, S., Togo, C.A., Limson, J.L., 2009. Application of multi-walled carbon nanotubes to enhance anodic performance of an Enterobacter cloacae-based fuel cell. African Journal of Biotechnology 8(24), 6927-6932.

Nevin, K.P., Hensley, S.A., Franks, A.E., Summers, Z.M., Ou, J.H., Woodard, T.L., Snoeyenbos-West, O.L., Lovley, D.R., 2011. Electrosynthesis of Organic Compounds from Carbon Dioxide Is Catalyzed by a Diversity of Acetogenic Microorganisms. Applied and Environmental Microbiology 77(9), 2882-2886.

Nevin, K.P., Richter, H., Covalla, S.F., Johnson, J.P., Woodard, T.L., Orloff, A.L., Jia, H., Zhang, M., Lovley, D.R., 2008. Power output and columbic efficiencies from biofilms of Geobacter

sulfurreducens comparable to mixed community microbial fuel cells. Environmental Microbiology 10(10), 2505-2514.

Nevin, K.P., Woodard, T.L., Franks, A.E., Summers, Z.M., Lovley, D.R., 2010. Microbial electrosynthesis: feeding microbes electricity to convert carbon dioxide and water to multicarbon extracellular organic compounds. Mbio 1(2), 1-4.

Nguyen, T.A., Lu, Y.Z., Yang, X.H., Shi, X.M., 2007. Carbon and steel surfaces modified by Leptothrix discophora SP-6: Characterization and implications. Environmental Science & Technology 41(23), 7987-7996.

Park, D.H., Kim, S.K., Shin, I.H., Jeong, Y.J., 2000. Electricity production in biofuel cell using modified graphite electrode with Neutral Red. Biotechnology Letters 22(16), 1301-1304.

Park, D.H., Laivenieks, M., Guettler, M.V., Jain, M.K., Zeikus, J.G., 1999. Microbial utilization of electrically reduced neutral red as the sole electron donor for growth and metabolite production. Applied and Environmental Microbiology 65(7), 2912-2917.

Park, D.H., Zeikus, J.G., 2000. Electricity generation in microbial fuel cells using neutral red as an electronophore. Applied and Environmental Microbiology 66(4), 1292-1297.

Park, D.H., Zeikus, J.G., 2003. Improved fuel cell and electrode designs for producing electricity from microbial degradation. Biotechnology and Bioengineering 81(3), 348-355.

Pham, C.A., Jung, S.J., Phung, N.T., Lee, J., Chang, I.S., Kim, B.H., Yi, H., Chun, J., 2003. A novel electrochemically active and Fe(III)-reducing bacterium phylogenetically related to Aeromonas hydrophila, isolated from a microbial fuel cell. Fems Microbiology Letters 223(1), 129-134.

Picot, M., Lapinsonniere, L., Rothballer, M., Barriere, F., 2011. Graphite anode surface modification with controlled reduction of specific aryl diazonium salts for improved microbial fuel cells power output. Biosensors and Bioelectronics 28(1), 181-188.

Pinson, J., Podvorica, F., 2005. Attachment of organic layers to conductive or semiconductive surfaces by reduction of diazonium salts. Chemical Society Reviews 34(5), 429-439.

Ploux, L., Ponche, A., Anselme, K., 2010. Bacteria/Material Interfaces: Role of the Material and Cell Wall Properties. Journal of Adhesion Science and Technology 24(13-14), 2165-2201.

Popov, A.L., Kim, J.R., Dinsdale, R.M., Esteves, S.R., Guwy, A.J., Premier, G.C., 2012. The effect of physico-chemically immobilized methylene blue and neutral red on the anode of microbial fuel cell. Biotechnology and Bioprocess Engineering 17(2), 361-370.

Powell, E.E., Mapiour, M.L., Evitts, R.W., Hill, G.A., 2009. Growth kinetics of Chlorella vulgaris and its use as a cathodic half cell. Bioresource technology 100(1), 269-274.

Prasad, D., Arun, S., Murugesan, A., Padmanaban, S., Satyanarayanan, R.S., Berchmans, S., Yegnaraman, V., 2007. Direct electron transfer with yeast cells and construction of a mediatorless microbial fuel cell. Biosensors and Bioelectronics 22(11), 2604-2610.

Qiao, Y., Li, C.M., Bao, S.J., Bao, Q.L., 2007. Carbon nanotube/polyaniline composite as anode material for microbial fuel cells. Journal of Power Sources 170(1), 79-84.

Rabaey, K., Boon, N., Siciliano, S.D., Verhaege, M., Verstraete, W., 2004. Biofuel cells select for microbial consortia that self-mediate electron transfer. Applied and Environmental Microbiology 70(9), 5373-5382.

Rabaey, K., Butzer, S., Brown, S., Keller, J., Rozendal, R.A., 2010. High Current Generation Coupled to Caustic Production Using a Lamellar Bioelectrochemical System. Environmental Science & Technology 44(11), 4315-4321.

Rabaey, K., Read, S.T., Clauwaert, P., Freguia, S., Bond, P.L., Blackall, L.L., Keller, J., 2008. Cathodic oxygen reduction catalyzed by bacteria in microbial fuel cells. The ISME Journal 2(5), 519-527.

Rabaey, K., Rodriguez, J., Blackall, L.L., Keller, J., Gross, P., Batstone, D., Verstraete, W., Nealson, K.H., 2007. Microbial ecology meets electrochemistry: electricity-driven and driving communities. The ISME Journal 1(1), 9-18.

Rabaey, K., Rozendal, R.A., 2010. Microbial electrosynthesis - revisiting the electrical route for microbial production. Nature Reviews Microbiology 8(10), 706-716.

Ringeisen, B.R., Biffinger, J.C., Pietron, J., Ray, R., Little, B., 2007. A biofilm enhanced miniature microbial fuel cell using Shewanella oneidensis DSP10 and oxygen reduction cathodes. Biosensors and Bioelectronics 22(8), 1672-1679.

Roberts, J.A., 2004. Inhibition and enhancement of microbial surface colonization: the role of silicate composition. Chemical Geology 212(3-4), 313-327.

Rozendal, R.A., Hamelers, H.V.M., Euverink, G.J.W., Metz, S.J., Buisman, C.J.N., 2006. Principle and perspectives of hydrogen production through biocatalyzed electrolysis. International Journal of Hydrogen Energy 31(12), 1632-1640.

Rozendal, R.A., Hamelers, H.V.M., Rabaey, K., Keller, J., Buisman, C.J.N., 2008. Towards practical implementation of bioelectrochemical wastewater treatment. Trends in Biotechnology 26(8), 450-459.

Rozendal, R.A., Leone, E., Keller, J., Rabaey, K., 2009. Efficient hydrogen peroxide generation from organic matter in a bioelectrochemical system. Electrochemistry Communications 11(9), 1752-1755.

Saito, T., Mehanna, M., Wang, X., Cusick, R.D., Feng, Y.J., Hickner, M.A., Logan, B.E., 2011. Effect of nitrogen addition on the performance of microbial fuel cell anodes. Bioresource technology 102(1), 395-398.

Sakakura, T., Choi, J.C., Yasuda, H., 2007. Transformation of carbon dioxide. Chemical Reviews 107(6), 2365-2387.

Schroder, U., 2007. Anodic electron transfer mechanisms in microbial fuel cells and their energy efficiency. Physical Chemistry Chemical Physics 9(21), 2619-2629.

Scott, K., Rimbu, G.A., Katuri, K.P., Prasad, K.K., Head, I.M., 2007. Application of modified carbon anodes in microbial fuel cells. Process Safety and Environmental Protection 85(B5), 481-488.

Shantaram, A., Beyenal, H., Raajan, R., Veluchamy, A., Lewandowski, Z., 2005. Wireless sensors powered by microbial fuel cells. Environmental Science & Technology 39(13), 5037-5042.

Sharma, T., Reddy, A.L.M., Chandra, T.S., Ramaprabhu, S., 2008. Development of carbon nanotubes and nanofluids based microbial fuel cell. International Journal of Hydrogen Energy 33(22), 6749-6754.

Shen, W.Z., Li, Z.J., Liu, Y.H., 2008. Surface chemical functional groups modification of porous carbon. Recent Patents on Chemical Engineering 1, 27-40.

Star, A., Joshi, V., Skarupo, S., Thomas, D., Gabriel, J.C.P., 2006. Gas sensor array based on metal-decorated carbon nanotubes. Journal of Physical Chemistry B 110(42), 21014-21020.

Steinbusch, K.J.J., Hamelers, H.V.M., Schaap, J.D., Kampman, C., Buisman, C.J.N., 2010. Bioelectrochemical Ethanol Production through Mediated Acetate Reduction by Mixed Cultures. Environmental Science & Technology 44(1), 513-517.

Strycharz, S.M., Gannon, S.M., Boles, A.R., Franks, A.E., Nevin, K.P., Lovley, D.R., 2010. Reductive dechlorination of 2-chlorophenol by Anaeromyxobacter dehalogenans with an electrode serving as the electron donor. Environmental Microbiology Reports 2(2), 289-294.

Strycharz, S.M., Woodard, T.L., Johnson, J.P., Nevin, K.P., Sanford, R.A., Loffler, F.E., Lovley, D.R., 2008. Graphite electrode as a sole electron donor for reductive dechlorination of tetrachlorethene by Geobacter lovleyi. Applied and Environmental Microbiology 74(19), 5943-5947.

Sun, J.J., Zhao, H.Z., Yang, Q.Z., Song, J., Xue, A., 2010. A novel layer-by-layer self-assembled carbon nanotube-based anode: Preparation, characterization, and application in microbial fuel cell. Electrochimica Acta 55(9), 3041-3047.

Tanaka, H., Aramata, A., 1997. Aminopyridyl cation radical method for bridging between metal complex and glassy carbon: cobalt(II) tetraphenylporphyrin bonded on glassy carbon for enhancement of CO2 electroreduction. Journal of Electroanalytical Chemistry 437(1-2), 29-35.

Tang, X.H., Guo, K., Li, H.R., Du, Z.W., Tian, J.L., 2011. Electrochemical treatment of graphite to enhance electron transfer from bacteria to electrodes. Bioresource technology 102(3), 3558-3560.

Taricska, J., Long, D., Chen, J.P., Hung, Y.-T., Zou, S.-W., 2007. Anaerobic Digestion. In: Wang, L., Shammas, N., Hung, Y.-T. (Eds.), Biosolids Treatment Processes, pp. 135-176. Humana Press.

Tender, L.M., Gray, S.A., Groveman, E., Lowy, D.A., Kauffman, P., Melhado, J., Tyce, R.C., Flynn, D., Petrecca, R., Dobarro, J., 2008. The first demonstration of a microbial fuel cell as a viable power supply: Powering a meteorological buoy. Journal of Power Sources 179(2), 571-575.

Ter Heijne, A., Hamelers, H.V.M., De Wilde, V., Rozendal, R.A., Buisman, C.J.N., 2006. A bipolar membrane combined with ferric iron reduction as an efficient cathode system in microbial fuel cells. Environmental Science & Technology 40(17), 5200-5205.

Terada, A., Yuasa, A., Tsuneda, S., Hirata, A., Katakai, A., Tamada, M., 2005. Elucidation of dominant effect on initial bacterial adhesion onto polymer surfaces prepared by radiation-induced graft polymerization. Colloid Surface B 43(2), 99-107.

Thrash, J.C., Van Trump, J.I., Weber, K.A., Miller, E., Achenbach, L.A., Coates, J.D., 2007. Electrochemical stimulation of microbial perchlorate reduction. Environmental Science & Technology 41(5), 1740-1746.

Tsai, H.Y., Wu, C.C., Lee, C.Y., Shih, E.P., 2009. Microbial fuel cell performance of multiwall carbon nanotubes on carbon cloth as electrodes. Journal of Power Sources 194(1), 199-205.

Virdis, B., Rabaey, K., Yuan, Z., Keller, J., 2008. Microbial fuel cells for simultaneous carbon and nitrogen removal. Water Research 42(12), 3013-3024.

von Sperling, M., 2007. Activated Sludge and Aerobic Biofilm Reactors. IWA Publishing.

Walker, S.L., 2005. The role of nutrient presence on the adhesion kinetics of Burkholderia cepacia G4g and ENV435g. Colloid Surface B 45(3-4), 181-188.

Wang, K.P., Liu, Y.W., Chen, S.L., 2011. Improved microbial electrocatalysis with neutral red immobilized electrode. Journal of Power Sources 196(1), 164-168.

Wang, P., Li, H.R., Du, Z.W., 2013. Deposition of Iron on Graphite Felts by Thermal Decomposition of Fe(CO)(5) for Anodic Modification of Microbial Fuel Cells. International Journal of Electrochemical Science 8(4), 4712-4722.

Wang, X., Cheng, S.A., Feng, Y.J., Merrill, M.D., Saito, T., Logan, B.E., 2009. Use of Carbon Mesh Anodes and the Effect of Different Pretreatment Methods on Power Production in Microbial Fuel Cells. Environmental Science & Technology 43(17), 6870-6874.

Whitehead, K.A., Verran, J., 2006. The effect of surface topography on the retention of microorganisms. Food and Bioproducts Processing 84(C4), 253-259.

Wrighton, K.C., Agbo, P., Warnecke, F., Weber, K.A., Brodie, E.L., DeSantis, T.Z., Hugenholtz, P., Andersen, G.L., Coates, J.D., 2008. A novel ecological role of the Firmicutes identified in thermophilic microbial fuel cells. The ISME Journal 2(11), 1146-1156.

Xing, D.F., Zuo, Y., Cheng, S.A., Regan, J.M., Logan, B.E., 2008. Electricity generation by Rhodopseudomonas palustris DX-1. Environmental Science & Technology 42(11), 4146-4151.

Yan, Z., Zhang, J.R., Fang, H.Q., 1999. Electrocatalytic oxidation of uric acid at cysteine modified glassy carbon electrode. Analytical Letters 32(2), 223-234.

Ye, Z., Hou, J., Ellis, M.W., 2012. Dependence of Electrochemical Performance On Anode Surface Roughness in Microbial Fuel Cells. 2012 Annual Meeting of AIChE, Pittsburgh, PA.

Yuan, Y., Kim, S., 2008. Polypyrrole-coated reticulated vitreous carbon as anode in microbial fuel cell for higher energy output. Bulletin of the Korean Chemical Society 29(1), 168-172.

Zhang, L.X., Zhou, S.G., Zhuang, L., Li, W.S., Zhang, J.T., Lu, N., Deng, L.F., 2008. Microbial fuel cell based on Klebsiella pneumoniae biofilm. Electrochemistry Communications 10(10), 1641-1643.

Zhang, T., Cui, C.Z., Chen, S.L., Ai, X.P., Yang, H.X., Ping, S., Peng, Z.R., 2006. A novel mediatorless microbial fuel cell based on direct biocatalysis of Escherichia coli. Chemical Communications (21), 2257-2259.

Zhang, T., Nie, H.R., Bain, T.S., Lu, H.Y., Cui, M.M., Snoeyenbos-West, O.L., Franks, A.E., Nevin, K.P., Russell, T.P., Lovley, D.R., 2013. Improved cathode materials for microbial electrosynthesis. Energy & Environmental Science 6(1), 217-224.

Zhang, X., Xia, X., Ivanov, I., Huang, X., Logan, B.E., 2014. Enhanced activated carbon cathode performance for microbial fuel cell by blending carbon black. Environmental Science & Technology 48(3), 2075-2081.

Zhang, Y., Franklin, N.W., Chen, R.J., Dai, H.J., 2000. Metal coating on suspended carbon nanotubes and its implication to metal-tube interaction. Chemical Physics Letters 331(1), 35-41.

Zhao, F., Rahunen, N., Varcoe, J.R., Chandra, A., Avignone-Rossa, C., Thumser, A.E., Slade, R.C.T., 2008. Activated carbon cloth as anode for sulfate removal in a microbial fuel cell. Environmental Science & Technology 42(13), 4971-4976.

Zhou, M., Chen, J., Freguia, S., Rabaey, K., Keller, J., 2013. Carbon and electron fluxes during the electricity driven 1,3-propanediol biosynthesis from glycerol. Environmental Science & Technology 47(19), 11199-11205.

Zhou, M.H., Chi, M.L., Luo, J.M., He, H.H., Jin, T., 2011. An overview of electrode materials in microbial fuel cells. Journal of Power Sources 196(10), 4427-4435.

Zhu, N.W., Chen, X., Zhang, T., Wu, P.X., Li, P., Wu, J.H., 2011. Improved performance of membrane free single-chamber air-cathode microbial fuel cells with nitric acid and ethylenediamine surface modified activated carbon fiber felt anodes. Bioresource technology 102(1), 422-426.

Zou, Y.J., Xiang, C.L., Yang, L.N., Sun, L.X., Xu, F., Cao, Z., 2008. A mediatorless microbial fuel cell using polypyrrole coated carbon nanotubes composite as anode material. International Journal of Hydrogen Energy 33(18), 4856-4862.

Zuo, Y., Xing, D.F., Regan, J.M., Logan, B.E., 2008. Isolation of the exoelectrogenic bacterium Ochrobactrum anthropi YZ-1 by using a U-tube microbial fuel cell. Applied and Environmental Microbiology 74(10), 3130-3137.

Appendix A

The effects of surface charge and hydrophobicity on anodic biofilm formation, community composition and current generation in bioelectrochemical systems

Kun Guo[a,b,c], Stefano Freguia[b], Paul G. Dennis[b,d], Xin Chen[e], Bogdan C. Donose[b], Jurg Keller[b], J. Justin Gooding[e], Korneel Rabaey[a,b,c*]

[a]Centre for Microbial Electrosynthesis, The University of Queensland, Brisbane, QLD 4072, Australia; [b]Advanced Water Management Centre, The University of Queensland, Brisbane, QLD 4072, Australia; [c]Laboratory of Microbial Ecology and Technology, Ghent University, Coupure Links 653, B-9000 Ghent, Belgium; [d]Australian Centre for Ecogenomics, School of Chemistry and Molecular Biosciences, The University of Queensland, Brisbane, Queensland 4072, Australia; [e]School of Chemistry, University of New South Wales, Sydney, NSW 2052, Australia.

Environmental Science & Technology. 2013, 47: 7563-7570.

GRAPHIC ABSTRACT

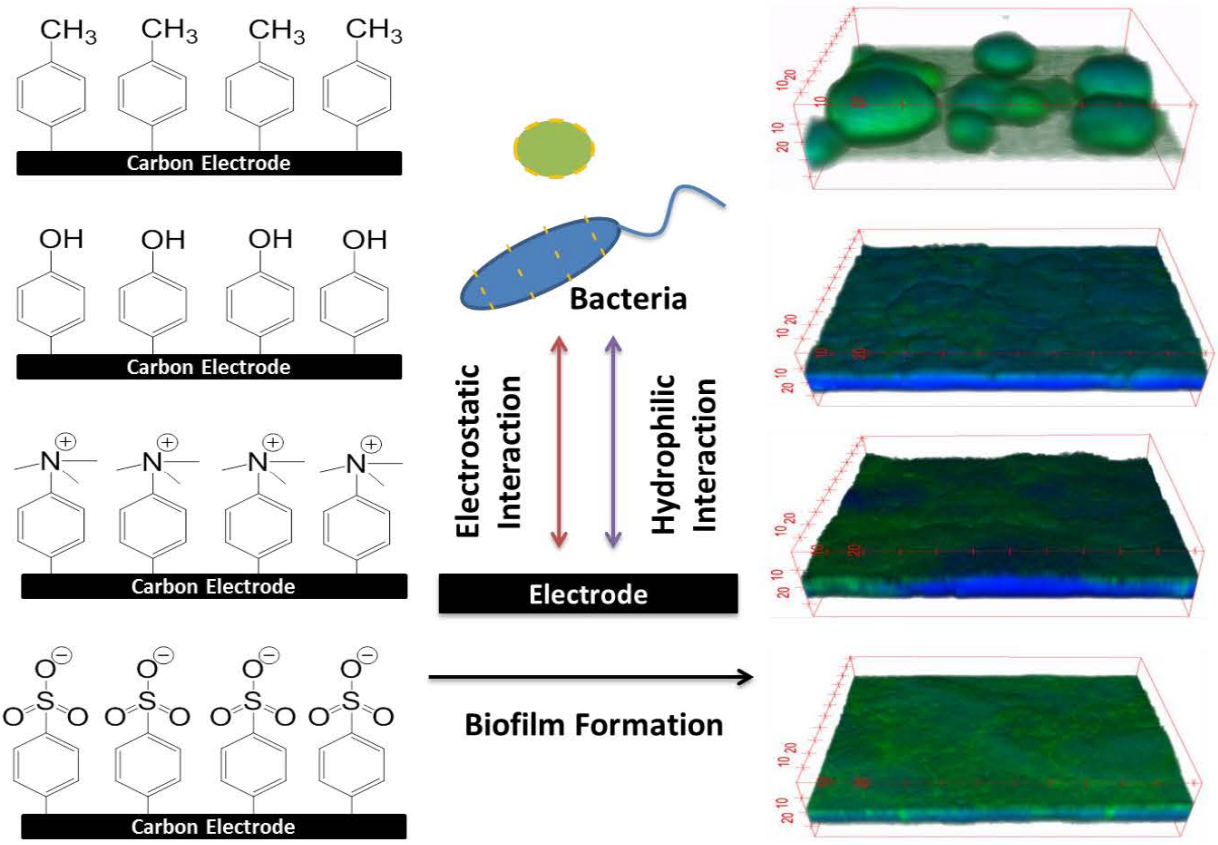

ABSTRACT

The focus of this study was to investigate the effects of surface charge and surface hydrophobicity on anodic biofilm formation, biofilm community composition, and current generation in bioelectrochemical systems (BESs). Glassy carbon surfaces were modified with –OH, $–CH_3$, $–SO_3^-$, or $–N^+(CH_3)_3$ functional groups by electrochemical reduction of aryl diazonium salts and then used as anodes with poised potential of -0.2 V (vs. Ag/AgCl). The average startup times and final current densities for the $–N^+(CH_3)_3$, –OH, $–SO_3^-$, and $–CH_3$, electrodes were (23 d, 0.204 mA/cm^2), (25.4 d, 0.149 mA/cm^2), (25.9 d, 0.114 mA/cm^2), and (37.2 d, 0.048 mA/cm^2), respectively. Biofilms on different surfaces were analyzed by non-turnover cyclic voltammetry (CV), fluorescence in situ hybridization (FISH), and 16S rRNA gene amplicon pyrosequencing. The results demonstrated that: 1) differences in the maximum current output between surface modifications was correlated with biomass quantity, and 2) all biofilms were dominated by *Geobacter* populations, but the composition of $–CH_3$-associated biofilms differed from those formed on surfaces with different chemical modification. This study shows that anode surface charge and hydrophobicity influences biofilm development and can lead to significant differences in BESs performance. Positively charged and hydrophilic surfaces were more selective to electroactive microbes (*e.g. Geobacter*) and more conducive for electroactive biofilm formation.

KEYWORDS

surface charge, surface hydrophobicity, biofilm formation, current generation, microbial fuel cells, bioelectrochemical systems

INTRODUCTION

Bioelectrochemical systems (BESs) are devices that use microbes as catalysts to drive oxidation and/or reduction reactions at electrodes. Applications for this promising technology include wastewater treatment, power production, bioremediation, and the production of valuable chemicals.[1] In the past decade, rapid progress has been made in BESs in terms of increasing current densities, cataloguing electroactive bacteria, improving understanding of the mechanisms of extracellular electron transfer (EET), producing desirable electrode materials, identifying efficient reactor configurations, and developing novel processes.[3-5] Attempts to scale-up BESs, however, indicate that practical application of this technology is limited by low current and power densities.[6-7]

Anodic electrode surface modification, such as acid soaking,[8] high temperature ammonia treatment,[9] heat treatment,[10] conductive polymer coating,[11] electrochemical oxidation,[12] carbon nanotube coating,[13] mediator grafting,[14] and surface functionalization by reduction of aryl diazonium salts[15] have been successful in increasing the current densities of BESs. These successes have been attributed to one or a combination of the following factors: 1) increased surface area, 2) improved electrode biocompatibility, and 3) facilitated electron transfer between electrode and bacteria.

Among those surface modification methods, reduction of aryl diazonium salts is among the most controlled methods to covalently graft various of functional groups to a carbon surface thereby finely modifying the surface's chemical properties.[16, 17] In the field of BESs, $–N(CH_3)_2$, $–NH_2$, $–CH_2COO^–$, $–CH_2PPh_3^+$, and $–B(OH)_2$ have been grafted to carbon surface using this method. Satio *et al.*[18] demonstrated that a small amount of nitrogen ($–N(CH_3)_2$) functionalization on carbon cloth was sufficient to enhance BES performance. Picot *et al.*[15] reported that, at lower degree at lower degree of surface modification, $–N(CH_3)_2$, $–NH_2$, and $–CH_2PPh_3^+$ modification increased the current output, $–CH_2COO^–$ decreased the current output. Lapinsonnière *et al.*[19] found that $–B(OH)_2$ modified electrodes promote biofilm adhesion and increase current output of BESs.

Whereas several studies have thus focused on increasing BES current outputs via surface modifications, the effect of surface chemistry (e.g. surface charge and surface hydrophobicity) on biofilm formation and diversity remains poorly understood. Therefore, in this study, we used electrochemical modification of aryl diazonium salts to graft $–N^+(CH_3)_3$, $–SO_3^-$, –OH, and $–CH_3$ functional groups to glassy carbon (GC) electrode surfaces, thereby, changing their surface charge and hydrophobicity. The modified GC surfaces were then used as anodes in acetate-fed BESs. The

effects of surface charge and hydrophobicity on anodic biofilm formation, community composition as well as current generation were systematically investigated by comparing the four modified electrodes.

MATERIALS AND METHODS

Electrode Preparation and Modification.

Glassy carbon (GC) plates (50 mm × 20 mm × 2 mm) (HTW, Germany) were used as anodes. Copper wires were glued on the backside of the plates by silver paint to make the external connection. Then the back and side of the plates were insulated by water proof epoxy glue, leaving an exposed (effective) surface area of 10 cm^2. The GC electrode surfaces were cleaned by polishing successively with 1.0, 0.3, and 0.05 μm Buehler alumina slurries for 3 min at each grade on a microcloth pad (Buehler, USA). After each polishing step, the electrodes were thoroughly rinsed with Milli-Q water, and then sonicated in Milli-Q water for 5 min.[20] Before modification, the electrodes were dried with nitrogen gas stream.

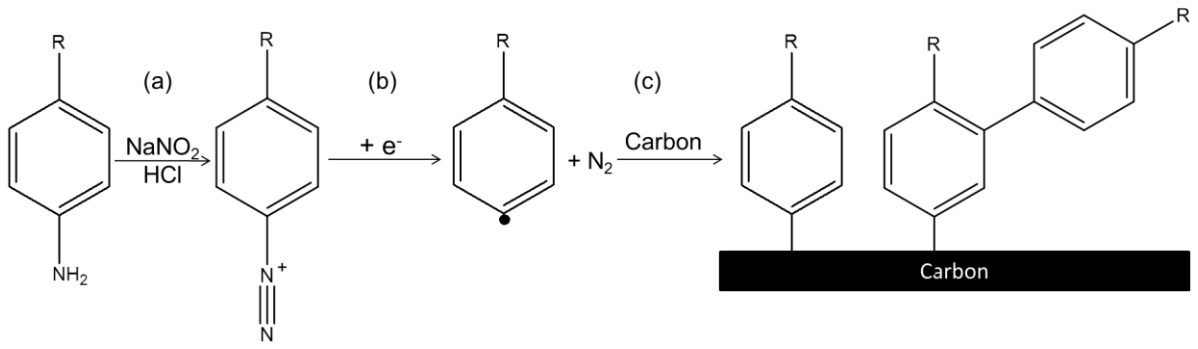

Figure 1. Procedure for electrochemical reduction of aryl diazonium salts: a) in situ generation of diazonium salts, b) electrochemical reduction of aryl diazonium salts and c) C–C bond formation. Candidate R groups: $–CH_3$, –OH, $–SO_3^-$, $–N^+(CH_3)_3$.

Functional groups were attached to the GC electrodes via electrochemical reduction of in-situ generated aryl diazonium salts (Fig. 1). Specifically, 1 mM of p-aniline derivatives with different functional groups (i.e. $–CH_3$, –OH, $–SO_3H$, $–N(CH_3)_3I$) were solubilized in 0.5 M HCl, to which 1 mM of $NaNO_2$ was added to generate the aryl diazonium salts. The mixture was sparged with high purity nitrogen gas for 30 min to remove the dissolved oxygen. Then, electrochemical reduction of the diazonium salts was carried out by chronocoulometry at a potential of -0.6 V (v.s Ag/AgCl) using a potentiostat (VMP3, Bio-Logic, USA). The reduction was stopped when a coulombic charge density of 0.1 mC/cm^2 was reached. This coating density was chosen based on the result that

at this coating density the surface electron transfer ability (measured by Ferricyanide cyclic voltammetry) was not significantly inhibited. After modification, the electrodes were thoroughly rinsed with Milli-Q water and then sonicated in Milli-Q water for 3 min.

Electrode Surface Characterization.

To check whether those functional groups were properly grafted, the electrode surfaces were analyzed by the following techniques:

(1) X-ray Photoelectron Spectroscopy (XPS):

XPS was used to determine the elemental composition of the electrode surfaces and was performed as described in Chen, *et al.*[21] Briefly, XPS spectra of non-modified and modified GC surfaces were collected using an EscaLab 250Xi spectrometer with a monochromated Al Kα source (1486.6 eV), hemispherical analyzer, and multichannel detector. The spectra were accumulated at a take-off angle of 90^{o} with a 0.79 mm^2 spot size at a pressure of less than 10-8 mbar. The pass energy for the survey scan is 100 eV and for the narrow scan 20 eV. Spectra were calibrated on the C1s peak (285.0 eV) and analyzed using the Avantage 4.54 software.

(2) Contact Angle Goniometry:

As a measure of surface hydrophobicity, contact angles with Milli-Q water were measured with sessile drop method using Rame-Hart 100-00 goniometer. Three different spots per substrate on three different substrates were measured to provide an average contact angle.

(3) Ferricyanide cyclic voltammetry:

The electron transfer ability of these four different modified surfaces was investigated by cyclic voltammetry (CV) using $K_3[Fe(CN)_6]$ as a redox probe. CV was performed by a VMP3 potentiostat in 0.1 mM $K_3[Fe(CN)_6]$ with 0.2 M KCl in MilliQ water, at 50 mV/s.

BES cell setup and operation.

Photos of each reactor component are provided in the supplementary information (Fig. S1). The BES cell was fabricated from a cylindrical container of 95 cm diameter and 100 cm height (700 mL). The reactor is a membrane-free BES cell (700 mL) with one common reference electrode, one common counter electrode and four working electrodes. A Ag/AgCl reference electrode (MF-2052, Bioanalytical Systems, USA) was placed in the center. Four working electrodes were arranged in a

circle with the electroactive side facing the reference electrode, and a titanium mesh surrounding the working electrodes was used as the counter electrode. The working electrodes and counter electrode were separated by a circular plastic mesh. Two same reactors were run in replicate. The electrodes were connected to a CHI 1000B Multi-Potentiostat (CH Instruments, Austin, TX, USA), which controlled the potential of each working electrode and recorded the current generated.

The reactor was filled with 400 mL of modified M9 medium with sodium acetate as the electron donor (6 g/ L Na_2HPO_4, 3 g/L KH_2PO_4, 0.5 g/L NH_4Cl, 0.5 g/L NaCl, 0.1 g/ L $MgSO_4 \cdot 7H_2O$, 14.6 mg/ L $CaCl_2$, 2 g/L CH_3COONa, and 1 mL/L of a mixed trace element solution[22]), sparged with high purity nitrogen gas for 30 min, and then inoculated with 200 mL fresh anodic effluent of an existing acetate-fed BE reactor in the lab which was originally started up with the effluent of the reactor reported by Dennis, *et al.* [23] and has been continuously running for more than one year. The potential of each anode was maintained at -0.2 V vs. Ag/AgCl (3.5 M KCl) and current generation was recorded using the potentiostat. From day three, the reactor was continuously fed media at a flow rate of 30 mL/h. A magnetic stirrer was used to mix the solution in the BES cell at a speed of 150 rpm. The experiments were performed in the dark at room temperature (20-25ºC).

Biofilm Characterization.

The current generation experiments were stopped on day 53, then the electrochemical activity of the biofilms was analyzed by non-turnover cyclic voltammetry (CV). After that, the reactors were opened. Half of the biofilm on each electrode was sampled by scraping the electrode surface with a sterile microscope slide for 16S rRNA gene amplicon pyrosequencing to characterize biofilm community composition, and the remaining half of the sample was subjected to fluorescence in situ hybridisation (FISH) for morphological characterization of the biofilm.

(1) Biofilm non-turnover CV:

Non-turnover CV was performed as follows: 1) the BES cell was drained and then filled with acetate (electron donor)-free medium, 2) biofilms were then starved for two days to deplete acetate that was absorbed into biofilm surfaces or stored within bacterial cells, 3) CVs were then performed within a potential window between -0.8 V and 0 V (vs. Ag/AgCl) at a scan rate of 1 mV/s. This information provided insight into the extracellular electron transfer mechanism of the biofilm.

(2) Fluorescence in situ hybridization (FISH):

Biofilm samples were subjected to FISH as previously described.[24] Eubacteria were targeted using EUB338-mix with FITC and *Geobacter* populations were targeted using Geo1A with Cy5. Labeled cells were visualized and z-stacks were captured using a Zeiss LSM 510 confocal laser scanning microscope. The maximum biofilm thickness, biofilm surface coverage, and suface *Geobacter* abundance were measured and analyzed using the ImageJ software (1.46r). The 3D biofilm images were reconstructed by the 3D viewer plugin of ImageJ. The amount of biomass was calculated based on the maximum biofilm thickness and biofilm surface coverage.

(3) 16S rRNA gene amplicon pyrosequencing and analysis:

DNA extraction, PCR amplification, sequencing, and data analysis were performed as described in Dennis *et al.* [23] Briefly, DNA was extracted using a MO BIO PowerBiofilm™ DNA Isolation Kit, and then universal 16S rRNA genes were amplified by PCR using primers 926F and 1392Rmodified on the 5' end to contain the 454 FLX Titanium Lib L adapters B and A, respectively.[25] The reverse primers also contained a sample-specific 5-6 base barcode sequence positioned between the primer sequence and the adapter. Sequencing was performed at the Australian Centre for Ecogenomics (The University of Queensland) on a 454 GS-FLX using the Titanium XLR70 kit (Roche). Sequences were quality filtered and dereplicated using the QIIME script split_libraries.py with the homopolymer filter deactivated,[26] checked for chimeras against the GreenGenes database using uchime ver. 3.0.617[27] and denoised using Acacia[28]. Sequences were then clustered at 97% similarity, representatives for each cluster were selected and assigned GreenGenes taxonomy using BLAST, and finally, tables with the abundance of different OTUs in each sample were generated. These steps are described by Cayford[29]and were performed using QIIME. Community composition was visualized using a heatmap and the effect of surface modification on the composition of microbial communities was assessed using Redundancy analysis (RDA) with subsequent Monte-Carlo permutation tests (999 permutations). Differences were investigated using Hellinger-transformed OTU abundances.[30] Generalized linear modeling (GLM) was used to determine whether variation in the maximum current output between samples could be attributed to community composition (primary axis sites scores from a principal component analysis of the community profiles) and/or biomass. All analyses were implemented using R 2.12.0 (R Development Core Team).

RESULTS

Electrode Surface Modification and Characterization.

XPS and water contact measurements indicated that all of the functional groups were successfully grafted onto the GC surfaces (Table 1). For example: 1) the percentage of nitrogen atoms increased 2.8 times from 1.89% on non-modified surfaces to 5.34% on $–N^+(CH_3)_3$ functionalized surfaces, 2) the obvious sulfur signal (4.54%) was observed on $–SO_3^-$ functionalized surfaces compared with the non-signaled unmodified surfaces, 3) $–CH_3$ functionalized surfaces were more hydrophobic than non-modified surfaces and its surface carbon ratios were about 7% higher than the non-modified, and 4) –OH functionalized surfaces were more hydrophilic than non-modified surfaces. Furthermore, the $–SO_3^-$ and $–N^+(CH_3)_3$ functionalized surfaces were more hydrophilic than the $–CH_3$ and –OH functionalized surfaces and their water contact angles were similar.

Table 1. The elemental composition and hydrophobicity of modified and non-modified electrode surfaces.

Surface	Elemental composition (%)					Water contact angle (º) (mean ± AD)
	C	N	O	S	I	
Non-modified	82.80	1.89	15.31	-	-	59.9 ± 2.6
-Ar–CH_3	89.51	1.94	8.54	-	-	80.2 ± 0.4
-Ar–OH	82.28	1.92	15.57	-	-	52.9 ± 1.1
-Ar–SO_3^-	80.63	1.67	13.17	4.54	-	10.0 ± 0.8
-Ar–$N^+(CH_3)_3$	88.36	5.34	5.82	-	0.49	15.0 ± 1.1

Cyclic voltammetry also indicated that the electrochemical properties of modified electrodes differed from those of non-modified electrodes (Fig. 2). Using negatively charged ferricyanide as a redox probe, an obvious peak increase was observed on $–N^+(CH_3)_3$ functionalized surfaces compared with that on non-modified surfaces because of electrostatic attraction, which means the positively charged $–N^+(CH_3)_3$ was attached to the surface. The opposite phenomenon was observed on $–SO_3^-$ functionalized surfaces, likely due to the negatively charged $–SO_3^-$ and electrostatic repulsion. The $–CH_3$ functionalized surface displayed a peak pair with broad separation (~250 mV), indicating a reduced electron transfer rate on this surface. The lower peak heights may be caused by

the hampered kinetics and possibly by the repulsive force that the hydrophobic surface exerts on ionic species such as ferricyanide. According to surface elemental composition and surface hydrophobicity investigation, the –OH terminated surface is similar to the non-modified surface, so its CV response is also similar to the non-modified surface. In summary, our results indicate that all the functional groups were successfully grafted to the electrode surfaces.

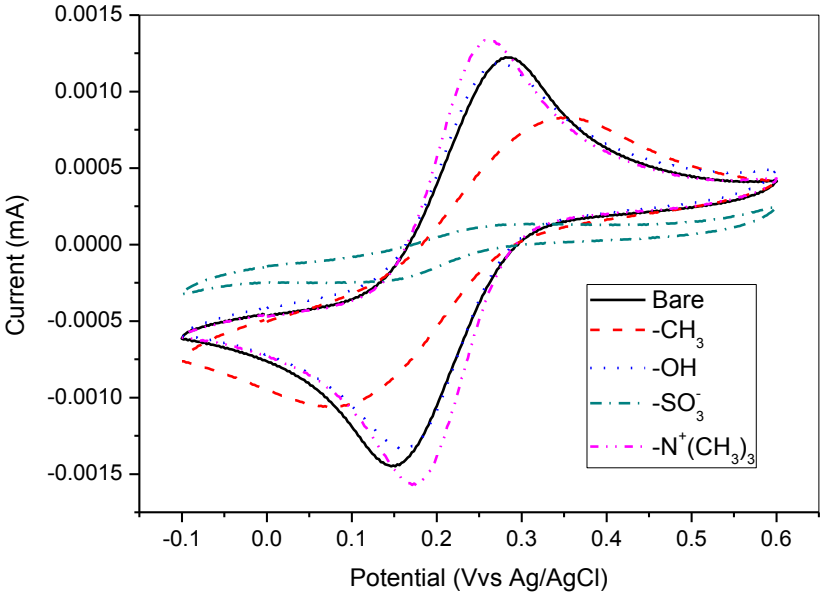

Figure 2. Cyclic voltammograms (50 mV/s) of bare and modified GC surfaces in 0.1 mM $K_3[Fe(CN)_6]$ and 0.2 M KCl solution. (CVs obtained in the second cycle)

Current generation.

In this study, the startup time of current ($t_{startup}$) and time needed to reach a stable current (t_{stable}) were defined as the time taken to the point when current exceeded 0.01 mA/cm^2 (the yellow line in the new Figure 3) and when current stopped logarithmic increase, respectively. The $t_{startup}$ and t_{stable} of the three hydrophilic surfaces ($–N^+(CH_3)_3$, $–SO_3^-$, and –OH) were around 25 days and within 38 days, while the $t_{startup}$ for hydrophobic surfaces ($–CH_3$) was longer than 34 days and they had not reached stable phase by the end of the experiment (day 53). The best performance in terms of both $t_{startup}$ and average current density at the stable stage (J_{stable}) were the $–N^+(CH_3)_3$ functionalized electrodes. The $t_{startup}$ of $–SO_3^-$ and –OH terminated surfaces were comparable to each other, but the J_{stable} of –OH terminated surfaces were more than 20% higher than the $–SO_3^-$ surfaces. The slowest rate of current increase was associated with $–CH_3$ functionalized electrodes. At the end of the experiment the current from the $–CH_3$ functionalized electrodes were still at least 2.5 times lower

than other modified electrodes. Statistical tests demonstrated that the $t_{startup}$ differences of the three hydrophilic surfaces ($–N^+(CH_3)_3$, $–SO_3^-$, and –OH) are not significant, but they are significantly different to that of the hydrophobic surface ($–CH_3$), and the final current outputs of the four modified surfaces are significantly different (Table S1).

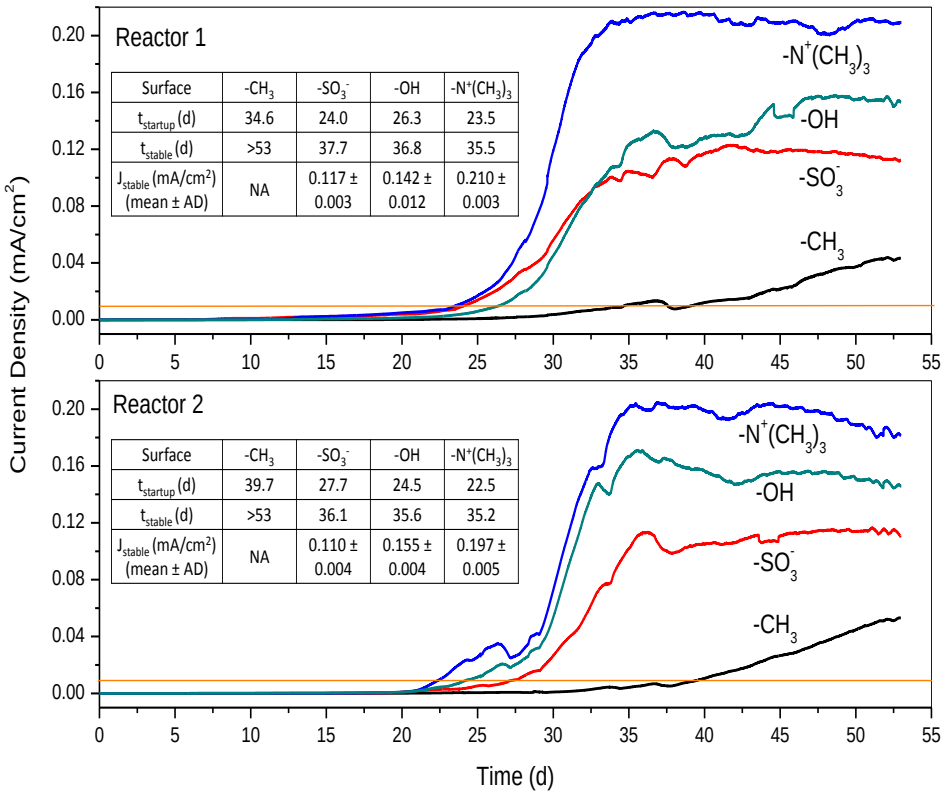

Figure 3. Current output over time of BE cells with different modified electrodes. The inset table compares the startup time of current ($t_{startup}$), time needed to reach a stable current (t_{stable}), and average current density at the stable stage (J_{stable}) of each electrode.

Prior to the comparative analysis just described, we performed an experiment in which a bare glassy carbon electrode was compared with the positively and negatively charged surfaces (Figure S5). The same start-up effect was observed, confirming earlier observation that surface modification may enhance start-up time. The control on the long run delivered higher current output, however, which was likely due to the high modifier loading used in this first test (~7mC/cm^2 of $–N^+(CH_3)_3$ and $–SO_3^-$). This was adapted later on for the experiments described previously. A bare glassy carbon control as such is considered debatable though; glassy carbon may have imperfections as the surface contains a range of oxygenated carbon species, which can also be protonated and

deprotonated. This is thus less defined as the modified surfaces. A surface modification with only benzene is not included either as this would create a hydrophobic surface. Considering that our study aims to compare the impact of charge on microbial biofilm formation and current formation rather than compare modified vs. unmodified electrodes we have therefore only reported the control data in the supplementary section.

Biofilm non-turnover CV.

After two days of starvation in acetate-free medium the current output of all biofilms were less than 20 μA, which made it possible to perform non-turnover CV. Non-turnover CV was also conducted on modified surfaces before inoculation and no redox peak was found in this scan range (Figure S3). Thus, the differences in CV profiles in Figure 4 are due to differences in biofilm composition/structure rather than surface modification. The redox peak height of biofilms followed the order – $N^+(CH_3)_3$ > –OH > $–SO_3^-$ >> $–CH_3$, which is consistent with the order of maximum current output of different biofilms. Differences in redox peak height is associated with the amount of redox active components present within the biofilms, so this indicates that the amount of biomass on different biofilms varied may be in the same order. In terms of peak positions, the reductive peaks at -500 mV and -400 mV and oxidative peak at -410 mV were present on all biofilm CV curves, while the oxidative peak at -100 mV was only observed on the CV curves of biofilms on the hydrophilic surfaces (namely $–N^+(CH_3)_3$, $–SO_3^-$, and –OH functionalized surfaces). Redox peak positions are correlated with different types of redox active components, so the absence of the -100 mV oxidation peak on the CV curve of $–CH_3$-associated biofilm may reflect a difference in the community composition of biofilm on $–CH_3$ functionalized surface relative to other samples. This hypothesis is somewhat corroborated by the FISH and sequence data (see below).

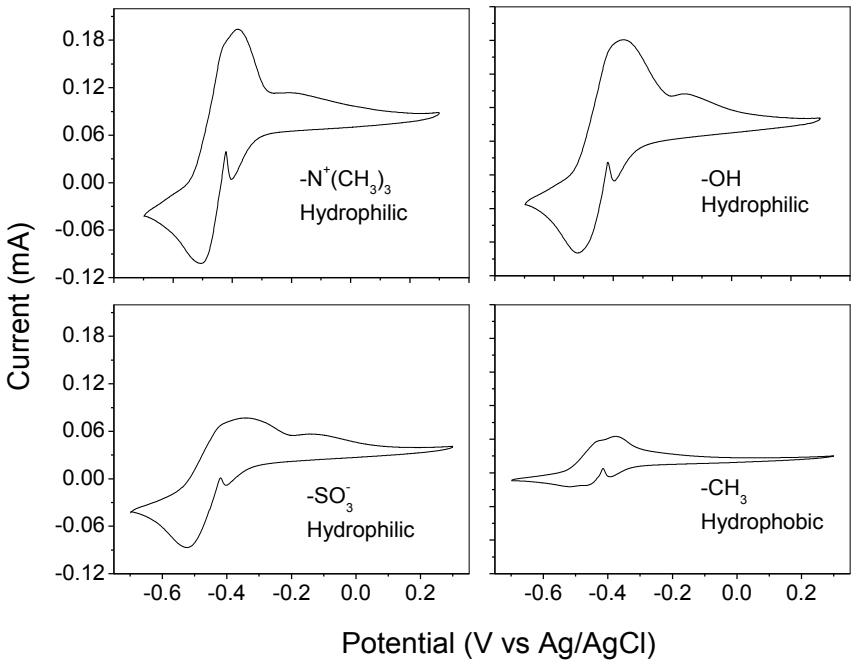

Figure 4. Non-turnover CV analyses of biofilms on different modified surfaces (scan rate: 1mV/s)

Biofilm FISH.

Figure 5 shows the representative CLSM 3D images of biofilms on different modified GC electrodes. The maximum thickness, surface coverage, amount of biomass, the abundance of *Geobacter* cells at the electrode surface of biofilms on different surfaces were compared in Table 2. FISH images indicate that *Geobacter* populations dominated the biofilms irrespective of surface functionalization (Fig. 5). Biofilms covered 100% of the surface area of $–N^+(CH_3)_3$, –OH, and $–SO_3^-$ functionalized electrodes but only around 30% of the surface area on $–CH_3$ functionalized electrodes. The maximum biofilm thicknesses followed the order $–CH_3 > –N^+(CH_3)_3 >$ –OH > $–SO_3^-$. It is likely that the biofilm was thicker on the $–CH_3$ functionalized electrodes because its patchy surface coverage facilitated greater diffusion of nutrients than would have been possible for the other more homogeneously distributed biofilms associated with $–N^+(CH_3)_3$, –OH, and $–SO_3^-$ surfaces. Calculated based on biofilm coverage and thickness data indicate that the amount of biomass associated with each electrode modification followed the order $–N^+(CH_3)_3 >$ –OH > $–SO_3^- > –CH_3$. Also, at the electrode surface, the *Geobacter* ratio of the $–CH_3$ biofilm (~40%) was about half as much as the biofilms on $–N^+(CH_3)_3$, –OH, and $–SO_3^-$ surfaces.

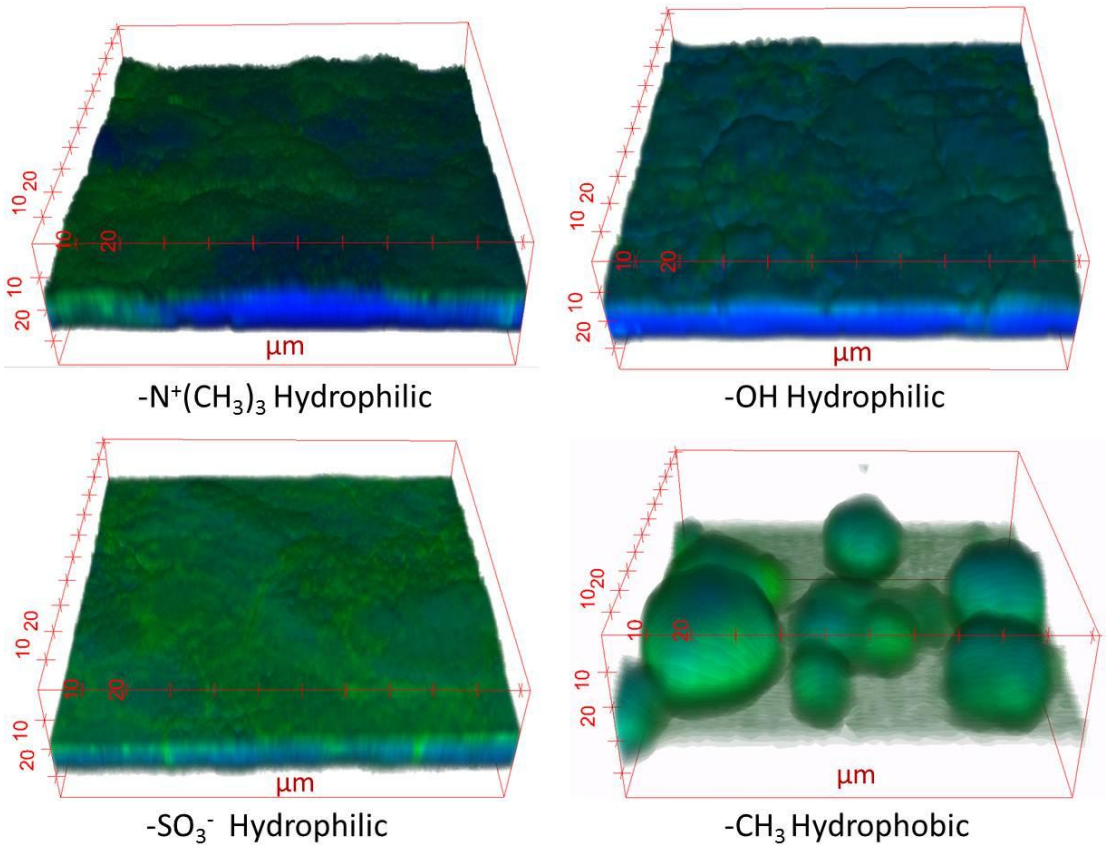

Figure 5. CLSM 3D images of biofilms on different modified GC electrodes. The biofilms were stained with EUB338mix-FITC (All bacteria, Green) and Geo1A-Cy5 (*Geobacter*, Blue).

Table 2. Comparison of biofilms on different surfaces

Surface	Thickness$_{max}$ (µm)		Coverage (%)		Biomass ($\mu m^3/\mu m^2$)		Surface $R_{Goebacter}$ (%)	
	R1	R2	R 1	R2	R1	R2	R1	R2
$-CH_3$	28.2	29.3	28.6	33.5	8.1	9.8	44.4	40.8
$-SO_3^-$	12.2	13.4	100	100	12.2	13.4	72.1	79.3
-OH	14.3	15.7	100	100	14.3	15.7	82.8	77.4
$-N^+(CH)_3$	16.4	17.1	100	100	16.4	17.1	80.3	83.5

Note: R1, Reactor 1; R2, Reactor 2; Surface $R_{Goebacter}$, the ratio of *Geobacter* cells at the electrode surface.

Biofilm pyrosequencing.

Pyrosequencing of 16S rRNA gene amplicons revealed that the biofilms were dominated by *Geobacter* populations, an observation that was also indicated by FISH (Fig. 6). There were two *Geobacter* populations that were present at more than 1% relative abundance (Fig. 6). The most similar *Geobacter* sp. to the most dominant of these populations, *Geobacter* 1, was *G. psychrophilus* (Fig. S2). The less dominant of these populations, *Geobacter* 2, was most similar to *G. sulfurreducens* (Fig. S2). Together the two *Geobacte*r populations in this study represented 70-92% relative abundance within each sample (Fig. 6). Most of the other populations present at more than 1% relative abundance (i.e. *Chlorobaculum*, *Clostridiales*, and *Bacteroidales* populations) were also observed in other mixed-culture anodic biofilm studies, [22, 31, 32] but their specific roles in the functioning of BESs are yet to be determined. The composition of microbial communities associated with the $–CH_3$ terminated surface was significantly different to that of those associated with other surface modification chemistries (P = 0.038, RDA). Methyl-group functionalized anodes were associated with larger abundances of *Chlorobaculum* and *Geobacter* 2 and a smaller abundance of *Geobacter* 1 when compared with other communities.

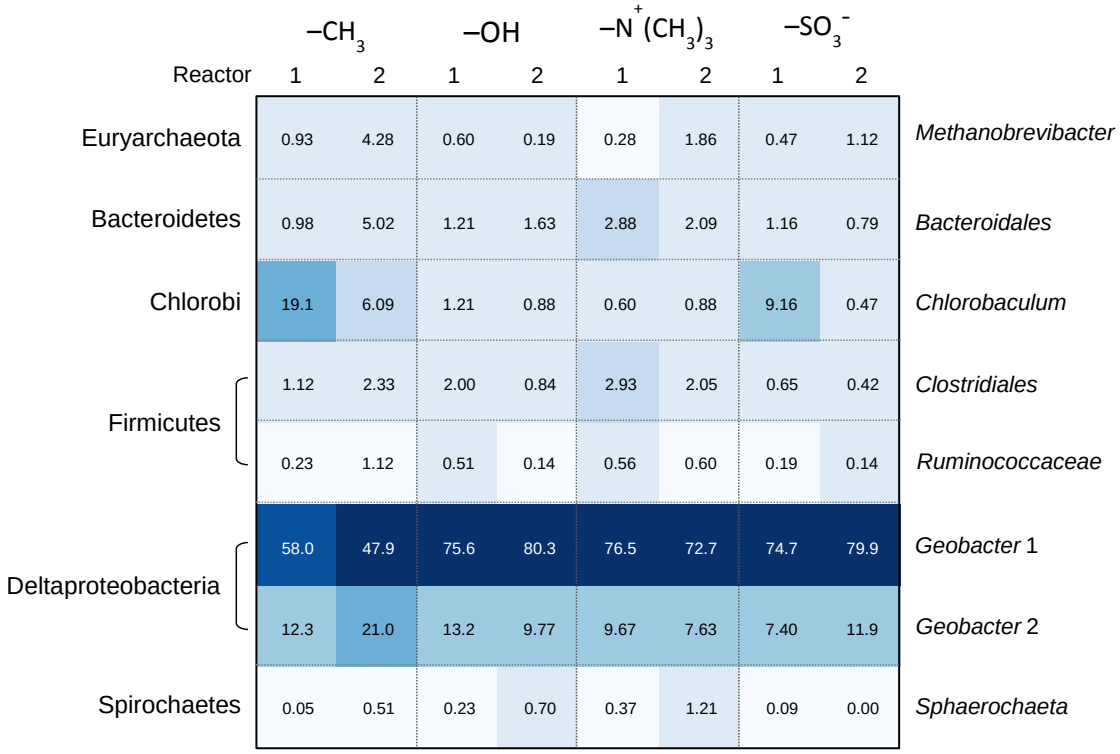

Figure 6. Percent relative abundances of microbial populations present at greater than 1% in any community.

DISCUSSION

Previous studies indicated that anodic current increases linearly with increasing of *G. sulfurreducens* electrode colonization and biofilm thickness. [33-35] Figure 3 shows that the current growth curves are "S" shaped with a lag phase, log phase, and a stable phase, which is according to the typical biofilm growth kinetics.[36] Hence, we can use the current versus time curve as the indicator of the biofilm formation process. The shorter the $t_{startup}$, the faster the bacterial initial adhesion. The $t_{startup}$ of the hydrophilic surfaces ($–N^+(CH_3)_3$, $–SO_3^-$, and –OH) were at least 9 days shorter than that of the hydrophobic surfaces ($–CH_3$). Although the $t_{startup}$ for the hydrophilic surfaces clustered together, it still can be seen from Figure 3 that $–N^+(CH_3)_3$ surfaces were always fastest to colonize. These results might be ascribed to the physicochemical interactions between bacteria and the modifying layers. Bacterial adhesion is affected by long-range forces (e.g. hydrophilic interactions, electrostatic interactions, van der Waals interactions) and short-range forces such as hydrogen bonding.[37] It is very likely that the $–N^+(CH_3)_3$, $–SO_3^-$, and –OH terminated surfaces not only make the surfaces more approachable for the planktonic bacteria because of hydrophilic interaction but also can potentially form hydrogen bonds that adhere bacteria to the electrode surface. Moreover, as bacterial surfaces are normally negatively charged at neutral pH, the $–N^+(CH_3)_3$ surfaces were more attractive to bacteria because of electrostatic forces, confirming earlier studies.[9,15] The FISH results showed that biofilms on different surfaces are different in surface coverage, thickness, and morphology. The amount of biomass on different surfaces followed the order $–N^+(CH_3)_3$ > –OH > $–SO_3^-$ >> $–CH_3$. Therefore, the effect of surface hydrophobicity on bacterial adhesion appears more pronounced than surface charge, and hydrophilic and positively-charged surfaces were more conducive to the initial adhesion and further biofilm growth of electrochemically active bacteria.

Besides $t_{startup}$, the final current output from different electrodes was also different from electrode to electrode, following the order $–N^+(CH_3)_3$ > –OH > $–SO_3^-$ >> $–CH_3$. The variation in the maximum current output was either from differences in extracellular electron transfer rate or differences in amount of biomass or differences in microbial community composition. As biofilm non-turnover CV shows that the peak positions do not change with the modifications, it is unlikely that surface modifications affected the kinetics of the redox reactions. The FISH results suggested that biofilms on all modified electrodes were dominated by *Geobacter* and that the community composition on $–CH_3$ functionalized surfaces was slightly different from the other biofilm samples. This observation was confirmed by the pyrosequencing data. The *Geobacter* populations occupied 70-92% abundance within all biofilms. The microbial community composition of the biofilms on $–N^+(CH_3)_3$,

–OH, and $–SO_3^-$ surfaces were not significantly different to each other ($P > 0.05$, RDA) but significantly different to that of the biofilm on $–CH_3$ surfaces ($P = 0.038$, RDA). The $–CH_3$ biofilms had lower abundances of *Geobacter* and larger abundances of *Chlorobaculum* comparing to the biofilms on the other modified surfaces. However, statistical analysis demonstrated that the variation in the maximum current output from different electrodes were not associated with the differences in microbial community composition ($P > 0.05$, GLM). The FISH results also showed that the amount of biomass on different surfaces followed the order $–N^+(CH_3)_3 > –OH > –SO_3^- >> –CH_3$. Statistical analysis demonstrated that the variation in the maximum current output from different electrodes were positively correlated with the differences in amount of biomass ($P < 0.001$, $R^2 = 0.937$) (Fig. S4). Therefore, it is the differences in amount of biomass that caused the variation in maximum current output rather than the differences in bacterial community composition.

Interestingly, the FISH results also showed that at the electrode interface, the relative *Geobacter* abundance on the hydrophobic surface ($–CH_3$, ~40%) was only about half of that of the biofilms on hydrophilic surfaces ($–N^+(CH_3)_3$, –OH, and $–SO_3^-$). Pyrosequencing demonstrated that the overall *Geobacter* ratio of the $–CH_3$ biofilm was also at least 10% lower than that of other three hydrophilic surfaces. Hence, we hypothesize that the surface hydrophobicity affects the initial attachment of *Geobacter* and the subsequent biofilm development is a further consequence.

As it has been reported that adding positively-charged functional groups such as $–NH_2$[9] and $–CH_2PPh_3^+$[15] could enhance the performance of BES, it is not surprising that the $–N^+(CH_3)_3$ terminated surfaces performed best among the four modifications. The biofilms are quite expectedly dominated by *Geobacter* because of inoculum and electron donor. The most important finding of this study is that hydrophilic surfaces are easier colonized by electroactive microbes (*e.g. Geobacter*) and more suitable for electroactive biofilm formation. It appears that "good" surfaces rather carry more biofilm than necessarily a different microbial community. This finding adds more support to the explanation why previously modifications such as acid soaking,[8] high temperature ammonia treatment,[9] heat treatment,[10] and electrochemical oxidation[12] all enhanced electrode performance.

ASSOCIATED CONTENT

Supporting Information. Five additional figures and 1 table. This material is available free of charge via the Internet at http://pubs.acs.org.

AUTHOR INFORMATION

Corresponding Author. *Email: korneel.rabaey@ugent.be; Phone: + 32 (0) 9/264 59 76; Fax: + 32 (0) 9/264 62 48

ACKNOWLEDGMENT

The authors would like to acknowledge Mr Kenn Lu from AWMC at UQ for the FISH training and mentorship and the anonymous reviewers for their valuable input. KG and KR are supported by strategic funding for the Centre for Microbial Electrosynthesis (UQ). KG is supported by UQ IPRS and Topup scholarships. KR is supported by the ERC via the ERC Starter Grant "Electrotalk".

REFERENCES

(1) Rabaey, K., Angenent, L., Schroder U., Eds. *Bioelectrochemical systems: from extracellular electron transfer to biotechnological application.* IWA Publishing: London; New York, 2010.

(2) Logan, B. E., Exoelectrogenic bacteria that power microbial fuel cells. *Nat. Rev. Microbiol.* **2009,** *7*, (5), 375-381.

(3) Schroder, U., Anodic electron transfer mechanisms in microbial fuel cells and their energy efficiency. *Phys. Chem. Chem. Phys.* **2007,** *9*, (21), 2619-2629.

(4) Zhou, M. H.; Chi, M. L.; Luo, J. M.; He, H. H.; Jin, T., An overview of electrode materials in microbial fuel cells. *J. Power Sources* **2011,** *196*, (10), 4427-4435.

(5) Du, Z. W.; Li, H. R.; Gu, T. Y., A state of the art review on microbial fuel cells: A promising technology for wastewater treatment and bioenergy. *Biotechnol. Adv.* **2007,** *25*, (5), 464-482.

(6) Logan, B. E.; Cusick, R.; Merrill, M. D.; Cheng, S. A.; Bryan, B.; Parker, D. S., Laboratory and field tests using microbial electrolysis cells for hydrogen production from agricultural and domestic wastewaters. *Abstr. Pap. Am. Chem. S.* **2010,** 239.

(7) Logan, B. E., Scaling up microbial fuel cells and other bioelectrochemical systems. *Appl. Microbiol. Biot.* **2010,** *85*, (6), 1665-1671.

(8) Zhu, N. W.; Chen, X.; Zhang, T.; Wu, P. X.; Li, P.; Wu, J. H., Improved performance of membrane free single-chamber air-cathode microbial fuel cells with nitric acid and ethylenediamine surface modified activated carbon fiber felt anodes. *Bioresour. Technol.* **2011,** *102*, (1), 422-426.

(9) Cheng, S. A.; Logan, B. E., High hydrogen yield from renewable resources using an improved beamr system. *Electrochem. Commun.* **2007,** *9*, (3), 492-496.

(10) Wang, X.; Cheng, S. A.; Feng, Y. J.; Merrill, M. D.; Saito, T.; Logan, B. E., Use of carbon mesh anodes and the effect of different pretreatment methods on power production in microbial fuel cells. *Environ. Sci. Technol*. **2009,** *43*, (17), 6870-6874.

(11) Lai, B.; Tang, X. H.; Li, H. R.; Du, Z. W.; Liu, X. W.; Zhang, Q., Power production enhancement with a polyaniline modified anode in microbial fuel cells. *Biosens. Bioelectron.* **2011,** *28*, (1), 373-377.

(12) Tang, X. H.; Guo, K.; Li, H. R.; Du, Z. W.; Tian, J. L., Electrochemical treatment of graphite to enhance electron transfer from bacteria to electrodes. *Bioresour. Technol.* **2011,** *102*, (3), 3558-3560.

(13) Nambiar, S.; Togo, C. A.; Limson, J. L., Application of multi-walled carbon nanotubes to enhance anodic performance of an Enterobacter cloacae-based fuel cell. *African J. Biotechnol.* **2009,** *8*, (24), 6927-6932.

(14) Park, D. H.; Kim, S. K.; Shin, I. H.; Jeong, Y. J., Electricity production in biofuel cell using modified graphite electrode with Neutral Red. *Biotechnol. Lett.* **2000,** *22*, (16), 1301-1304.

(15) Picot, M.; Lapinsonniere, L.; Rothballer, M.; Barriere, F., Graphite anode surface modification with controlled reduction of specific aryl diazonium salts for improved microbial fuel cells power output. *Biosens. Bioelectron.* **2011,** *28*, (1), 181-188.

(16) Gooding, J. J., Advances in interfacial design sensors: Aryl diazonium salts for electrochemical biosensors and for modifying carbon and metal electrodes. *Electroanal.* **2008,** *20*, (6), 573-582.

(17) Mahouche-Chergui, S.; Gam-Derouich, S.; Mangeney, C.; Chehimi, M. M., Aryl diazonium salts: a new class of coupling agents for bonding polymers, biomacromolecules and nanoparticles to surfaces. *Chem. Soc. Rev.* **2011,** *40*, (7), 4143-4166.

(18) Saito, T.; Mehanna, M.; Wang, X.; Cusick, R. D.; Feng, Y. J.; Hickner, M. A.; Logan, B. E., Effect of nitrogen addition on the performance of microbial fuel cell anodes. *Bioresour. Techno.* **2011**, *102*, (1), 395-398.

(19) Lapinsonnière, L.; Picot, M.; Poriel, C.; Barrière, F., Phenylboronic acid modified anodes promote faster biofilm adhesion and increase microbial fuel cell performances. *Electroanal.* **2013**, *25*, (3), 601-605.

(20) Liu, G. Z.; Chockalingham, M.; Khor, S. M.; Gui, A. L.; Gooding, J. J., A Comparative Study of the Modification of Gold and Glassy Carbon Surfaces with Mixed Layers of In Situ Generated Aryl Diazonium Compounds. *Electroanal.* **2010,** *22*, (9), 918-926.

(21) Strycharz-Glaven, S. M.; Tender, L. M., Study of the Mechanism of Catalytic Activity of G. Sulfurreducens Biofilm Anodes during Biofilm Growth. *ChemSusChem* **2012,** *5*, (6), 1106-1118.

(22) Rabaey, K.; Ossieur, W.; Verhaege, M.; Verstraete, W., Continuous microbial fuel cells convert carbohydrates to electricity. *Water Sci. Technol.* **2005,** *52*, (1-2), 515-523.

(23) Dennis, P. G.; Guo, K.; Imelfort, M.; Jensen, P.; Tyson, G. W.; Rabaey, K., Spatial uniformity of microbial diversity in a continuous bioelectrochemical system. *Bioresour. Technol.* **2012,** *129C*, 599-605.

(24) Amann, R. I., Fluorescently labelled, rRNA-targeted oligonucleotide probes in the study of microbial ecology. *Molecular Ecology* **1995,** *4*, (5), 543-554.

(25) Engelbrektson, A.; Kunin, V.; Wrighton, K. C.; Zvenigorodsky, N.; Chen, F.; Ochman, H.; Hugenholtz, P., Experimental factors affecting PCR-based estimates of microbial species richness and evenness. *Isme J.* **2010,** *4*, (5), 642-647.

(26) Caporaso, J. G.; Kuczynski, J.; Stombaugh, J.; Bittinger, K.; Bushman, F. D.; Costello, E. K.; Fierer, N.; Pena, A. G.; Goodrich, J. K.; Gordon, J. I.; Huttley, G. A.; Kelley, S. T.; Knights, D.;

Koenig, J. E.; Ley, R. E.; Lozupone, C. A.; McDonald, D.; Muegge, B. D.; Pirrung, M.; Reeder, J.; Sevinsky, J. R.; Tumbaugh, P. J.; Walters, W. A.; Widmann, J.; Yatsunenko, T.; Zaneveld, J.; Knight, R., QIIME allows analysis of high-throughput community sequencing data. *Nat. Methods* **2010,** *7*, (5), 335-336.

(27) Edgar, R. C.; Haas, B. J.; Clemente, J. C.; Quince, C.; Knight, R., UCHIME improves sensitivity and speed of chimera detection. *Bioinformatics* **2011,** *27*, (16), 2194-2200.

(28) Bragg, L.; Stone, G.; Imelfort, M.; Hugenholtz, P.; Tyson, G. W., Fast, accurate error-correction of amplicon pyrosequences using Acacia. *Nat. Methods* **2012,** *9*, (5), 425-426.

(29) Cayford, B. I.; Dennis, P. G.; Keller, J.; Tyson, G. W.; Bond, P. L., High-throughput amplicon sequencing reveals distinct communities within a corroding concrete sewer system. *Appl. Environ. Microb.* **2012,** *78*, (19), 7160-7162.

(30) Legendre, P.; Gallagher, E. D., Ecologically meaningful transformations for ordination of species data. *Oecologia* **2001,** *129*, (2), 271-280.

(31) Zhang, G. D.; Zhao, Q. L.; Jiao, Y.; Wang, K.; Lee, D. J.; Ren, N. Q., Efficient electricity generation from sewage sludge using biocathode microbial fuel cell. *Water. Res.* **2012,** *46*, (1), 43-52.

(32) Zhang, G. D.; Zhao, Q. L.; Jiao, Y.; Wang, K.; Lee, D. J.; Ren, N. Q., Biocathode microbial fuel cell for efficient electricity recovery from dairy manure. *Biosens. Bioelectron.* **2012,** *31*, (1), 537-543.

(33) Marsili, E.; Sun, J.; Bond, D. R., Voltammetry and growth physiology of geobacter sulfurreducens biofilms as a function of growth stage and imposed electrode potential. *Electroanal.* **2010,** *22*, (7-8), 865-874.

(34) Reguera, G.; Nevin, K. P.; Nicoll, J. S.; Covalla, S. F.; Woodard, T. L.; Lovley, D. R., Biofilm and nanowire production leads to increased current in Geobacter sulfurreducens fuel cells. *Appl. Environ. Microb.* **2006,** *72*, (11), 7345-7348.

(35) Speers, A. M.; Reguera, G., Electron donors supporting growth and electroactivity of geobacter sulfurreducens anode biofilms. *Appl. Environ. Microb.* **2012,** *78*, (2), 437-444.

(36) Capdeville B. ; Nguyen K. M., Kinetics and Modelling of Aerobic and Anaerobic Film Growth. *Water. Sci. Technol.* **1990**, *22*, (1-2), 149–170.

(37) Ploux, L.; Ponche, A.; Anselme, K., Bacteria/material interfaces: role of the material and cell wall properties. *J. Adhes. Sci. Technol.* **2010**, *24*, (13-14), 2165-2201.

SUPPORTING INFORMATION

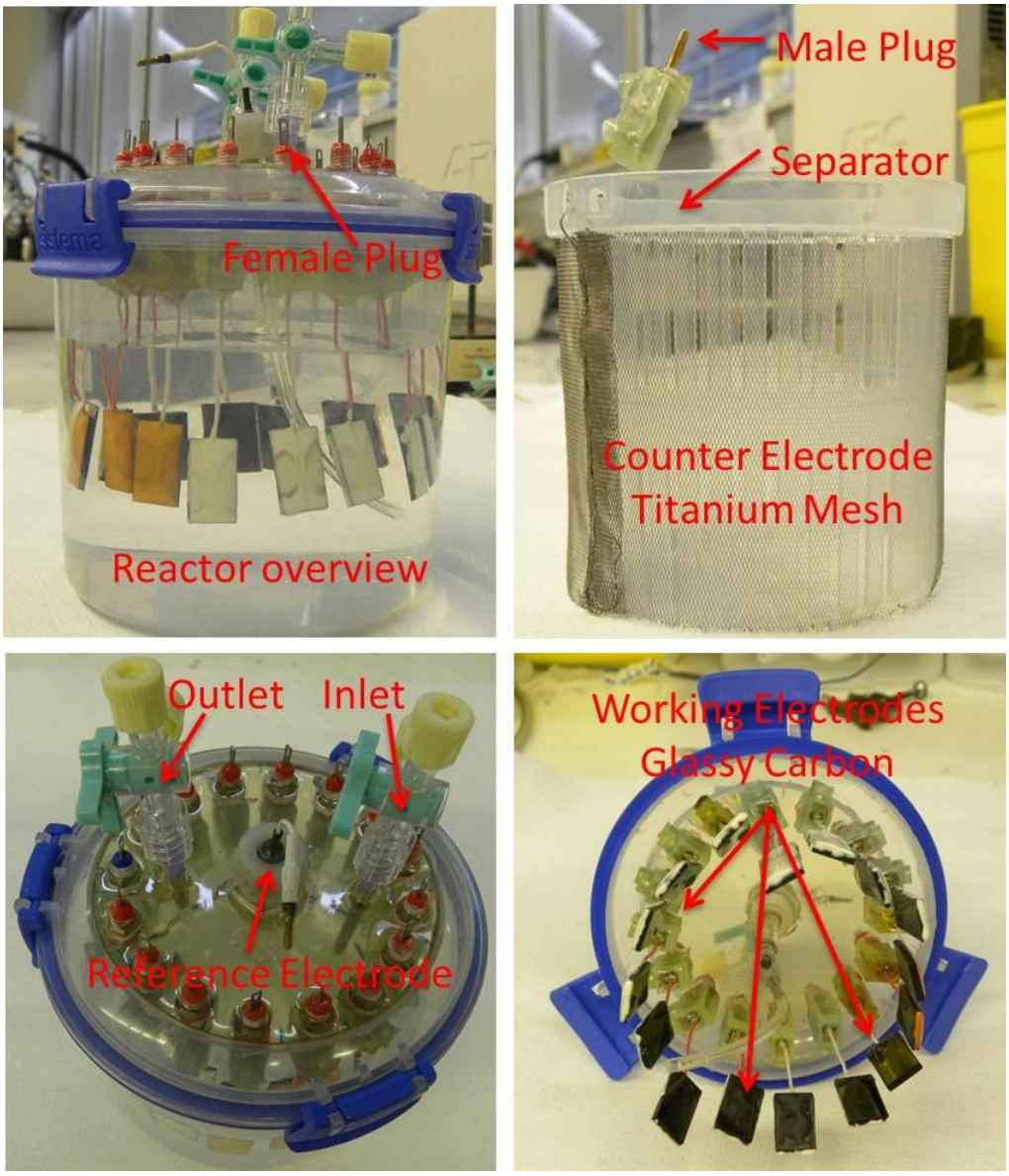

Figure S1. Photos of the BES reactor

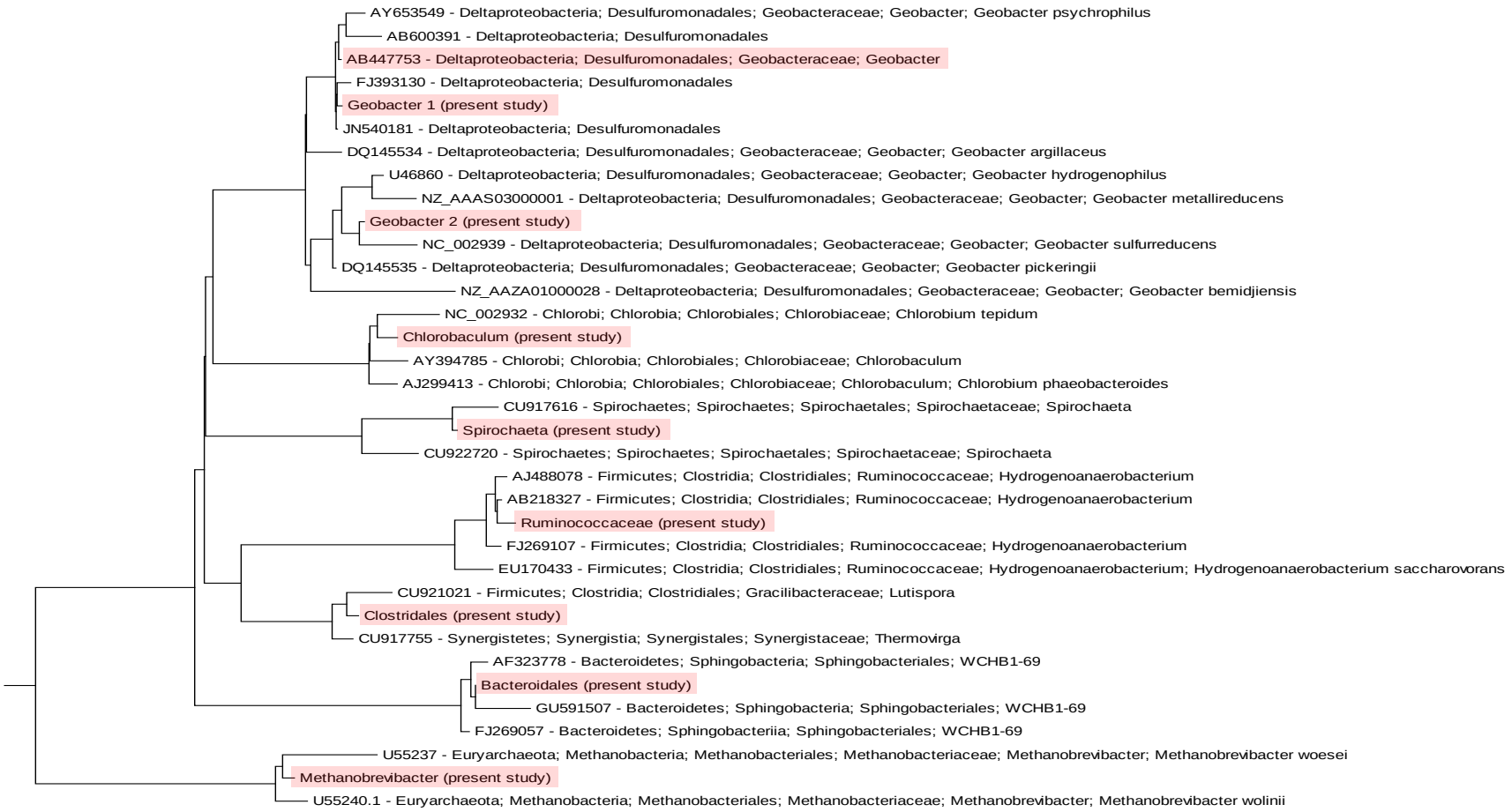

Figure S2. Phylogenetic neighbourhood of OTUs present at more than 1% relative abundance in this study (shaded) relative to the most similar full length 16S rRNA gene sequences in the greengenes database. The representative sequences for each OTU was inserted into the greengenes tree by maximum parsimony using Arb.

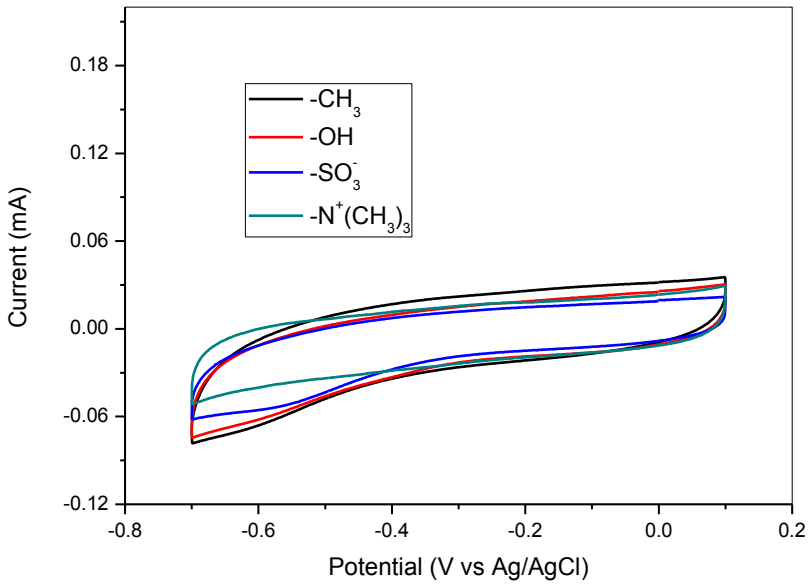

Figure S3. CVs for each of the modified electrodes in sterile media without acetate before inoculations (scan rate: 10mV/s)

Table S1. Tukey's Honestly Significant Difference (HSD) test of startup time and current output

	Startup time	Current output
–OH vs $–N^+(CH_3)_3$	ns	**
–OH vs $–SO_3^-$	ns	*
$–SO_3^-$ vs $–CH_3$	*	**
$–N^+(CH_3)_3$ vs $–CH_3$	*	***
–OH vs $–CH_3$	*	***
$–SO_3$ vs $–N^+(CH_3)_3$	ns	***

Note: P > 0.05 (ns), P < 0.05 (*), P < 0.01 (**), P < 0.001 (***)

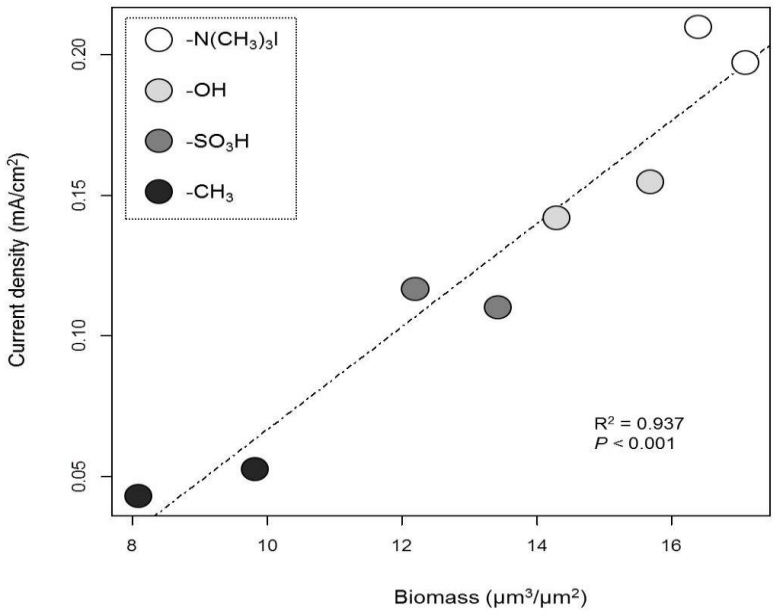

Figure S4. The correlations of amount of biomass and current density

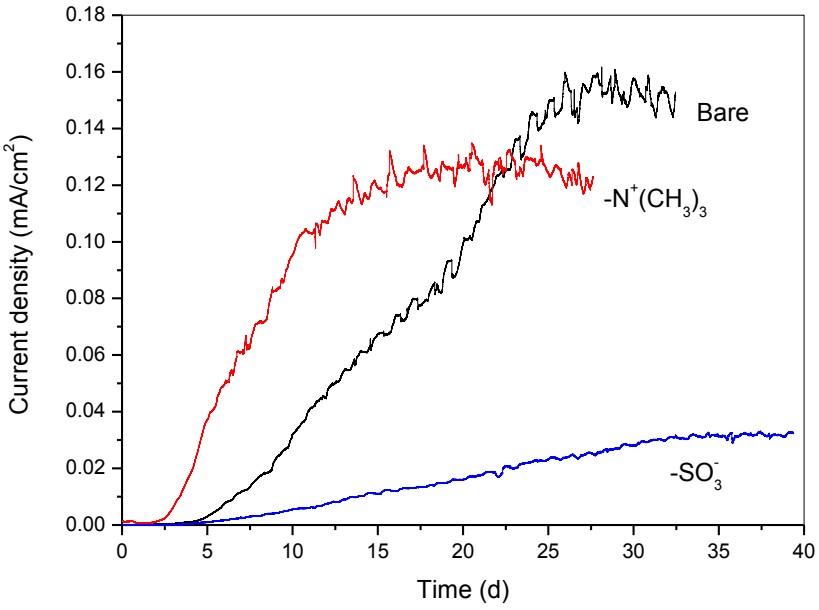

Figure S5. Current output over time of BE cells with bare GC electrode and modified GC electrodes. Surface modified by cyclic voltammetry and the coating density was around 7 mC/cm^2.

Appendix B

Surfactant treatment of carbon felt enhances anodic microbial electrocatalysis in bioelectrochemical systems

Kun Guo [a,b,c], Alexander H. Soeriyadi [d], Sunil A. Patil [a], Antonin Prévoteau [a], Stefano Freguia [b], J. Justin Gooding [d], Korneel Rabaey [a,b,c*]

[a] Laboratory of Microbial Ecology and Technology, Ghent University, Coupure Links 653, B-9000 Ghent, Belgium; [b] Centre for Microbial Electrosynthesis, The University of Queensland, Brisbane, QLD 4072, Australia; [c] Advanced Water Management Centre, The University of Queensland, Brisbane, QLD 4072, Australia; [d] School of Chemistry, University of New South Wales, Sydney, NSW 2052, Australia

* Corresponding author: korneel.rabaey@ugent.be +3292645976

Electrochemistry Communication. 2014, 39: 1-4.

Graphic Abstract

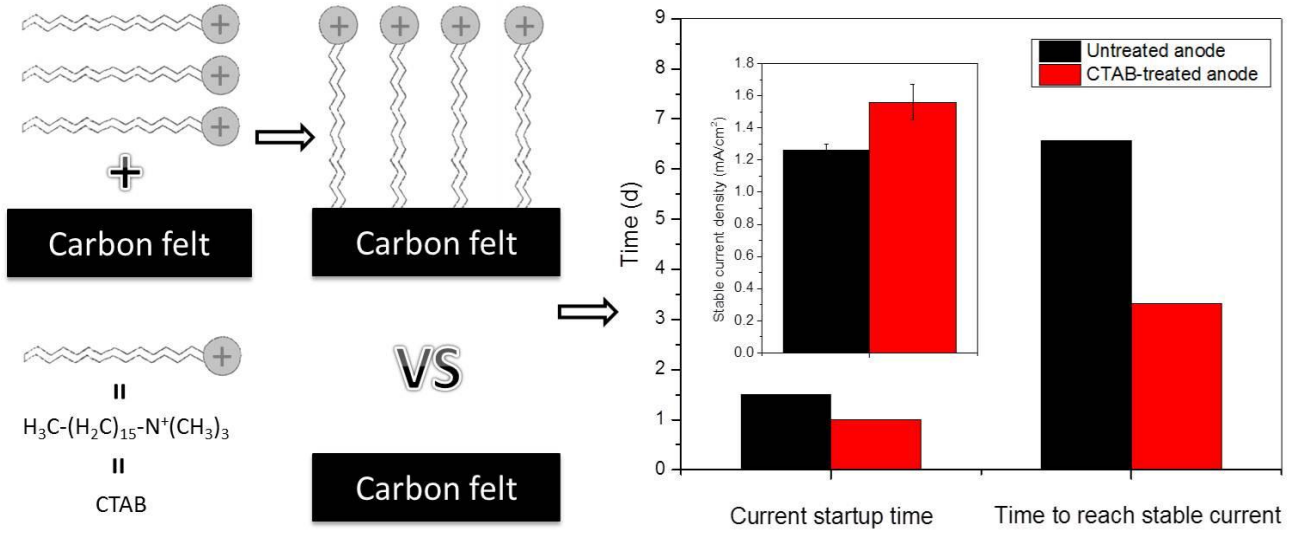

Abstract

This study reports a simple and effective method to make carbon felt surface hydrophilic and positively-charged by means of cetyltrimethylammonium bromide (CTAB) soaking. X-ray photoelectron spectroscopy and cyclic voltammetry indicated that CTAB could form a surfactant layer on carbon felt surface with the polar heads exposing outwardly. In a acetate-fed bioanode, the start-up time of current production and the time to reach stable current output at the CTAB-treated felt anodes were 36.1% and 49.4% shorter than the untreated anodes, respectively. Moreover, the maximum current output with these treated electrodes was 23.8% higher than the untreated counterparts. These results indicate that the CTAB treatment of carbon felt accelerates the anodic biofilm formation and enhances current output of BESs.

Keywords: Cetyltrimethylammonium bromide, carbon felt, surface modification, surfactant, biofilm formation, bioelectrochemical systems

1. Introduction

Carbon felt has been widely used as electrode material in microbial bioelectrochemical systems (BESs) due to its high porosity, low cost, and limited corrosion sensitivity. Since the surfaces of commercial carbon felts are rather hydrophobic, which is not optimal for bacterial attachment and biofilm formation, pre-treatment may enhance their electrocatalytic performance. Previously, several pre-treatment methods such as the use of ammonia [1], heat [2], acid [3, 4], electrochemical oxidation [5], NaOH/HCl soaking [6], and plasma [7] have been reported to improve the surface wettability of carbon surfaces and enhance current outputs of BESs. However, strong acids, harsh conditions or expensive equipment are used in these methods, and most of them are quite time-consuming. Here we propose a simple and effective "surfactant soaking" pre-treatment method for carbon felt.

Surfactants, molecules with a hydrophilic head and a long hydrophobic tail, have been widely used in electrode surface treatments for different purposes [8]. It has been reported that cetyltrimethylammonium bromide (CTAB), a cationic surfactant, could form a compact monolayer on carbon paste electrodes [9] and on activated carbon surfaces [10] with the polar head facing away from the electrode, which made the electrode surface hydrophilic and positively-charged. Moreover, our previous study demonstrated that the hydrophilic and positively-charged surfaces are more selective to electroactive microbes and more conducive to biofilm formation in BESs [11]. Therefore, the aim of this study was to test whether CTAB treatment can make carbon felt surface hydrophilic and positively charged, and thereby enhance anodic biofilm formation and current outputs of BESs.

2. Materials and Methods

2.1 Electrode treatment

Carbon felt (ALFA43199, Alfa Aesar) electrodes were cut into pieces of 20 mm x 10 mm x 3.18 mm (projected surface area 2 cm^2). Ti wire (Ø 0.25 mm, Advent Research Materials, UK) woven into the carbon felt was used to make external connections. For surface treatment, the electrodes were firstly soaked in 500 mL vigorously stirred (1000 rpm) CTAB (Sigma-Aldrich) solution (2 mM) for 5 min and then rinsed three times in 500 mL vigorously stirred (1000 rpm) deionized water for 5 min. The untreated electrodes were only rinsed in deionized water with the same protocol.

2.2 Characterization of the electrode surfaces

As a measure of surface hydrophobicity, contact angles with Milli-Q water were analyzed with sessile drop method using a Rame-Hart 100-00 goniometer. In order to confirm the hydrophobicity, water absorption experiments were conducted in test tubes with Milli-Q water. The surface elemental composition was analyzed by X-ray photoelectron spectroscopy (XPS) as described in Guo et al [11]. The electrochemical properties of these electrodes were studied by cyclic voltammetry using a VSP potentiostat (Biologic, France).

2.3 BES set-up and operation

Bioelectrochemical experiments were conducted using a CHI 1000C Multi-Potentiostat (CH Instruments, Austin, TX, USA) with a custom-made membrane-free bottle-type BES reactor (600 mL) [6] hosting a Ag/AgCl (3 M KCl) reference electrode, a stainless steel mesh counter electrode and several CTAB-treated and untreated working electrodes positioned geometrically identical relative to the counter. The reactor was firstly filled with 400 mL of modified M9 medium [6] with 2 g/L sodium acetate (24.4 mM) as substrate and then sparged with nitrogen for 30 min to remove dissolved oxygen. It was inoculated with 100 mL anodic effluent from an existing acetate-fed BES reactor operated with the same medium. The bioelectrocatalytic performance of all electrodes was investigated by chronoamperometry at an applied potential of -0.2 V vs. Ag/AgCl. The reactor was firstly run in a fed-batch mode and then switched to a continuous mode as described below. The reactor medium was continuously mixed using a magnetic stirrer rotating at 200 rpm. At the end of chronoamperometry experiment, biofilms on treated and untreated electrodes were analyzed by cyclic volatmetry within a potential window between -0.8 V and 0 V (vs. Ag/AgCl) at a scan rate of 1 mV/s. These experiments were conducted in a 28°C temperature-controlled room.

3. Results and Discussion

3.1 Electrode surface hydrophobicity

The effect of the detergent treatment on hydrophobicity was assessed by water contact angle measurements and water absorption observations. The water contact angles of the untreated, control electrodes were greater than 120°. Comparatively, with CTAB-treated electrodes the water droplet would immediately penetrate the felt that resulted in a contact angle lower than 10° (Fig. 1a). It was also noticed in the water absorption experiment that the treated felt sunk to the bottom of Milli-Q water quickly, whereas the untreated felt remained floating at the top of the water level (Fig. 1b). These results demonstrated that the hydrophobic carbon felt surface could be transformed into

hydrophilic in a couple of minutes only by 2mM CTAB soaking. Compared to the existing carbon electrode treatment methods mentioned in the introduction, no strong acid nor harsh environment, expensive equipment or complex set-up were involved in CTAB treatment.

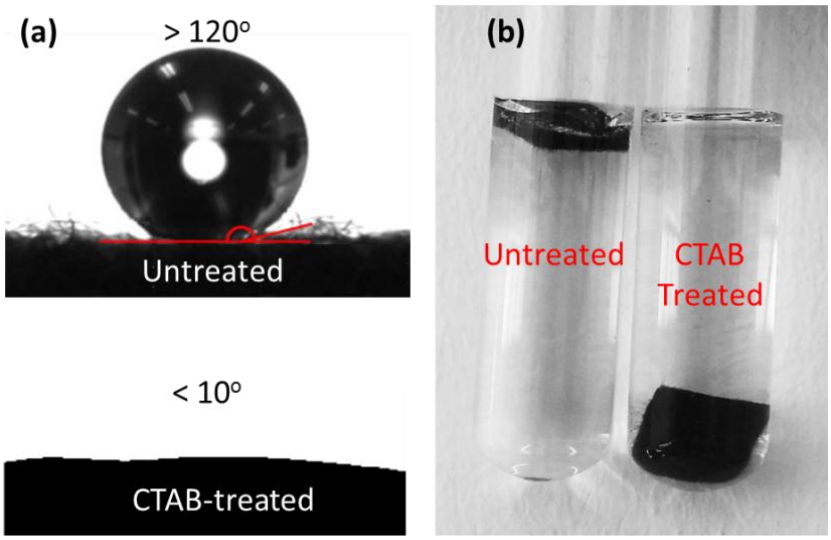

Figure 1. Water contact angle (a) and water absorption (b) images of untreated and CTAB-treated carbon felts.

3.2 Elemental composition of electrode surfaces

The atomic composition of the electrode surfaces were determined by XPS and reported in Fig. 2. These analyses revealed that: 1) the nitrogen content of CTAB-treated surfaces (0.96%) was higher than that of the untreated surfaces (0.3%); 2) 24% of the nitrogen content of CTAB-treated surfaces could be attributed to $-N^{+}(CH_3)_3$; 3) bromine was not present in either surface, but the oxygen content of the CTAB-treated surface increased from 5.6% to 6.9% with respect to the untreated surface. Since $-N^{+}(CH_3)_3$ is the characteristic functional group of the CTAB molecule, these results indicate that detergent molecules were absorbed on the carbon felt surface. The absence of bromine on CTAB-treated surface is likely due to the fact that the bromine ion could be easily washed away by water during rising and replaced by some oxygen-containing anions (e.g. OH^{-}).

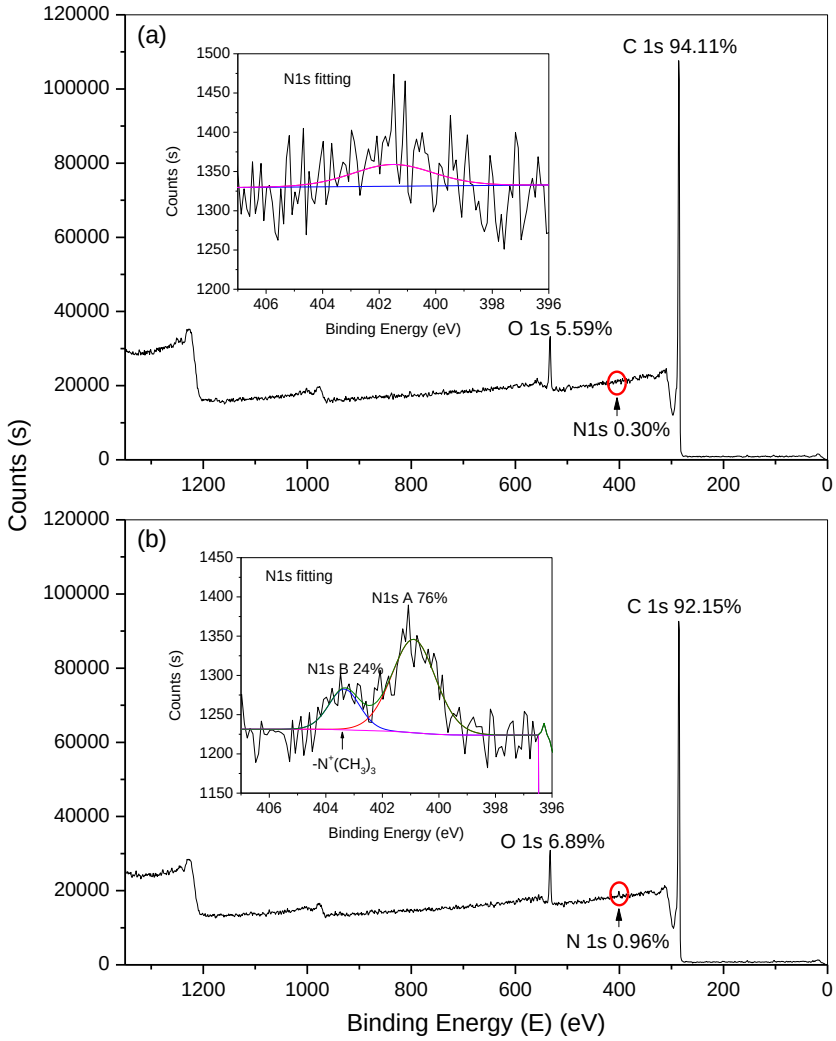

Figure 2. XPS spectra of (a) untreated and (b) CTAB-treated carbon felt surfaces showing elemental composition. Inset figures show N1s peak fitting and assignment.

It has been reported that cationic surfactants such as HDTMA [12], DTAB [13], TTAB [13], and most importantly CTAB [10] could form a film on the substrate surface via hydrophobic bonding. As the carbon felt surface is quite hydrophobic, it is very likely that detergent formed a film on the electrode surface via hydrophobic interaction between electrode surface and the non-polar tail of detergent, and left the polar head of the detergent ($-N^{+}(CH_3)_3$) exposed to the outside. As a result, the detergent modified carbon felt surface became hydrophilic.

3.3 Electrochemical characterization of electrodes materials

CVs were performed in PB and PB with ferrocyanide solution (Fig. 3). Calculated from the capacitive current in the CVs recorded in PB (Fig. 3a), the apparent capacitance shows a 4.7 fold increase with the CTAB treatment, from 161 ± 32 to 757 ± 143 μF (mean ± SD, n = 3). CVs recorded in PB with ferrocyanide present features of a typical quasi-reversible process (Fig. 3b). The electrode treated with CTAB exhibited around five times higher peak current density (1.21 ± 0.17 mA/cm^2) than the untreated surfaces (0.24 ± 0.7 mA/cm^2). Since the real electrode surface area is not expected to change considerably after treatment, these results strongly suggest that the surface area wetted by the buffer dramatically increased with the CTAB-treatment. It can also be seen from Fig. 3b that the peak separations of the untreated and CTAB-treated surfaces were both around 130 mV. The similar peak separations (~130 mV) indicates that any putative impact of the CTAB-treatment on the electron transfer kinetics was not measurable. These results confirmed our hypothesis that there was a CTAB layer formed on the electrode surface (see section 3.1). This layer made the surface hydrophilic, hence most of the treated-felt surface must be in intimate contact with the solution, increasing the surface available for heterogeneous electron transfer.

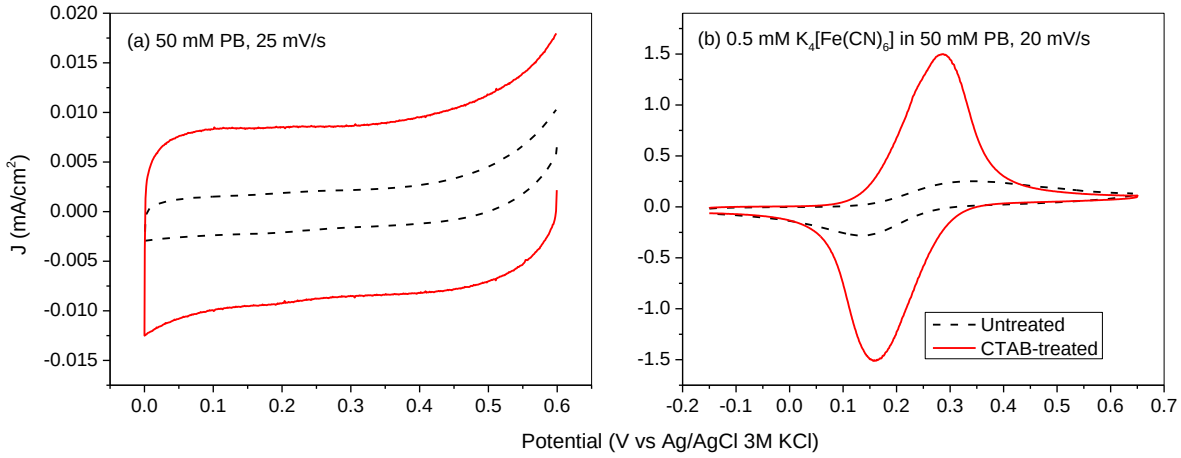

Figure 3. CVs of untreated and CTAB-treated carbon felt (a) in phosphate buffer (PB) and (b) PB with ferrocyanide. CVs were recorded with a correction level of 80% of the ohmic drop which was measured by current interrupt method.

3.4 Performance of untreated and CTAB-treated carbon felts as anodes in BES

Fig. 4a shows the bioelectrocatalytic current generation over time at the untreated and CTAB-treated electrodes. The reactor was firstly run in a fed-batch mode to allow the bacteria to attach to

the electrodes. After two batch cycles, the reactor was switched to a continuous flow mode to maintain the maximum current output. The medium feed rate was changed from 30 to 40 mL/h on day 6 because it was noticed that the former rate was not able to maintain the maximum current output of the treated electrodes. The start-up time ($t_{startup}$) of current generation of the untreated and CTAB-treated electrodes were 36 h and 23 h, respectively. The CTAB-treated electrodes reached a stable stage current densities (j_{stable}) of 1.56 ± 0.11 mA/cm^2 (mean ± SD) within 3.32 days, while the current outputs of the untreated electrodes stopped increase and stabilized around 1.26 ± 0.04 mA/cm^2 (mean ± SD) after 6.56 days. The experiments were continued for up to 30 days revealing consistently higher currents for the CTAB treated electrodes. Turnover CVs (Fig. 4b) indicate that the oxidation of acetate started from -0.4 V onwards and reached a plateau from -0.25 V on at both untreated and untreated electrodes. The current density plateau of the untreated and treated were 1.69 and 1.32 mA/cm^2, respectively.

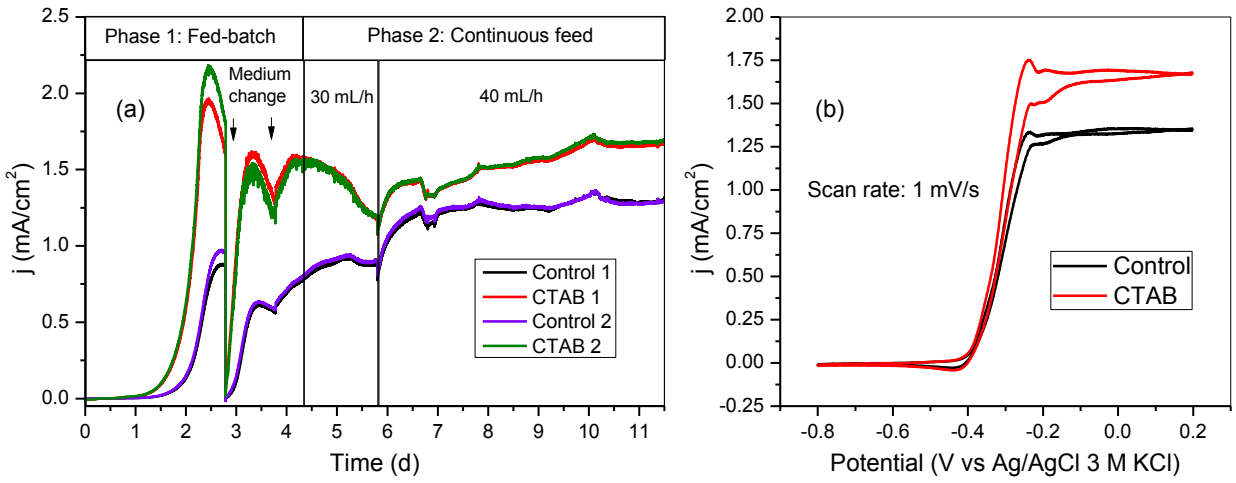

Figure 4. Bioelectrocatalytic current generation (a) and representative turnover CVs recorded at the end of the chronoamperometry (b) on untreated and CTAB-treated carbon felts.

Since previous publications have reported that BES current linearly increased with growth of the electroactive biofilm [14], the $t_{startup}$ and time to j_{stable} (t_{stable}) can be used as indicators of initial biofilm formation and biofilm maturing. The $t_{startup}$ and t_{stable} of the CTAB-treated electrodes were 36.1% and 49.4% shorter than those of the untreated electrodes, respectively. Hence, CTAB treatment could accelerate initial attachment of bacteria and biofilm formation at carbon felt surface. Turnover CVs indicated that surfactant treatment did not affect the kinetics of extracellular electron transfer between bacteria and electrode, hence the current density difference between the untreated and treated electrodes was likely due to the different amount of biomass on their surfaces.

This can be attributed to the fact that the CTAB treatment makes the carbon felt surface hydrophilic and positively-charged by introducing the $-N^{+}(CH_3)_3$ groups. Hydrophilic surfaces are more approachable for bacteria colonization and surface positive charges can also attract the negatively-charged bacteria to attach the electrode surfaces [11]. Besides CTAB, other detergents such as SDS, TMBC and Umonium 38® were also tested. We also compared the CTAB treatment with NaOH/HCl soaking. These results (data not shown) demonstrated that CTAB-treated carbon felt outperformed other pretreatment strategies in terms of $t_{startup}$ and I_{stable}.

4. Conclusion

CTAB soaking is a simple and effective way to make carbon felt surfaces hydrophilic and positively-charged. This is attributed to the ability of CTAB to form a layer on the carbon felt surface via hydrophobic bonding and to expose the polar heads to the solution. CTAB treatment significantly accelerated start-up time and development of an electroactive biofilm on carbon felt surface and slightly enhanced the current output of BESs.

References

[1] S.A. Cheng, B.E. Logan, Electrochem. Commun. 9 (2007) 492.

[2] X. Wang, S.A. Cheng, Y.J. Feng, M.D. Merrill, T. Saito, B.E. Logan, Environ. Sci. Technol. 43 (2009) 6870.

[3] N.W. Zhu, X. Chen, T. Zhang, P.X. Wu, P. Li, J.H. Wu, Bioresour. Technol. 102 (2011) 422.

[4] Y.J. Feng, Q. Yang, X. Wang, B.E. Logan, J. Power Sources 195 (2010) 1841.

[5] X.H. Tang, K. Guo, H.R. Li, Z.W. Du, J.L. Tian, Bioresour. Technol. 102 (2011) 3558.

[6] K. Guo, X. Chen, S. Freguia, B.C. Donose, Biosens. Bioelectron. 47 (2013) 184.

[7] V. Flexer, M. Marque, B.C. Donose, B. Virdis, J. Keller, Electrochim. Acta 108 (2013) 566.

[8] R. Vittal, H. Gomathi, K.J. Kim, Adv. Colloid Interface Sci. 119 (2006) 55.

[9] S.S. Shankar, B.E.K. Swamy, U. Chandra, J.G. Manjunatha, B.S. Sherigara, Int. J. Electrochem. Sci. 4 (2009) 592.

[10] A. Gurses, M. Yalcin, M. Sozbilir, C. Dogar, Fuel Process Technol. 81 (2003) 57.

[11] K. Guo, S. Freguia, P.G. Dennis, X. Chen, B.C. Donose, J. Keller, J.J. Gooding, K. Rabaey, Environ. Sci. Technol. 47 (2013) 7563.

[12] S.H. Xu, S.A. Boyd, Environ. Sci. Technol. 29 (1995) 312.

[13] C. Serpi, A. Voulgaropoulos, S. Girousi, Electroanal. 25 (2013) 2493.

[14] G. Reguera, K.P. Nevin, J.S. Nicoll, S.F. Covalla, T.L. Woodard, D.R. Lovley, Appl. Environ. Microbiol. 72 (2006) 7345.

Appendix C

Spontaneous modification of carbon surface with neutral red from its diazonium salts for bioelectrochemical systems

Kun Guo [a, b]*, Xin Chen [c], Stefano Freguia [a], Bogdan C. Donose [a]

[a] Advanced Water Management Centre, The University of Queensland, Brisbane, QLD 4072, Australia

[b] Centre for Microbial Electrosynthesis, The University of Queensland, Brisbane, QLD 4072, Australia

[c] School of Chemistry, University of New South Wales, Sydney, NSW 2052, Australia

* Corresponding author: k.guo@awmc.uq.edu.au

Biosensors & Bioelectronics. 2013, 47 (C):184-189.

Highlights

- A new and simple method for neutral red (NR) surface modification.
- Covalently graft NR onto carbon surfaces was achieved by spontaneous reduction of in situ generated NR diazonium salts.
- The NR-modified electrodes showed a good stability when stored in PBS solution in the dark.
- The NR-modified electrodes produced 3.63±0.36 times higher current than the unmodified electrodes.

Abstract:

This study introduces a novel and simple method to covalently graft neutral red (NR) onto carbon surfaces based on spontaneous reduction of *in situ* generated NR diazonium salts. Immobilization of neutral red on carbon surface was achieved by immersing carbon electrodes in NR-$NaNO_2$-HCl solution. The functionalized electrodes were characterized by cyclic voltammetry (CV), atomic force microscope (AFM), and X-ray photoelectron spectroscopy (XPS). Results demonstrated that NR attached in this way retains high electrochemical activity and proved that NR was covalently bound to the carbon surface via the pathway of reduction of aryl diazonium salts. The NR-modified electrodes showed a good stability when stored in PBS solution in the dark. The current output of an acetate-oxidising microbial bioanode made of NR-modified graphite felts were 3.63 ± 0.36 times higher than the unmodified electrodes, which indicates that covalently bound NR can act as electron transfer mediator to facilitate electron transfer from bacteria to electrodes.

Keywords: neutral red, aryl diazonium salts, spontaneous modification, extracellular electron transfer, bioelectrochemical systems

1. Introduction

Bioelectrochemical systems (BESs) which use bacteria as catalysts to drive oxidation and/or reduction reactions at solid-state electrodes are considered as a novel, promising technology for wastewater treatment, power production and valuable chemicals production (Rabaey 2010). However, at present, the technology appears to be constrained by low current density mainly resulting from the low rate of extracellular electron transfer between bacteria and electrode. It has been previously shown that immobilization of electron transfer mediators, such as neutral red (NR) (Park et al. 2000; Park and Zeikus 2003; Wang et al. 2011), methylene blue (MB) (Popov et al. 2012), anthraquinone-1,6-disulfonic acid (AQDS) (Lowy and Tender 2008; Lowy et al. 2006), and 1,4-naphthoquinone (NQ) (Lowy et al. 2006), onto electrode surface is an efficient way to facilitate electron transfer from bacteria to electrode. Among those mediators, NR was considered as one of the ideal mediators for BES anodes as it possesses a redox potential of -0.325 V vs. normal hydrogen electrode (NHE) which is rather close to the -0.32 V (vs. NHE) of NAD^+/NADH couple (Park and Zeikus 1999). Since the latter locates at the low-potential end of the electron transfer chain in microbial respiration, a NR-immobilized electrode has the potential to harvest most of the energy released from the microbial oxidation of organic substrates.

So far, two methods have been employed to immobilize NR to carbon electrodes. The first is a chemical method which grafts NR to carbon surface through the amidation reaction between carboxylated carbon and the primary amine of NR (Jeykumari and Narayanan 2007; Wang et al. 2011). NR immobilized in this way is tightly anchored to the carbon surface as the linkage is an amido bond. However, the disadvantage of this method is that large amount of nitric/sulphuric acids and organic solvents are required to carboxylate the carbon surface and set off the amidation reaction, respectively. Electropolymerization of NR is the other method to immobilize NR to carbon surface, which is generally carried out by means of cyclic voltammetry (CV) between -0.2 V and 1.2 V vs. SCE in a NR solution with sodium nitrate (Chen and Gao 2007b). Polymerized NR (PNR) retains the electrochemical properties of the NR monomer as well as enhances the conductivity of the electrode. Hence, it has been used as an insoluble redox mediator for sensors and biosensors (Pauliukaite and Brett 2008). Comparing to the amidation reaction method, this procedure is much simpler and more environmentally friendly. However, the modification system is complex as a potentiostat, 3-electrode system and an external power source are required. Moreover, since the PNR is just deposited and not chemically bound to the electrode surface, the electrical connection is not as strong as for covalent bonding. Therefore, new, simple and environmentally friendly methods need to be developed.

Electrochemical reduction of in situ generated aryl diazonium salts has been widely used to covalently modify carbon surfaces (Chehimi 2012; Gooding 2008). Aryl diazonium salts ($N\equiv N^+$-Ar-R) can be easily and rapidly prepared in one step from a wide range of aromatic amines. Electrochemical reduction of diazonium salts can be carried out either by CV or poising the electrode potential. However, it has been recently found that some diazonium salts could be reduced spontaneously by the electrode substrates (Mahouche-Chergui et al. 2011). Among them, one of the electron transfer mediators, anthraquinone (AQ), has been covalently bound to the carbon surface using this method (Aulenta et al. 2011; Seinberg et al. 2008).

Since there is a primary aromatic amine group in the NR molecule and the structure of NR is similar to AQ, we hypothesised that NR could be covalently bound to carbon surfaces via spontaneous reduction of its diazonium salts. This work shows experimental evidence that NR can be covalently grafted to glassy carbon surfaces via spontaneous reduction as well as electrochemical reduction. Our results also revealed that significantly enhanced current densities were obtained for acetate-oxidising microbial bioanodes made of graphite felt modified with NR via spontaneous reduction of its *in situ* generated diazonium salts. Compared with the two previously mentioned methods, spontaneous modification provides a simpler and more environmentally friendly route to covalently graft neutral red to carbon surface.

2. Materials and Methods

2.1 Electrodes Modification

2.1.1 Electrodes and electrode pre-treatment

Two types of carbon electrodes were used, glassy carbon (GC) plates (HTW, Germany, 20 mm × 10 mm × 2 mm with an effective surface area of 20 mm × 10 mm) and graphite felts (Morgan, Australia, 40 mm × 30 mm × 2 mm). GC electrodes were used to study the mechanism of the modification procedure, and graphite felts were utilized as a BES anode for current generation test. Before modification, GC plates were polished successively in 1.0, 0.3, and 0.05 μm alumina slurries for 3 minutes at each grade. The electrodes were thoroughly rinsed with deionised (DI) water and then sonicated in Milli-Q water for 5 min between polishing steps (Liu et al. 2010). After that, the electrodes were dried with a nitrogen gas stream. Graphite felts were immersed successively in 1 M NaOH for 12 h and then 1 M HCl for 12 h, followed by rinsing with DI water.

2.1.2 Electrode modification

NR diazonium salts were in situ generated by diazonation of NR (1 mM) with $NaNO_2$ (1 mM) in HCl (0.5M) solution (Liu et al. 2010). Reduction of NR diazonium salts was carried out either by electrochemical reduction or spontaneous reduction at room temperature. For the electrochemical reduction, electrodes were immersed in NR diazonium salts solution and polarized at a potential of -0.4 V (vs NHE) for 1 h. For the spontaneous reduction, electrodes were just immersed in NR diazonium salts solution for 3 h. Figure 1 shows the proposed mechanism of carbon surface modification with neutral red via both electrochemical and spontaneous reduction of its diazonium salt.

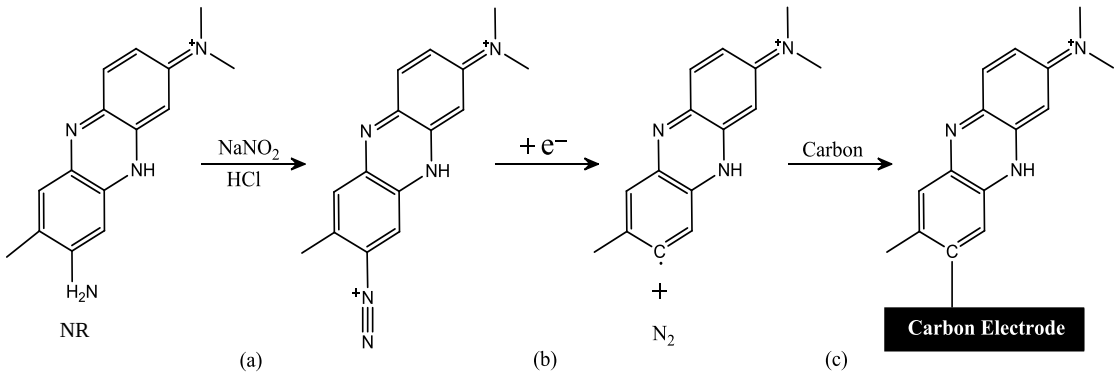

Fig. 1 Proposed mechanism of modification of carbon surface with neutral red via both electrochemical and spontaneous reduction of its diazonium salts (a) *in situ* generation of diazonium salts (b) reduction of diazonium salts (c) C-C bond formation.

To prove that the formation of NR diazonium salts is essential for the NR immobilization, GC electrodes were also immersed in NR (1mM)-$NaNO_2$ (1 mM) solution and NR (1mM)-HCl (0.5M) solution for 3h at room temperature as controls. At the end of modification, all the electrodes were successively sonicated in ethanol, acetonitrile, DI water for 5 min each to thoroughly remove the physically adsorbed species.

2.2 Characterization of NR-modified electrodes

2.2.1 Cyclic voltammetry

The surface electrochemical properties were characterized by cyclic voltammetry (CV). All the CV experiments were carried out in an oxygen-free 0.1 M and pH 7 phosphate buffer solution (PBS) in the bioelectrochemical (BE) cell described below. In order to remove the oxygen from the solution,

the BE cell was sparged with high purity nitrogen for 30 min before the start of the CV. The CV was conducted at a potential window between -0.8 V to 0 V (vs. Ag/AgCl) at various scan rates.

2.2.2 Surface analysis

The surface morphology of the NR-modified electrodes was analysed by a MFP-3D AFM (Asylum Research, USA) placed on an anti-vibration table (Herzan, USA) located in an acoustic isolation chamber (TMC, USA). All samples were imaged in AC mode employing HA-NC Etalon (NT-MDT, Russia) cantilevers, at loading setpoint under 100 mV and scan rate of 0.3 Hz. The surface elemental composition was analysed by XPS. The X-ray photoelectron spectra were collected on an EscaLab 250Xi spectrometer with a monochromated Al Ka source (1486.6 eV), hemispherical analyzer and multichannel detector. The spectra were corrected with reference to carbon C1s (284.5 eV) and analysed using Avantage 4.54 software.

2.2.3 Stability

The stability of the spontaneously NR-modified electrodes was tested by measuring its CV response (0 to −0.8 V vs. Ag/AgCl, 50 mV/s) in 0.1 M PBS (pH 7.0). Firstly, we compared the decrease in current response of three modified electrodes after continuously conducing CV for 100 cycles. Secondly, we measured their remaining CV current response after keeping them in PBS solution in dark.

2.3 Bioelectrochemical cell setup and operation

2.3.1 Bioelectrochemical cell setup

All the electrodes were tested in a membrane-free BE cell (700 mL) with one common reference electrode, one common counter electrode and 4 working electrodes. In particular, the BE cell was fabricated from a cylindrical container of 95 cm diameter and 100 cm height; A Ag/AgCl reference electrode (MF-2052, Bioanalytical Systems, USA) was placed in the centre; working electrodes were arranged in a circle around the reference electrode; and a titanium mesh surrounding the working electrodes was used as the counter electrode. The working electrodes and counter electrode were separated by a plastic basket which was also used to keep the counter electrode in shape (photos of each reactor component are provided in the supplementary information Figure S1). The electrodes were connected to a CHI 1000B Multi-Potentiostat (CH Instruments, Austin, TX, USA), which controlled the potential of each working electrode and recorded the current generated.

2.3.2 BE cell operation

For the CV tests of the electrodes, the BE cell was filled with 600 mL 0.1 M PBS (pH 7.0) and then followed the CV procedure mentioned above. For the current generation tests, the reactor was firstly filled with 400 mL medium and then sparged with high purity nitrogen for 30 min to remove dissolved oxygen. After that, the reactor was inoculated with 200 mL fresh anodic effluent of an existing acetate-fed BE reactor in the lab which was originally started up with the effluent of the reactor reported by Dennis, et al. (2012) and has been continuously running for more than one year. The potential of each anode was set as -0.2 V vs Ag/AgCl and the current generated was recorded by the potentiostat. From day 2.5, the reactor was switched to a continuous mode and the medium was pumped into the reactor at a flow rate of 30 mL/h. A magnetic stirrer was used to mix the solution in the BE cell at a speed of 150 rpm. All the experiments were done at room temperature and the BE cell was covered with aluminium foil to keep the reactor in dark. The medium used was a modified M9 medium with sodium acetate as the electron donor, which contains 6 g/ L Na_2HPO_4, 3 g/L KH_2PO_4, 0.5 g/L NH_4Cl, 0.5 g/L NaCl, 0.1 g/ L $MgSO_4 \cdot 7H_2O$, 14.6 mg/ L $CaCl_2$, 2 g/L NaAc, and 1 mL/L of a mixed trace element solution as described in Rabaey, et al. (2005).

3. Results and Discussion

3.1 Surface modification of GC with neutral red

To check whether NR was covalently bound to the GC surface, GC plates with different modification methods were tested by CV in oxygen free PBS solution. Fig. 2 shows the CV curves obtained. As can be seen from the figure, bare electrodes and electrodes immersed in NR-HCl solutions did not show any obvious reversible redox peaks, while electrodes immersed in NR-$NaNO_2$ and NR-$NaNO_2$-HCl solutions all showed an obvious pair of symmetric peaks with a midpoint redox potential around -0.55V (vs Ag/AgCl) which is very close to the redox potential of NR (-0.52 V vs Ag/AgCl) (Park and Zeikus 1999). The peaks appeared regardless of whether the modification was electrochemically assisted or spontaneous. As all the treated electrodes were successively sonicated in ethanol, acetonitrile, DI water for 5 min at each solution to thoroughly remove the physically adsorbed species before the CV analysis, the redox peaks at this potential must be associated with a form of NR which is strongly bound to the GC surfaces. The forward and reverse peak separation was dependent on peak height and in all cases greater than 0.1 V, indicating quasi-reversibility and/or counter ion mass transfer limitations. The peak height increased approximately 4-fold from the NR-$NaNO_2$ treated electrode (curve 3) to the electrochemically and spontaneously modified electrodes (curves 4 and 5). This peak height increase indicates an

increased effective mediator concentration and/or reduced activation energy on the electrode surface.

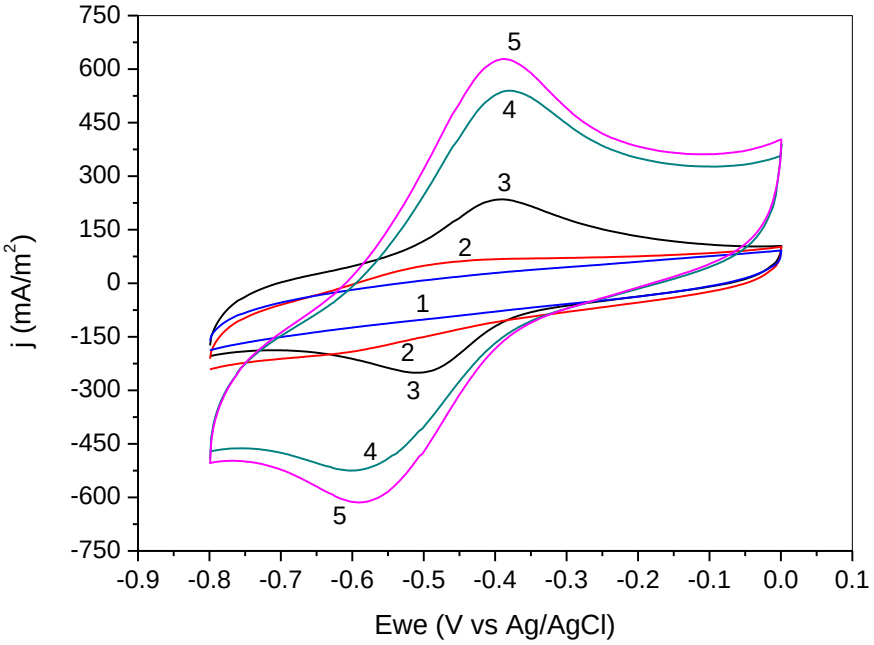

Fig. 2 Cyclic voltammograms of GC plates with different treatments in oxygen-free PBS (0.1M, pH 7.0) at a scan rate of 50 mV/s. Curves: (1) bare; (2) NR-HCl treated; (3) NR-$NaNO_2$ treated; (4) NR-$NaNO_2$-HCl electrochemically modified; (5) NR-$NaNO_2$-HCl spontaneously modified surface.

It also can be seen from the figure that the peak current of NR-$NaNO_2$ treated electrode is much smaller than that for NR-$NaNO_2$-HCl treated ones. This result indicated that the addition of $NaNO_2$ is essential for the NR immobilization and that the acid environment enhances this process, which is likely due to fact that the *in situ* generated diazonium salts are not stable at pH > 2 (Pinson and Podvorica 2005). For the electrodes immersed in NR-$NaNO_2$-HCl solution, both electrochemical reduction method and spontaneous reduction method were applied. The electrodes modified via electrochemical reduction and spontaneous reduction showed similar CV curves with comparable peak height and peak location. This result corroborates our hypothesis that NR could be covalently bound to carbon surface via spontaneous reduction of its diazonium salt. Spontaneous modification with diazonium salts was previously achieved from acid and neutral aqueous solution, and the proposed mechanism for spontaneous grafting was that the diazonium salt obtains an electron from the electrode, resulting in the formation of aryl free radicals (Combellas et al. 2005; Dyke and Tour 2003; Strano et al. 2003).

3.2 Surface characterization of spontaneous NR-modified GC

3.2.1 Atomic force microscope

Fig. 3(a), (b) and (c) show the AFM micrographs of bare GC, electrochemically and spontaneously NR-modified GC surface. The surface roughness (RMS) values for them are 3.8 nm, 4.1nm and 5.0 nm, respectively. The slight increase of surface roughness suggests that few molecular layers of NR are attached to the GC surface. Increasing the spontaneous functionalisation time from 3h to 12h resulted in a significant thickness increase of the NR layer. Fig. 3(d) shows AFM 3D rendering of the boundary area of a spontaneous NR-modified GC plates after 12h functionalisation. The thickness of NR layer in this case reached as high as 40nm. Such a thick layer indicates that NR could form a multilayer structure on the GC surface. The formation of the organic layer is due to the reaction of the aryl radical with the surface, while the growth of the layer is due to the attacks of aryl radical to the first grafted aryl group (Chehimi 2012; Pinson and Podvorica 2005).

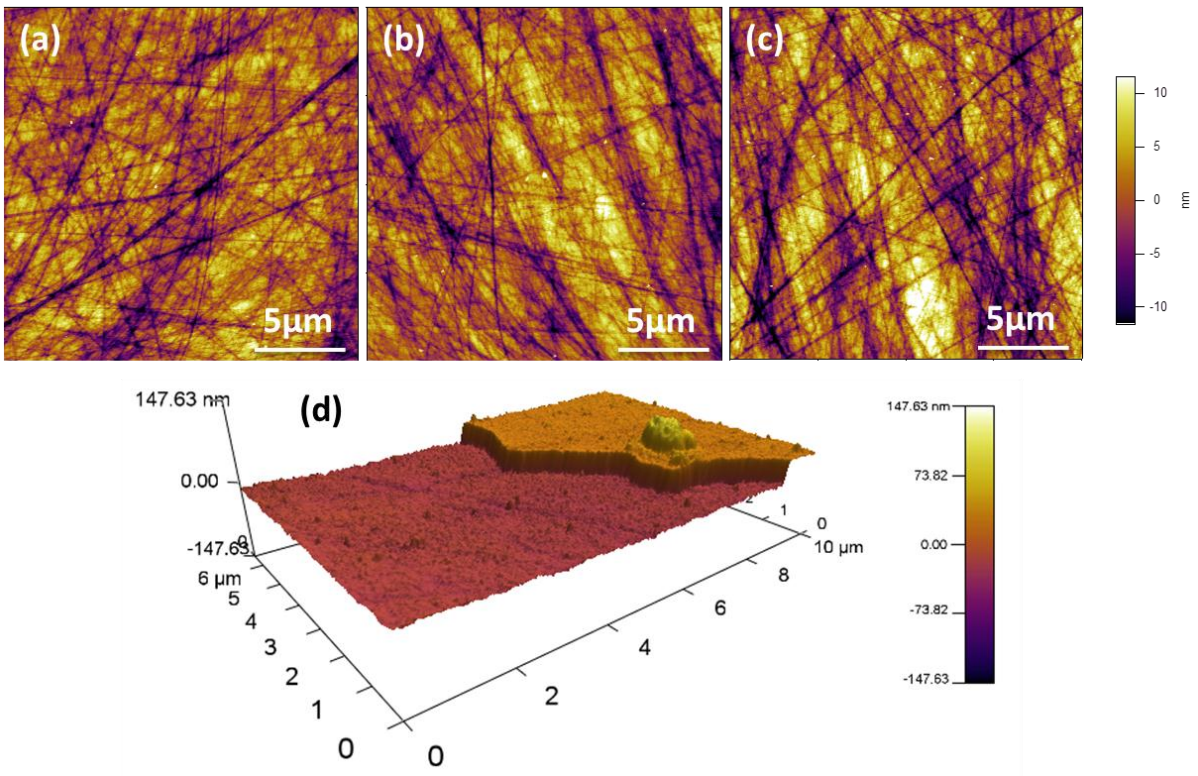

Fig. 3(a) AFM micrographs of Bare GC; (b)electrochemically NR-modified GC; (c) spontaneously NR-modified GC (3 hr modification) and (d) AFM 3D topographical mapping of the boundary area of a spontaneous NR-modified GC plate (12 hr modification)

3.2.2 XPS

All the XPS spectra and peak fitting are included in the supplementary information Figure S2-4. Table 1 displays the XPS results of the bare and NR-coated glassy carbon surfaces. It can be seen that, in comparison to the bare GC, the nitrogen content of NR-coated surfaces increased significantly. Also, chlorine is present in the NR-coated surfaces. The additional nitrogen and the chlorine are characteristic to NR hydrochloride. To distinguish between different nitrogen elements, the high resolution N1s peaks of the NR-coated surfaces were fitted using Avantage 4.54 software. Hereby, a surface that was physically coated with NR by simple adsorption is compared with the spontaneously modified surface described above. The N1s peak of physically coated surface was split into two peaks, one at 399.1 eV (N1sA) and the other one at 400.0 eV (N1sB). According to the literature, N1sA may be attributed to the imine (-N=) and amine (-NH- and $–NH_2$) nitrogens, while N1sB is likely from the positively-charged nitrogen atom in $=N^+(CH_3)_2$ (Chen and Gao 2007a). The N1sA/ N1sB ratio (2.95:1) is very close to the theoretical value for NR (3:1). For the spontaneously modified surfaces, besides the previous two peaks, another peak can be fitted at 401.5 eV, very close to the binding energy of nitrogen in NO_2^- group. The NO_2^- group comes originally from the unreacted $NaNO_2$ and is electrostatically attracted to the electrode surface by the positively-charged $=N^+(CH_3)_2$ group in the NR molecule. The N1sA/ N1sB ratios of the electrochemically modified surfaces was 2.04:1 which is very close to the theoretical value 2:1 for covalently bound NR, if we assume that the $–NH_2$ group in NR was lost during reduction of its diazonium salt (see Figure 1), while the N1sA/ N1sB ratios of the spontaneously modified surfaces is 1.80:1 which is slightly lower than the theoretical value. As a possible explanation for the missing N, it was previously shown that some diazonium groups ($-N^+\equiv N$) can also be transformed to azo groups (-N=N-) and then bound to the electrode surface via N-C bond, and the binding energy for the azo group is around 400 eV (Doppelt et al. 2007). In other words, some $–NH_2$ groups from NR molecules were not transformed to nitrogen gas but ended up with -N=N- groups during spontaneous reduction, which makes the N1sA/ N1sB ratio of the spontaneously modified surfaces less than 2:1.

Table 1. Elemental contents and atomic ratios of bare and NR-coated glassy carbon

Element	Bare GC	NR-coated GC			Binding Energy (eV)	Peak assignment
		Physically absorbed	Spontaneously modified	Electrochemically modified		
C1s (%)	88.99	86.24	88.33	89.63	---	---
O1s (%)	9.96	7.71	6.68	6.07	---	---
Cl2p (%)	**0**	**0.87**	**0.63**	**0.55**	---	---
N1s (%)	**1.06**	**5.17**	**4.36**	**3.76**	---	---
N1s A(%)	0.88	3.86	2.24	2.31	399.1	C-N*=C; -N*H_2
N1s B (%)	0	1.31	1.25	1.13	400.0	=N*$^{+}$$(CH_3)_2$; -N*=N*-
N1s C (%)	0.18	0	0.88	0.32	401.5	-N*O_2
N1s A/ N1s B	---	**2.95:1**	**1.80:1**	**2.04:1**	---	---

3.2.3 Stability of the NR-modified GC Electrodes

The stability of the modified electrode was tested by measuring the decrease in current during potential cycles from 0 to −0.8 V at a scan rate of 50 mV/s in 0.1 M PBS (pH 7.0). The NR-modified glassy carbon showed a high stability. After subjected to 100 cycles, the electrodes showed almost no decrease in the voltammetric current and retained >99% of their initial value. Moreover, longer-term storage stability of the NR-modified electrode was also significant. For instance, the electrodes were found to retain 94.5 ± 3.5% of their initial activity after more than 2 weeks' preservation in PBS solution in the dark. However, only 50.2 ± 5.3% of their initial activity was retained if they were kept in PBS solution exposed to light. This is likely due to the fact that neutral red molecular is not stable when it is exposed to light.

3.3 Performance of bare and NR-modified graphite felts as microbial bioanodes

To test the effect of NR-modification via spontaneous reduction of NR diazonium salts on the current generation during microbial anodic acetate oxidation, graphite felt rather than glassy carbon was used as the anode material because it possesses a higher specific surface area and allows for faster start-up time (Wei et al. 2011). Fig.4 shows the time course of current density for the bare and NR-modified graphite felts. Both electrodes showed a fast start-up as the current started to increase 12 hours after the inoculation. On day 2, the current hit a peak value and started to drop, which was very likely due to the depletion of substrate in the BE reactor because of bacteria growth, biofilm formation and current generation. Thereafter, from day 2.5, the BE reactor was switched to a continuous mode with a feed flow rate of 30 mL/h. After that, the current recovered gradually and then increased significantly in the following few days. The current density of the bare and NR-modified electrodes stopped increasing and started to fluctuate around 1049.9 ± 51.9 mA/m^2 and 4100.6 ± 71.2 mA/m^2 from day 7 and day 7.5, respectively. Thus, the current output of the modified electrode was about 3.7 times higher than the unmodified electrode. In another two tests, the modified electrodes produced 3.1 and 4.1 times more current than the bare surface.

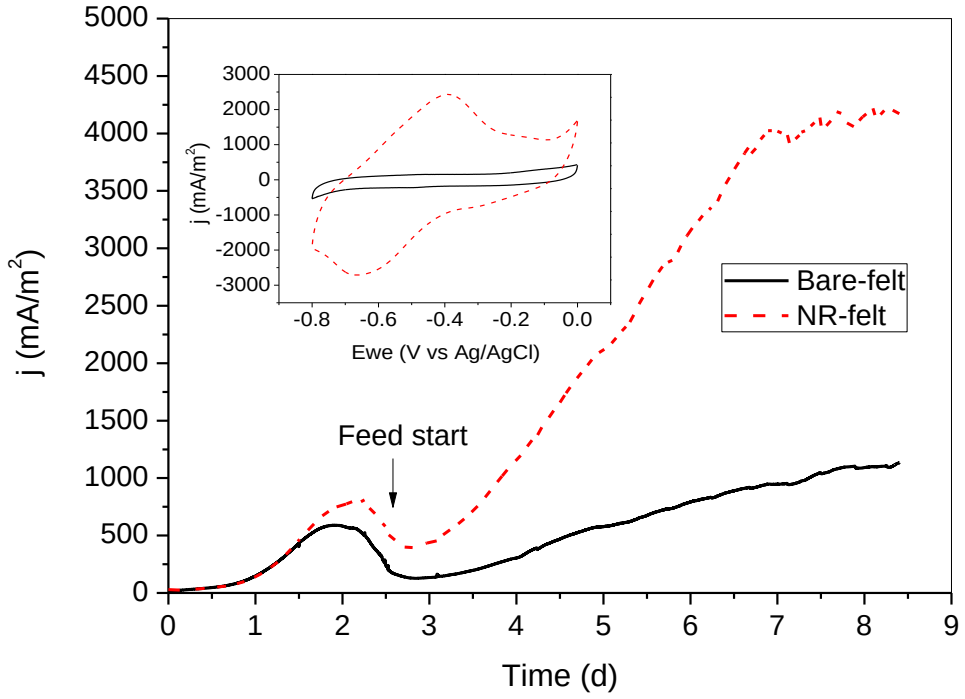

Fig. 4 Current generation of acetate-oxidising BE reactor with bare and NR-modified graphite felts. The inset: cyclic voltammograms (50 mV/s) of bare and NR-modified graphite felts in oxygen-free 0.1 M PBS (pH 7.0).

These results demonstrated that the NR covalently bound to the electrode surface via spontaneous reduction of NR diazonium salts can act as an electron transfer mediator to facilitate electron transfer from bacteria to electrodes. The maximum current density of the unmodified graphite felt in this study is 1.0 A/m^2 which is slightly lower than the 1.1 A/m^2 achieved by Park and Zeikus (2003) using NR-modified woven graphite (via one-step amidation reaction) and 1.5 A/m^2 achieved by Wang et al. (2011) using NR-modified carbon paper (via stepwise amidation reaction) even though the specific surface area of graphite felt is much higher than the others, while NR-modified graphite felt (via spontaneous reduction of NR diazonium salts) produced 3 to 4 times more current than the other NR-modified electrodes. Therefore, spontaneous reduction of NR diazonium salts is an efficient way to covalently bond NR to carbon surface and enhance the performance of bioanodes in bioelectrochemical systems.

4. Conclusion

Immobilization of neutral red onto carbon electrodes was achieved via spontaneous reduction of *in situ* generated NR diazonium salts. The immobilized NR could withstand sonication in water, ethanol and acetonitrile rinses, which indicates a covalent bonding between NR moieties and the electrode surface. The formation of NR diazonium salts was essential for the NR immobilization, indicating that that NR was covalently grafted to the electrode surface via the pathway of reduction of aryl diazonium salts. The NR-modified electrodes showed a good electrochemical activity with a midpoint redox potential of -0.5 V (vs. Ag/AgCl) which is slightly higher than the standard redox potential of NR. AFM results demonstrated NR modification slightly increased the surface roughness and NR might form a multilayer on the surface. XPS demonstrated that most of the primary amino groups ($-NH_2$) of molecular NR were lost during immobilization. These results further proved that NR was covalently grafted to the electrode surface via reduction of its diazonium salts. The NR-modified electrodes showed good stability when stored in PBS solution in the dark. Moreover, the current output of NR-modified graphite felt electrodes when used as bioanodes in BESs were 3.63 ± 0.36 times higher than the unmodified electrodes, which demonstrated the effectiveness of covalently bound NR as insoluble redox mediator during the microbial anodic oxidation of acetate.

Acknowledgements

The authors would like to acknowledge Prof. Korneel Rabaey and Dr. Jens Kroemer at CEMES for being the driver of this research area, Prof. Jurg Keller at AWMC for his continuous mentorship and Prof. Justin Gooding at UNSW for providing facilities and support towards electrode modifications and XPS analysis. This work was performed in part at the Queensland node of the Australian National Fabrication Facility, a company established under the National Collaborative Research Infrastructure strategy to provide nano- and microfabrication facilities for Australia's researchers.

References

Aulenta, F., Ferri, T., Nicastro, D., Majone, M., Papini, M.P., 2011. New Biotechnology 29(1), 126-131.

Chehimi, M.M., 2012. Aryl Diazonium Salts. Wiley-VCH.

Chen, C.X., Gao, Y.H., 2007a. Materials Chemistry and Physics 102(1), 24-30.

Chen, C.X., Gao, Y.H., 2007b. Electrochimica Acta 52(9), 3143-3148.

Combellas, C., Delamar, M., Kanoufi, F., Pinson, J., Podvorica, F.I., 2005. Chemistry of Materials 17(15), 3968-3975.

Dennis, P.G., Guo, K., Imelfort, M., Jensen, P., Tyson, G.W., Rabaey, K., 2012. Bioresource technology 129C, 599-605.

Doppelt, P., Hallais, G., Pinson, J., Podvorica, F., Verneyre, S., 2007. Chemistry of Materials 19(18), 4570-4575.

Dyke, C.A., Tour, J.M., 2003. Nano Letters 3(9), 1215-1218.

Gooding, J.J., 2008. Electroanalysis 20(6), 573-582.

Jeykumari, D.R.S., Narayanan, S.S., 2007. Nanotechnology 18(12).

Liu, G.Z., Chockalingham, M., Khor, S.M., Gui, A.L., Gooding, J.J., 2010. Electroanalysis 22(9), 918-926.

Lowy, D.A., Tender, L.M., 2008. Journal of Power Sources 185(1), 70-75.

Lowy, D.A., Tender, L.M., Zeikus, J.G., Park, D.H., Lovley, D.R., 2006. Biosensors and Bioelectronics 21(11), 2058-2063.

Mahouche-Chergui, S., Gam-Derouich, S., Mangeney, C., Chehimi, M.M., 2011. Chemical Society Reviews 40(7), 4143-4166.

Park, D.H., Kim, S.K., Shin, I.H., Jeong, Y.J., 2000. Biotechnology Letters 22(16), 1301-1304.

Park, D.H., Zeikus, J.G., 1999. Journal of Bacteriology 181(8), 2403-2410.

Park, D.H., Zeikus, J.G., 2003. Biotechnology and Bioengineering 81(3), 348-355.

Pauliukaite, R., Brett, C.M.A., 2008. Electroanalysis 20(12), 1275-1285.

Pinson, J., Podvorica, F., 2005. Chemical Society Reviews 34(5), 429-439.

Popov, A.L., Kim, J.R., Dinsdale, R.M., Esteves, S.R., Guwy, A.J., Premier, G.C., 2012. Biotechnology and Bioprocess Engineering 17(2), 361-370.

Rabaey, K., 2010. Bioelectrochemical systems. IWA Publishing, London; New York.

Rabaey, K., Ossieur, W., Verhaege, M., Verstraete, W., 2005. Water Science and Technology 52(1-2), 515-523.

Seinberg, J.M., Kullapere, M., Maeorg, U., Maschion, F.C., Maia, G., Schiffrin, D.J., Tammeveski, K., 2008. Journal of Electroanalytical Chemistry 624(1-2), 151-160.

Strano, M.S., Dyke, C.A., Usrey, M.L., Barone, P.W., Allen, M.J., Shan, H.W., Kittrell, C., Hauge, R.H., Tour, J.M., Smalley, R.E., 2003. Science 301(5639), 1519-1522.

Wang, K.P., Liu, Y.W., Chen, S.L., 2011. Journal of Power Sources 196(1), 164-168.

Wei, J.C., Liang, P., Huang, X., 2011. Bioresource technology 102(20), 9335-9344.

Supplementary Information

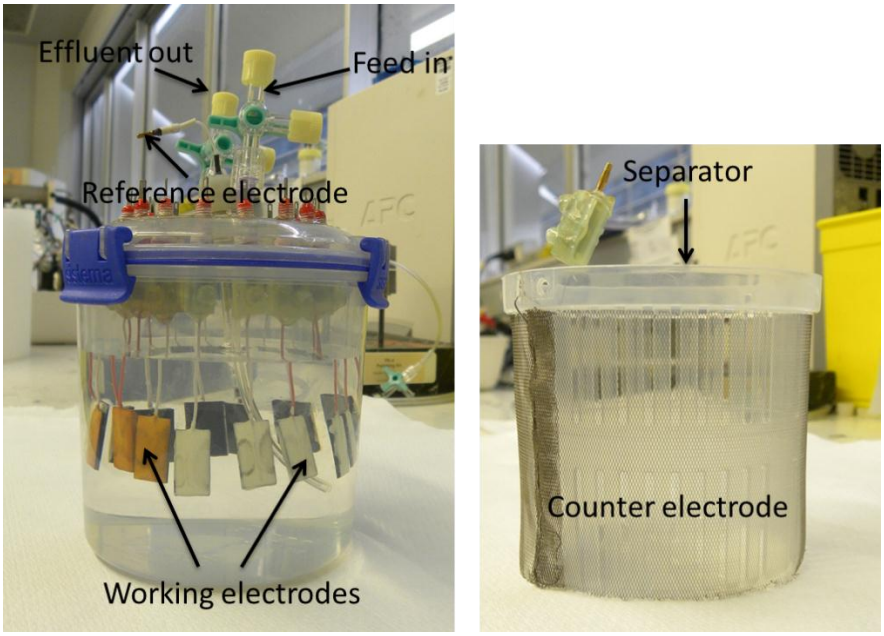

Fig. S1 Photos of the bioelectrochemical cell

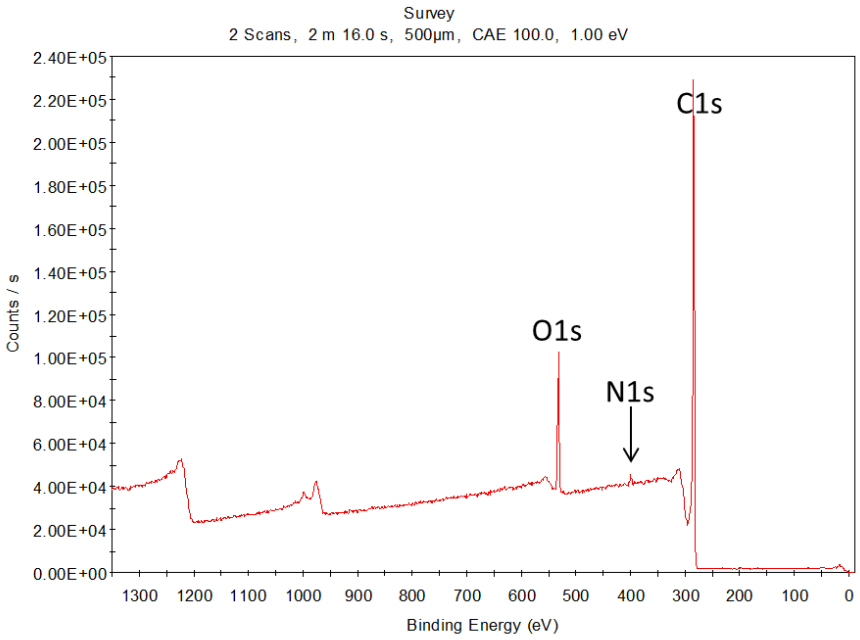

Fig. S2 Surface elements survey of the Bare GC electrode

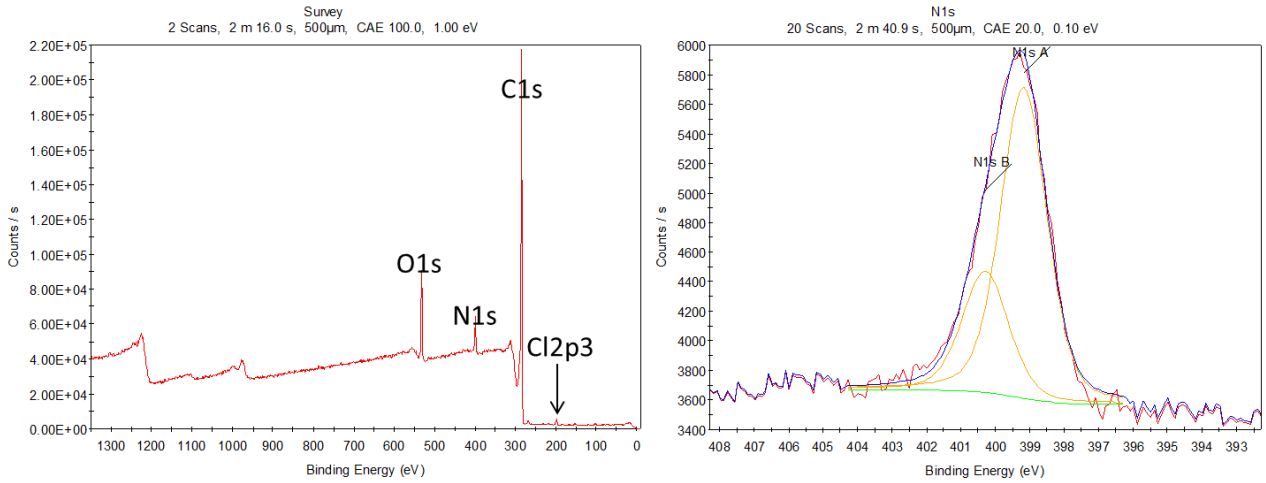

Fig. S3 Surface elements survey and N1s peaking fitting of the GC surface with NR physically absorbed

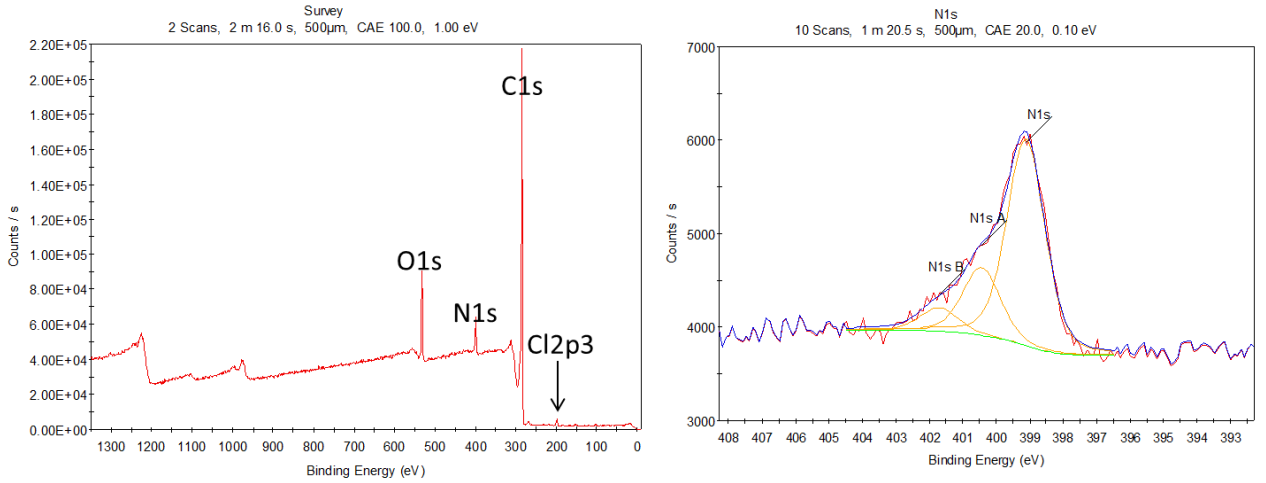

Fig. S4 Surface elements survey and N1s peaking fitting of the GC surface spontaneously modified with NR

Appendix D

Flame oxidation of stainless steel felt enhances anodic biofilm formation and current output in bioelectrochemical systems

Kun Guo,[a,b,c] Bogdan C. Donose,[b] Alexander H. Soeriyadi,[d] Antonin Prévoteau,[a] Sunil A. Patil,[a] Stefano Freguia,[b] J. Justin Gooding,[d] and Korneel Rabaey[a,b,c*]

[a] Laboratory of Microbial Ecology and Technology, Ghent University, Coupure Links 653, B-9000, Ghent, Belgium; [b] Centre for Microbial Electrosynthesis, The University of Queensland, Brisbane, QLD 4072, Australia; [c] Advanced Water Management Centre, The University of Queensland, Brisbane, QLD 4072, Australia; [d] School of Chemistry, University of New South Wales, Sydney, NSW 2052, Australia

* Corresponding author: Tel: +3292645976; E-mail: korneel.rabaey@ugent.be

Submitted to Environmental Science & Technology. 2014.

GRAPHIC ABSTRACT

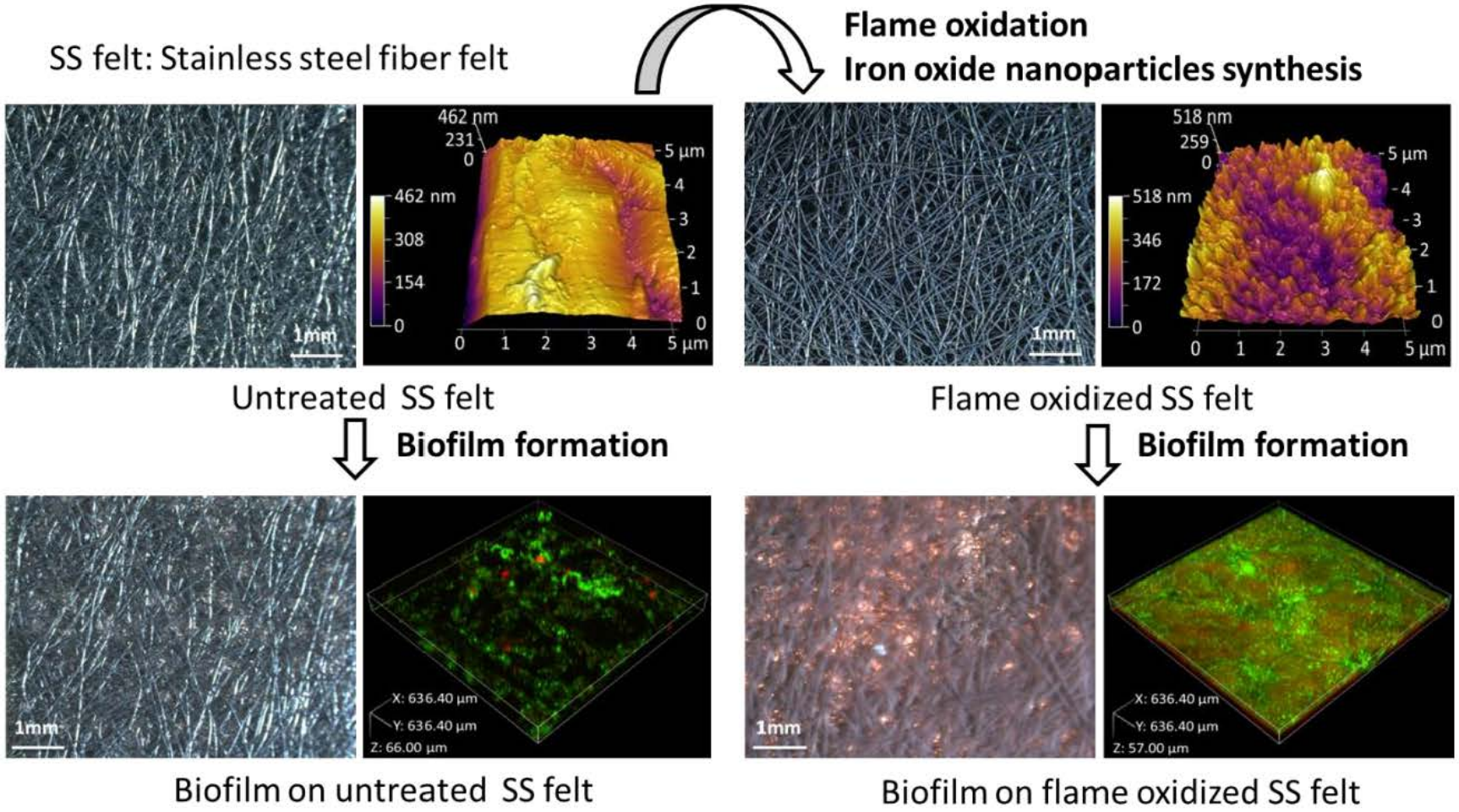

ABSTRACT

Stainless steel (SS) can be an attractive material to create large electrodes for microbial bioelectrochemical systems (BESs), due to its low cost and high conductivity. However, poor biocompatibility limits its successful application today. Here we report a simple and effective method to make SS electrodes biocompatible by means of flame oxidation. Physicochemical characterization of electrode surface indicated that iron oxide nanoparticles (IONPs) were generated *in situ* on SS felt surface by flame oxidation. IONPs-coating dramatically enhanced the biocompatibility of SS felt and consequently resulted in a robust electroactive biofilm formation at its surface in BESs. The maximum current densities reached at IONPs-coated SS felt electrodes were 16.5 times and 4.8 times higher than the untreated SS felts and carbon felts, respectively. Furthermore, the maximum current density achieved with the IONPs-coated SS felt (1.92 mA/cm^2, 27.42 mA/cm^3) is one of the highest current densities reported thus far. These results demonstrate for the first time that flame oxidized SS felts could be a good alternative to carbon-based electrodes for achieving high current densities in BESs. Most importantly, high conductivity, excellent mechanical strength, strong chemical stability, large specific surface area, and comparatively low cost of flame oxidized SS felts offer exciting opportunities for scaling-up of the anodes for BESs.

KEYWORDS

stainless steel felt, surface modification, flame oxidation, iron oxide nanoparticles, biocompatibility, bioelectrochemical systems

INTRODUCTION

Microbial bioelectrochemical systems (BESs) are bioreactors that use microbes as catalysts to drive oxidation and/or reduction reactions at electrodes.[1] The applications of BESs range from wastewater treatment and electricity generation to the production of valuable chemicals.[2-5] Currently, the practical application of this technology is limited by low current density and high cost.[6, 7] Since electrodes play a key role in determining the current density and the cost of BESs, they have drawn increasing interest with regard to the materials and structures. The ideal electrode for BESs should possess following features: (1) high conductivity; (2) good biocompatibility; (3) strong chemical stability; (4) large specific surface area; (5) excellent mechanical strength; and (6) low cost.[8, 9]

Carbon materials have been widely used as electrodes in BESs because of their biocompatible, corrosion-resistant and inexpensive properties. However, scale-up of carbon-based electrodes is limited by relatively high resistivity and low mechanical strength.[7, 9, 10] Stainless steel (SS) materials are commonly used in industries, due to their good corrosion resistance, great mechanical strength, high conductivity and easily up-scalable characteristics. The major limitation in their use as anodes in BESs is poor biocompatibility and relative low current density comparing to carbon materials.[11, 12] Recently, high current density was achieved on SS foam using soil leachate as microbial inoculum.[13] However, the price of the SS foam (thickness 6.35 mm) is about 2.5 and 26 times higher than carbon foam (thickness 6.35 mm) and carbon felt (thickness 6.35 mm), respectively (calculated based on the 2014 values from http://www.goodfellow.com and http://www.alfa.com). Therefore, surface modifications of inexpensive SS with cheap and biocompatible materials is considered as an attractive strategy to utilize SS electrodes for several BES applications. Surface modification with carbon nanoparticles has been proved to be an efficient way to enhance the biocompatibility and current production of SS electrodes. Recently, it is reported that graphene coating increased the current density of SS felt from 0.0035 to 0.61mA/cm^2 in BESs.[14]

Besides CNTs, iron oxides are also biocompatible and have been used to modify carbon electrodes to enhance their performance in BESs.[15-117] More importantly, it has been demonstrated that iron oxide could be *in situ* generated on SS surface via oxidation of SS at high temperature or by exposure to oxidizing flame.[18-20] Hence, iron oxide coated SS electrodes might be attractive for BESs as they fit the criteria outlined before. Sintered SS fibre felt (SS felt) is a commercially available and cheap filter material for gas and liquid filtration. It has an open 3D macroporous structure with large specific surface area, high corrosion resistance, excellent mechanical strength

and uniform aperture distribution.[21] These properties make it an ideal backbone for electrode design in BESs. Flame oxidation of SS is an energy efficient, rapid and scalable process compared with the high temperature oxidation in furnace. Therefore, the aim of this study was to synthesize iron oxide nanoparticles (IONPs) on SS felt via the flame oxidation method and to investigate its performance as an anode in BESs.

MATERIALS AND METHODS

Electrode Preparation and Modification.

SS felt (316L, Lierfilter, China) was cut into pieces of 20 × 10 × 0.7 mm (projected surface area 2 cm^2, volume 0.14 cm^3) as substrate. The specifications of this SS felt are shown in Table S1. Oxidation of SS felt was conducted using a Bunsen burner employing natural gas as fuel. In order to yield a strong oxidizing flame, the air hole was completely open to generate a 13 cm long "roaring" blue flame. Before insertion into the flame, the SS felt was thoroughly cleaned in acetone and dried by a stream of nitrogen gas. Then, the SS felt was perpendicularly inserted into the tip of the inner flame (~1200 °C) that was 5 cm above the nozzle of burner. After 60 s, the SS felt was removed from the flame and allowed to cool to ambient temperature.

Electrode Surface Characterization.

The BET surface area of the untreated and flame oxidized SS felt was determined with a Micromeritics Tristar 3000 using nitrogen gas.[22] The surface capacitance was analyzed using cyclic voltammetry (CV) in M9 medium at different scan rates (2.5, 5, 10, 25, 50 and 80 mV/s). The surface topography was characterized by stereomicroscopy (Leica S8APO, Belgium), scanning electron microscopy (SEM, JEOL 7800F, operated at 5 kV), and atomic force microscopy (AFM, MFP-3D, Asylum Research, USA).[23] The surface chemical composition and the electrochemical properties were analyzed by X-ray photoelectron spectroscopy (XPS),[23] confocal Raman microscopy,[24] and cyclic voltammetry (CV).

BES setup and operation.

The efficacy of both untreated and flame oxidized SS felt electrodes as microbial anodes was tested in a custom-made BES reactor (Fig. 1). This high-throughput BES reactor allowed within an identical geometry simultaneous testing of eight working electrodes (WE, SS felt anodes) with the use of one counter electrode (CE, SS mesh cathode), and one reference electrode (RE, Ag/AgCl 3 M KCl). WEs 1, 3, 5, and 7 were untreated SS felts, and the others were flame oxidised SS felts. All

electrochemical experiments were conducted with a CHI 1000C Multi-Potentiostat (CH Instruments, Austin, TX, USA). The anodic chamber was filled with 400 mL of modified M9 medium (pH = 7) with 2 g/L (24 mM) sodium acetate as the electron donor.[25] The medium was sparged with nitrogen for 30 min to ensure anaerobic conditions and then inoculated with 50 mL fresh anodic effluent of an existing acetate-fed BES which is rich in *Geobacter*.[26] The cathodic chamber was filled with oxygen-free M9 buffer medium. The potential of each anode was set at -0.2 V *vs.* Ag/AgCl and current generation was recorded using chronoamperometry (CA). A magnetic stirrer was used to mix the solution continuously in the BES at a speed of 350 rpm unless stated otherwise. These experiments were conducted in the dark at 28 °C in a temperature-controlled room.

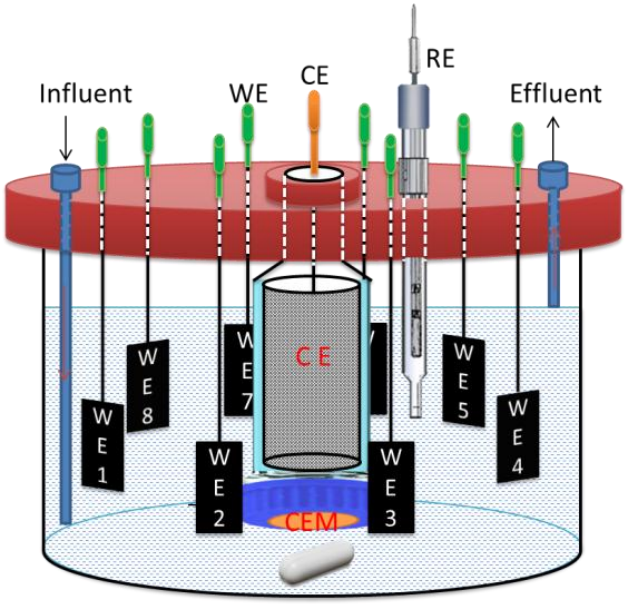

Figure 1. Schematic of the BES reactor setup

Biofilm Characterization.

At the end of CA experiment, CV was conducted in the same medium to investigate the electrochemical activity of the biofilms at the electrodes under acetate turnover condition. CVs were performed within a potential window between -0.8 V and 0.2 V (vs. Ag/AgCl) at a scan rate of 1 mV/s. After completion of electrochemical experiments, half of the biofilms on the electrodes were observed directly by a stereomicroscopy (Leica S8APO, Belgium), and the other half were subjected to Live/Dead staining. The stained biofilms were visualized and z-stacks were captured using a confocal laser scanning microscope (CLSM, Nikon C1, The Netherlands). CLSM image data were processed by Fiji software.

RESULTS

Electrode Surface Modification and Characterization.

After flame oxidation, the weight of the electrodes increased by 3.24 ± 0.65% (Average ± SD, n = 3), and the BET surface area increased from 461 to 719 m^2/m^2. Based on the CVs in M9 medium (Fig. S1), the apparent surface capacitance of the untreated and treated electrodes are 1.94 and 3.65 mF/cm^2, respectively. The increase of the capacitance is consistent with the increase of the BET surface area. Figure 2 shows the surface topography of the untreated and flame oxidized SS felts.

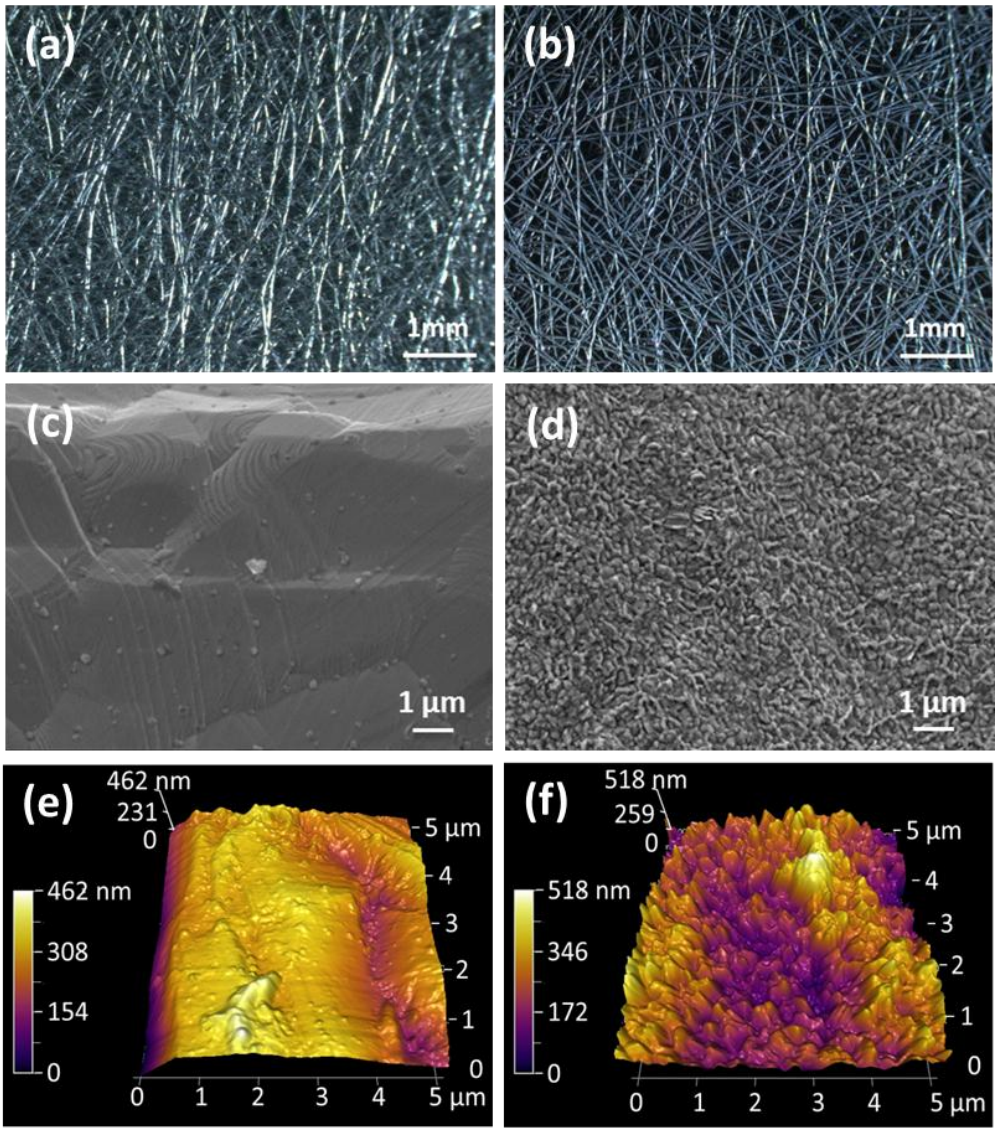

Figure 2. Representative light microscope images (a, b), SEM images (c, d), and AFM micrographs (e, f) of untreated (left column) and flame oxidized (right column) SS felt electrodes.

Stereomicroscope images (Fig. 2a and 2b) provide a macro-scale view of the materials and clearly show the 3D, fibrous and porous structure of the SS felts. The diameter of the SS fiber is about 25 μm. The oxidized SS surface became darker and less shining than the untreated SS surface. SEM images of single SS fibres (Fig. 2c and 2d) reveal that the oxidized SS electrodes were uniformly covered with nanoparticles of diameter ranging from 100 to 400 nm. AFM images (Fig. 2e and 2f) show the 3D structure of the electrode surface. AFM results also reveal that the surface average roughness (Ra) of the untreated and oxidized surfaces were 75 and 151 nm, respectively. These results demonstrate that flame oxidation of the SS felt uniformly generated nanoparticles on the SS felt surface.

In order to understand the surface chemical composition and the electrochemical properties of the untreated and SS felts, XPS, Raman microscopy, and CV experiments were conducted (Fig. 3). As can be seen from Fig. 3a and 3b, after flame oxidation, the surface iron and oxygen content increased from 4.76% and 42.24% to 13.25% and 54.61% respectively, while the carbon and chromium content decreased from 45.59% and 1.76% to 28.37% to 0%, respectively. The detailed surface atomic composition of the untreated and flame oxidized electrode defined by XPS is reported in Table S2. Further high-resolution narrow scans of the iron and oxygen, and peak fitting (Fig. S2) indicates that: 1) 10.9% of the iron in the untreated surface could be assigned to Fe(0), while the iron in oxidized samples were just iron oxide and 2) more oxygen in the oxidized samples were attributed to the metal oxides (84.8% compared to 52.92%). Raman spectra indicate that the surface of the untreated SS felt was mainly composed of γ-FeOOH, $MnCr_2O_4$, and $FeCr_2O_4$ (Fig. 3c, peak assignment based on literature[27-30]), while the flame oxidized SS felt surface was dominated by α-Fe_2O_3 (Fig. 3d, peak assignment based on literature[28, 29]). The CVs further highlight (Fig. 3e and 3f) that the iron oxide was generated on SS felt surface after flame oxidation. The redox peaks in the -0.4 to 0 V region at both untreated and flame oxidized SS felts are likely due to a reversible transition of oxidation state of Fe/Cr in the solid state,[30, 31] while the reduction peaks at -0.6 V and -0.8 V at the flame oxidized SS felt could be attributed to the reductive dissolution of Fe_2O_3 as Fe^{2+} in the solution.[32-34] These results indicate that the nanoparticles generated on SS felt surface by flame oxidation are iron oxide nanoparticles (IONPs).

The chemical composition of the surface of untreated SS felt is quite complex, because it contains a chromium-rich oxide film (~5 nm) that prevents it from further oxidation.[30] Furthermore, there could also be adventitious organic matter adsorbed on the SS mesh surface. When such material is exposed to high temperature oxidizing flame, the adsorbates burns off, the passive layer breaks down and rapid corrosion occurs. Therefore, the substantive drop in carbon ratio is likely due to the

fact that the flame treatment burns off most of the adsorbed adventitious organic materials, while the increase in the iron and oxygen contents is due to the generation of iron oxide on the SS surface.

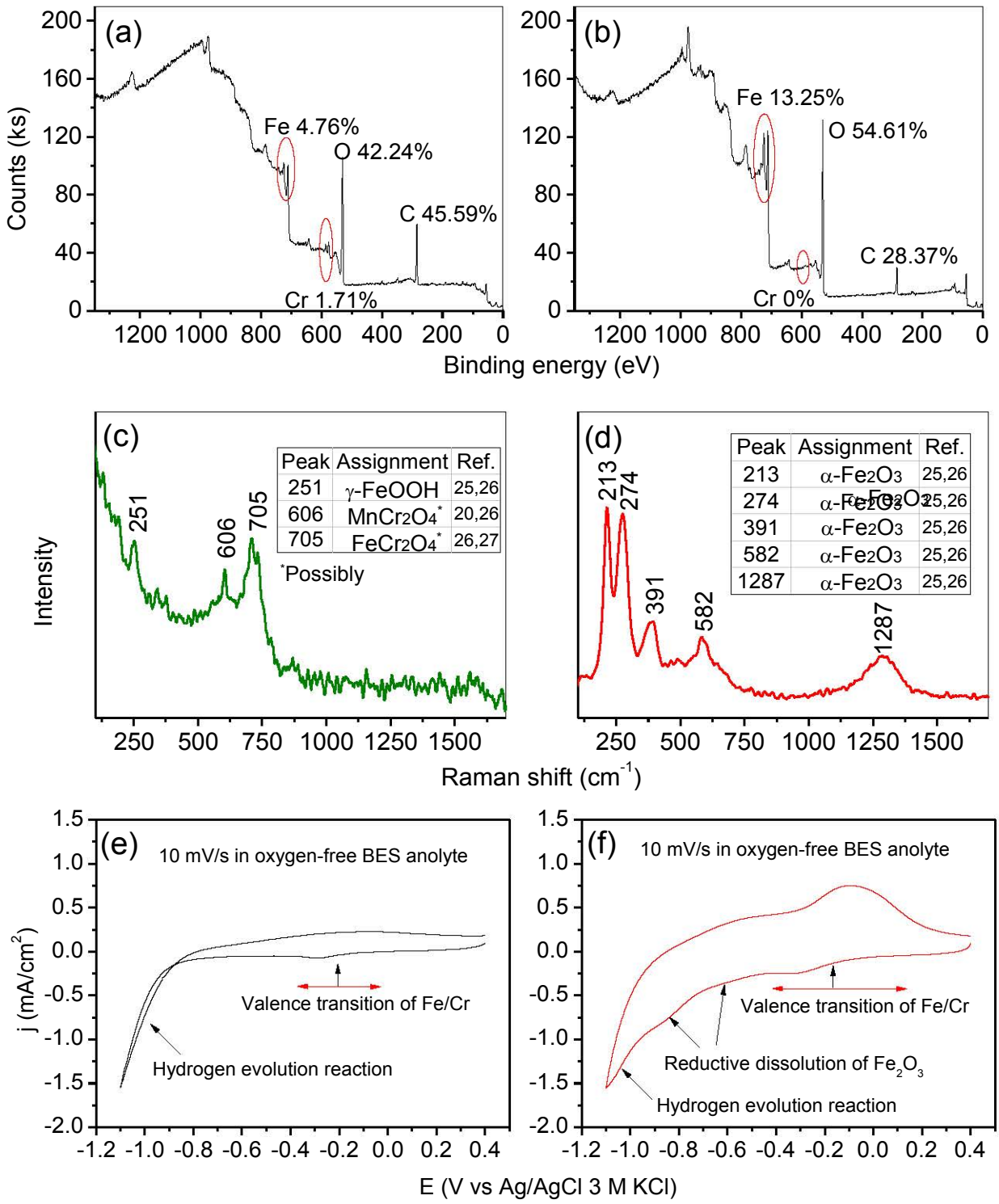

Figure 3. Representative XPS spectra (a, b), Raman spectra (c, d), and CVs (e, f) of untreated (left column) and flame oxidized (right column) SS felt electrodes.

Bioelectrocatalytic Performance.

Fig. 4 shows the bioelectrocatalytic current generation over time at the untreated and flame oxidised electrodes. The reactor was firstly run in a fed-batch mode to allow the bacteria to attach to the electrodes. After three batch cycles, the reactor was switched to a continuous-flow mode with a flow rate of 40 mL/h oxygen free medium to maintain the maximum current output. It can be seen from the figure that the bioelectrocatalytic current at the oxidized electrodes increased very quickly during the batch mode operation and reached a maximum current density (J_{max}) of 1.92 ± 0.08 mA/cm^2 (27.42 ± 1.14 mA/cm^3) in the third batch cycle. Whereas the current at the untreated electrodes, increased slowly and attained a J_{max} of 0.06 ± 0.01 mA/cm^2 (0.85 ± 0.14 mA/cm^3) during the same experimental period. When the reactor was switched to continuous mode operation, the current density at the flame-oxidized electrodes stabilized at around 1.51 ± 0.10 mA/cm^2 (21.56 ± 1.38 mA/cm^3) from day 7, while the current density at the untreated electrodes gradually increased and stabilized at around 0.11 ± 0.01 mA/cm^2 (1.51 ± 0.10 mA/cm^3) from day 12. In order to test the effect of mass transfer on the current density, the stirring rate was increased from 350 rpm to 500 rpm on day 11, and then to 650 rpm on day 12. The current density of the oxidized electrodes sharply increased by 7% and 5% on each step of the stirring rate increase, while the current density of the untreated electrodes gradually increased by 14% and 7% accordingly. On day 13, the stirring rate was switched back to 350 rpm. The current density of the untreated and treated electrodes both dropped sharply and stabilized at their original values. These observations demonstrate that the current density of the electrodes could be enhanced by improving the mass transfer.

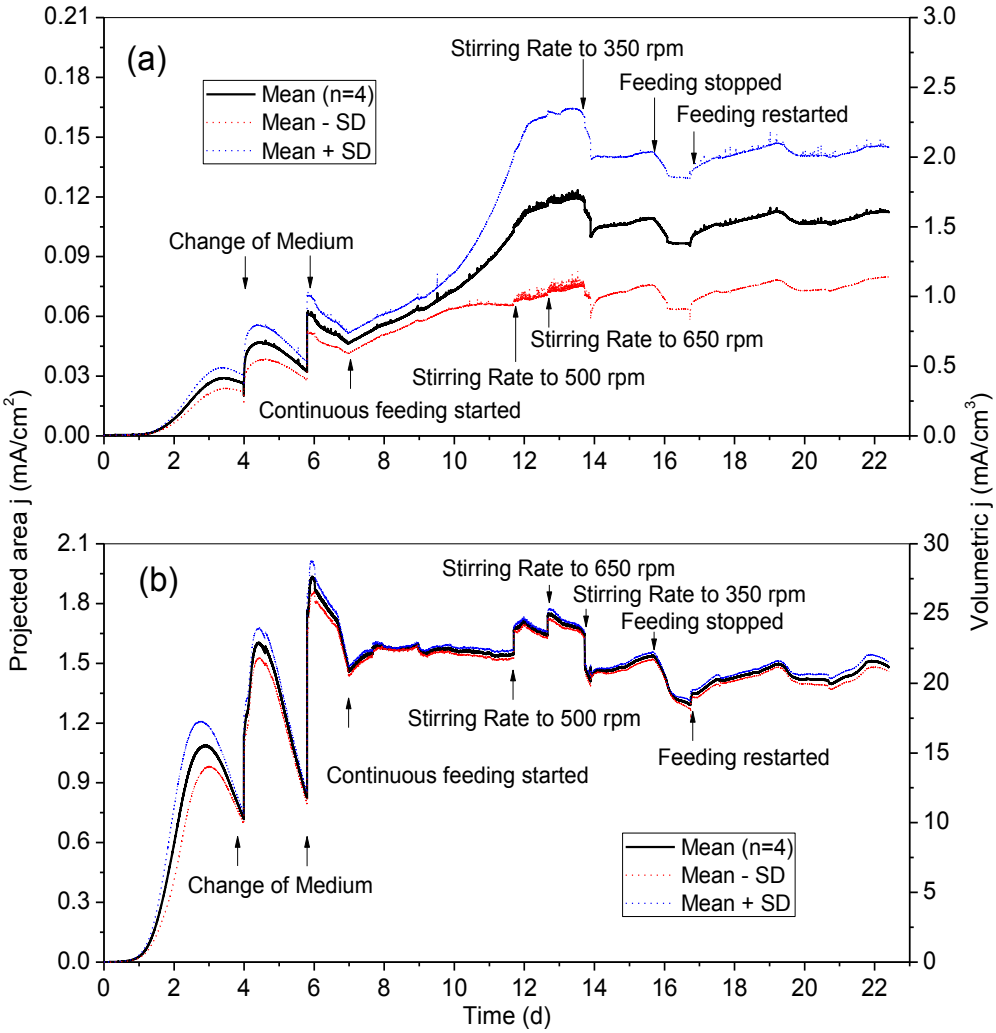

Figure 4. Bioelectrocatalytic current generation at untreated (a) and flame oxidized (b) SS felt electrodes. (Chronoamperometry, anodic potential set at - 0.2 V *vs.* Ag/AgCl)

Characterization of Electrocatalytically Active Biofilm.

After CA experiments, CV was conducted in the same medium to investigate the electrochemical activity of the biofilms at the electrodes under acetate turnover condition. The CVs at both untreated and flame oxidized electrodes exhibited the classic sigmoidal shape for anodic biofilms under turnover conditions.[24] At both untreated and flame oxidized electrodes, the acetate oxidation current started around -0.45 V *vs.* Ag/AgCl and reached a plateau from -0.2 V (Fig. 5a and 5b). These plateau current densities are logically similar to the current densities recorded at the end of the respective CA experiments. These results indicate the biofilm-associated extracellular electron transfer to electrodes and thus the generation of current.

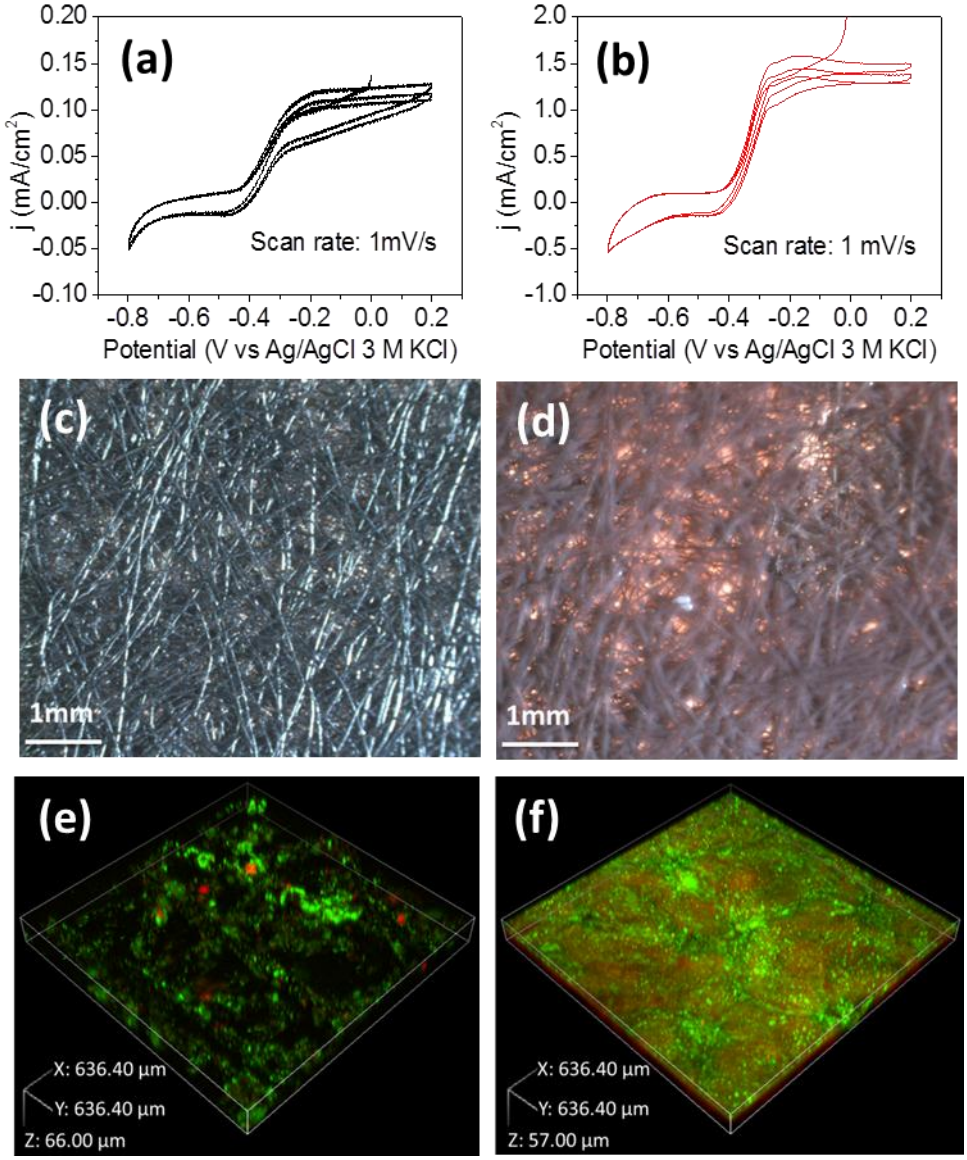

Figure 5. Representative turnover CVs (a, b), light microscope images (c, d), and CLSM images (e, f) of biofilms on untreated (top row) and flame oxidized (bottom row) SS felt electrodes.

Stereo microscopy images clearly show that a thick and reddish biofilm uniformly covered the whole surface area of the oxidized SS felt electrode, while almost no biofilm was observed on the untreated SS felt electrode (Fig. 5c and 5d). The red colour of the biofilm indicates that the oxidized electrodes were colonized with large amounts of *Geobacter* species.[25] It can be seen from CLSM biofilm images (Fig 5e and 5f) that bacteria only attached to certain points on the untreated SS felt, but covered the entire electrode surface of oxidized SS felt and formed a thick (~40 µm) biofilm. These results clearly reveal that flame oxidation considerably enhances the biocompatibility of SS

felt electrodes and the maximum current output is positively correlated with the biofilm coverage on these electrodes.

DISCUSSION

The electrochemical and microscopic results clearly demonstrate that the flame oxidation of SS felt dramatically enhanced the anodic biofilm formation and current output in BESs. It has been shown that an increase in surface roughness on stainless steel from 40 to 300 nm significantly increases the bacterial adhesion strength.[36] It has also been reported that iron oxide coating consistently enhances the bacterial adhesion to carbon and glass surfaces due to its positive charge and good biocompatibility.[17, 37] In the presented study, flame oxidation not only increased the surface roughness of SS felt from 75 to 151 nm but also burned off the chromium-rich passive layer and generated IONPs on the SS felt surface. Thus, the significant improvement of biocompatibility and current output of SS felt is attributed to a combined effect of the surface topography and surface chemical composition.

Flame treatment broke down the chromium oxide layer and generated iron oxide layer on the top of the surface. Thus, flame treatment might make SS felt surface less corrosion-resistant. However, cyclic voltammetry results (Fig. S3) indicate that flame oxidized SS felts are slightly more corrosion-resistant than untreated SS felt. Both the untreated and flame oxidizes SS felts show an onset potential of corrosion at about 0.4 V vs. Ag/AgCl), but the lower positive currents recorded after flame treatment suggest a decrease of the corrosion kinetics. Since the onset potential of corrosion current is 0.6 V higher than the normal operational potential of anode (-0.2 V vs Ag/AgCl), theoretically no corrosion will occur to the untreated and treated SS felt anode in BESs. Practically, no corrosion current was observed on the anodic biofilm CVs in Figure 5a and 5b up to 0.2V vs Ag/AgCl. Therefore, the corrosion resistance of the untreated and treated SS felts is high enough for the purpose of using them as bioanodes in BESs.

Table 1 summarizes the maximum current densities achieved so far with different 3D-structured anode materials in acetate-fed BESs. In comparison to other reported 3D-structured materials, flame oxidized SS felt shows very good bioelectrocatalytic performance. In terms of projected surface area current density, the oxidized SS felt delivers slightly lower current output than the carbon fibre mat, CNT-RVC and SS foam. On the other hand, taking the thickness of the electrode into account, the volumetric current density of the oxidized SS felt (27.42 mA cm^{-3}) is the highest amongst them. To our knowledge, this value represents the highest reported values for acetate-fed BESs. Due to different reactor designs, medium compositions, microbial inoculum, operational conditions

(temperature, convection, potential, etc.), it may be not very convincing to compare our results with the existing reports. Hence, we also tested carbon felt electrodes in the same reactor under the similar set of experimental conditions.[26] The projected surface area current density and the volumetric current density of flame oxidized SS felt are 23% and 4.8 times, respectively, higher than carbon felt. These results clearly demonstrate that flame oxidized SS felt electrodes could be a good alternative to carbon-based electrodes for achieving high current densities in BESs.

Table 1. Bioelectrocatalytic current densities obtained at different electrode materials in acetate-fed BESs.

Electrode material	$j_{projected}$[a] (mA/cm^2)	$j_{volumetric}$[b] (mA/cm^3)	T[d] (°C)	Acetate (mM)	Bulk Price[e] ($/m^2$)	Ref.
Carbon fibre mat	3.0	20	35	10	NA	38
CNT-RVC[c]	6.8	10.3	20	20	NA	24
Carbon felt	1.56	4.72	28	24	50-150	26
SS foam	7.25	11.42	40	20	2500-5000	13
Untreated SS felt	0.0035	0.035	33	12	30-100	14
Graphene-SS felt	0.61	6.1	33	12	NA	14
Untreated SS felt	0.11	1.57	28	24	30-100	This study
Oxidized SS felt	1.92	27.42	28	24	NA	This study

[a] Projected area current density. [b] Volumetric current density. [c] CNTs-coated reticulated vitreous carbon.
[d] Operation temperature. [e] 2014 values from http://www.alibaba.com/

Table 1 also lists the bulk prices of carbon felt, SS foam, and SS felt. Since SS foam is not widely used and produced, its current price is tens of times higher than the carbon felt and SS felt. Thus, scale-up of SS foam for BES anode might be limited by the high price in the near future. SS felt is commercially available at large scale and its price is about 50% lower than carbon felt, so it has a great advantage in capital cost. In this study, Bunsen burner loaded with natural gas (flow rate 1L/min) was used to treat SS felt and it took one min to treat 2 cm^2 of SS felt. Thus, 5 m^3 of natural gas is needed for the treatment of 1 m^2 of SS felt. The price of natural gas in Europe is around 0.75 $/$m^3$ (Source from Http://ec.europa.eu/eurostat/), thus the cost for flame treatment of SS felt is about 3.75 $/$m^2$. Even after combining both the material cost and the treatment cost, the price of flame oxidized SS felt remains significantly cheaper than carbon felt electrode. More importantly, large scale flame sprayers are also available. If larger flame sprayer rather than Bunsen burner is used, the time needed for treatment of per square metre of SS felt will be dramatically reduced.

In summary, as stated earlier, the advantages of SS felt over carbon materials include high conductivity, good corrosion resistance, excellent mechanical strength, scale-up possibility and low capital cost. Flame oxidation easily generates *in situ* iron oxide film on SS felt and make its surface biocompatible without reducing the corrosion resistance. Notably, flame oxidized SS felt meets all requirements of the ideal anode materials for BESs. Most importantly, bigger size SS felts are commercially available and they can be easily fabricated into different configurations (e.g. pleated felt). Moreover, flame spray is also an energy efficient, rapid, and scalable process. Attributed to the aforementioned advantages, flame oxidized SS felt holds exciting opportunities for scaling-up of anode and for achieving high current densities in BESs.

ASSOCIATED CONTENT

Supporting Information. Two additional tables and three figures. This material is available free of charge via the Internet at http://pubs.acs.org.

AUTHOR INFORMATION

Corresponding Author. *Email: korneel.rabaey@ugent.be; Phone: + 32 (0) 9/264 59 76; Fax: + 32 (0) 9/264 62 48

ACKNOWLEDGMENT

The authors would like to acknowledge Mr Zhi Zhang from UQ for the SEM imaging and Mrs Chenjing Shang from Ugent for the CLSM imaging. KG is supported by UQ IPRS and UGent Joint-PhD co-funding scholarships. KR is supported by the European Research Council Starter Grant “ELECTROTALK”. This work was performed in part at the Queensland node of the Australian National Fabrication Facility, a company established under the National Collaborative Research Infrastructure Strategy to provide nano and micro-fabrication facilities for Australia’s researchers.

REFERENCES

(1) Rabaey, K.; Rodriguez, J.; Blackall, L. L.; Keller, J.; Gross, P.; Batstone, D.; Verstraete, W.; Nealson, K. H., Microbial ecology meets electrochemistry: electricity-driven and driving communities. *Isme J.* **2007,** *1*, (1), 9-18.

(2) Min, B.; Logan, B. E., Continuous electricity generation from domestic wastewater and organic substrates in a flat plate microbial fuel cell. *Environ. Sci. Technol.* **2004,** *38*, (21), 5809-5814.

(3) Du, Z. W.; Li, H. R.; Gu, T. Y., A state of the art review on microbial fuel cells: A promising technology for wastewater treatment and bioenergy. *Biotechnol. Adv.* **2007,** *25*, (5), 464-482.

(4) Guo, K.; Tang, X. H.; Du, Z. W.; Li, H. R., Hydrogen production from acetate in a cathode-on-top single-chamber microbial electrolysis cell with a mipor cathode. *Biochem. Eng. J. l* **2010,** *51*, (1-2), 48-52.

(5) Rabaey, K.; Rozendal, R. A., Microbial electrosynthesis - revisiting the electrical route for microbial production. *Nat. Rev. Microbiol.* **2010,** *8*, (10), 706-716.

(6) Logan, B. E., Scaling up microbial fuel cells and other bioelectrochemical systems. *Appl. Microbiol. Biot.* **2010,** *85*, (6), 1665-1671.

(7) Rozendal, R. A.; Hamelers, H. V. M.; Rabaey, K.; Keller, J.; Buisman, C. J. N., Towards practical implementation of bioelectrochemical wastewater treatment. *Trends Biotechno.* **2008,** *26*, (8), 450-459.

(8) Logan, B. E.; Hamelers, B.; Rozendal, R. A.; Schrorder, U.; Keller, J.; Freguia, S.; Aelterman, P.; Verstraete, W.; Rabaey, K., Microbial fuel cells: Methodology and technology. *Environ. Sci. Technol.* **2006,** *40*, (17), 5181-5192.

(9) Zhou, M. H.; Chi, M. L.; Luo, J. M.; He, H. H.; Jin, T., An overview of electrode materials in microbial fuel cells. *J. Power Sources* **2011,** *196*, (10), 4427-4435.

(10) Rosenbaum, M. A.; Franks, A. E., Microbial catalysis in bioelectrochemical technologies: status quo, challenges and perspectives. *Appl. Microbiol. Biot.* **2014,** *98*, (2), 509-518.

(11) Dumas, C.; Mollica, A.; Feron, D.; Basseguy, R.; Etcheverry, L.; Bergel, A., Marine microbial fuel cell: Use of stainless steel electrodes as anode and cathode materials. *Electrochim. Acta* **2007,** *53*, (2), 468-473.

(12) Dumas, C.; Basseguy, R.; Bergel, A., Electrochemical activity of Geobacter sulfurreducens biofilms on stainless steel anodes. *Electrochim. Acta* **2008,** *53*, (16), 5235-5241.

(13) Ketep, S. F.; Bergel, A.; Calmet, A.; Erable, B., Stainless steel foam increases the current produced by microbial bioanodes in bioelectrochemical systems. *Energ. Environ. Sci.* **2014**, 7, 1633-1637.(14) Hou, j.; Liu, Z.; Yang, S.; Zhou, Y. Three-dimensional macroporous anodes based on stainless steel fiber felt for high-performance microbial fuel cells. *J. Power Sources* **2014,** 258, 204-209.

(15) Ling, D.; Hyeon, T., Chemical design of biocompatible iron oxide nanoparticles for medical applications. *Small* **2013,** *9*, (9-10), 1450-66.

(16) Lowy, D. A.; Tender, L. M.; Zeikus, J. G.; Park, D. H.; Lovley, D. R., Harvesting energy from the marine sediment-water interface II - Kinetic activity of anode materials. *Biosens. Bioelectron.* **2006,** *21*, (11), 2058-2063.

(17) Wang, P.; Lai, B.; Li, H. R.; Du, Z. W., Deposition of Fe on graphite felt by thermal decomposition of Fe(CO)(5) for effective cathodic preparation of microbial fuel cells. *Bioresource technol.* **2013,** *134*, 30-35.

(18) Huntz, A. M.; Reckmann, A.; Haut, C.; Sévérac, C.; Herbst, M.; Resende, F. C. T.; Sabioni, A. C. S., Oxidation of AISI 304 and AISI 439 stainless steels. *Materials Sci. Eng. A* **2007,** *447*, (1–2), 266-276.

(19) Li, L. F.; Jiang, Z. H.; Riquier, Y., High-temperature oxidation of duplex stainless steels in air and mixed gas of air and CH4. *Corros. Sci.* **2005,** *47*, (1), 57-68.

(20) Dobler, K.; Kreye, H.; Schwetzke, R., Oxidation of stainless steel in the high velocity oxy-fuel process. *J. Therm. Spray Tech.* **2000,** *9*, (3), 407-413.

(21) Liu, P. S.; Liang, K. M., Review functional materials of porous metals made by P/M, electroplating and some other techniques. *J. Mater. Sci.* **2001,** *36*, (21), 5059-5072.

(22) De Decker, J.; Bogaerts, T.; Muylaert, I.; Delahaye, S.; Lynen, F.; Van Speybroeck, V.; Verberckmoes, A.; Van der Voort, P., Covalent immobilization of the Jacobsen catalyst on mesoporous phenolic polymer: A highly enantioselective and stable asymmetric epoxidation catalyst. *Mater. Chem. Phys.* **2013,** *141*, (2-3), 967-972.

(23) Guo, K.; Chen, X.; Freguia, S.; Donose, B. C., Spontaneous modification of carbon surface with neutral red from its diazonium salts for bioelectrochemical systems. *Biosens. Bioelectron.* **2013,** *47*, (0), 184-189.

(24) Flexer, V.; Chen, J.; Donose, B. C.; Sherrell, P.; Wallace, G. G.; Keller, J., The nanostructure of three-dimensional scaffolds enhances the current density of microbial bioelectrochemical systems. *Energ. Environ. Sci.* **2013,** *6*, (4), 1291-1298.

(25) Guo, K.; Freguia, S.; Dennis, P. G.; Chen, X.; Donose, B. C.; Keller, J.; Gooding, J. J.; Rabaey, K., Effects of surface charge and hydrophobicity on anodic biofilm formation, community composition, and current generation in bioelectrochemical systems. *Environ. Sci. Technol.* **2013,** *47*, (13), 7563-70.

(26) Guo, K.; Soeriyadi, A. H.; Patil, S. A.; Prévoteau, A.; Freguia, S.; Gooding, J. J.; Rabaey, K., Surfactant treatment of carbon felt enhances anodic microbial electrocatalysis in bioelectrochemical systems. *Electrochem. Commun.* **2014,** *39*, (0), 1-4.

(27) Wesełucha-Birczyńska, A.; Dutkiewicz, J.; Bielańska, E.; Lityńska-Dobrzyńska, L.; Kozicki, M.; Łasocha, W.; Rafalska-Łasocha, A.; Najbar, M., Raman microspectroscopy as a unique method of the investigation of acid proof steel foil oxidation. *Opt.Photonics J.* **2013,** *3*, (5A), 7-12.

(28) de Faria, D. L. A.; Venâncio Silva, S.; de Oliveira, M. T., Raman microspectroscopy of some iron oxides and oxyhydroxides. *J. Raman Spectrosc.* **1997,** *28*, (11), 873-878.

(29) Farrow, R. L.; Benner, R. E.; Nagelberg, A. S.; Mattern, P. L., Characterization of surface oxides by Raman spectroscopy. *Thin Solid Films* **1980,** *73*, (2), 353-358.

(30) Sudesh, T. L.; Wijesinghe, L.; Blackwood, D. J., Electrochemical & optical characterisation of passive films on stainless steels. *J. Phys.Conf. Ser.* **2006,** *28*, (1), 74.

(31) Adekunle, A. S.; Ozoemena, K. I., Voltammetric and impedimetric properties of nano-scaled gamma-Fe2O3 catalysts supported on multi-walled carbon nanotubes: catalytic detection of dopamine. *Int. J. Electrochem. Sc.* **2010,** *5*, (12), 1726-1742.

(32) Schmuki, P.; Buchler, M.; Virtanen, S.; Isaacs, H. S.; Ryan, M. P.; Bohni, H., Passivity of iron in alkaline solutions studied by in situ XANES and a laser reflection technique. *J. Electrochem. Soc.* **1999,** *146*, (6), 2097-2102.

(33) Ramasubramanian, N.; Preocanin, N.; Davidson, R. D., Analysis of passive films on stainless-steel by cyclic voltammetry and auger-spectroscopy. *J. Electrochem. Soc.* **1985,** *132*, (4), 793-798.

(34) Ogura, K.; Majima, T., Formation and reduction of the passive film on iron in phosphate-borate buffer solution. *Electrochim. Acta* **1978,** *23*, (12), 1361-1365.

(35) Le Bozec, N.; Compère, C.; L'Her, M.; Laouenan, A.; Costa, D.; Marcus, P., Influence of stainless steel surface treatment on the oxygen reduction reaction in seawater. *Corros. Sci.* **2001,** *43*, (4), 765-786.

(36) Boyd, R. D.; Verran, J.; Jones, M. V.; Bhakoo, M., Use of the atomic force microscope to determine the effect of substratum surface topography on bacterial adhesion. *Langmuir* **2002,** *18*, (6), 2343-2346.

(37) Li, B. K.; Logan, B. E., Bacterial adhesion to glass and metal-oxide surfaces. *Colloid Surf. B* **2004,** *36*, (2), 81-90.

(38) Chen, S.; Hou, H.; Harnisch, F.; Patil, S. A.; Carmona-Martinez, A. A.; Agarwal, S.; Zhang, Y.; Sinha-Ray, S.; Yarin, A. L.; Greiner, A.; Schroder, U., Electrospun and solution blown three-dimensional carbon fiber nonwovens for application as electrodes in microbial fuel cells. *Energ. Environ. Sci.* **2011,** *4*, (4), 1417-1421.

Supporting Information

Table S1. Specifications of the sintered SS fiber felt

Part Number	Material	Filter rating (um)	Porosity (%)	Thickness (mm)
316L-40	316L SS	35.0-45.0	78	1.0

Table S2. Surface atomic composition of the bare and flame oxidized SS felts

Electrode	Surface elemental composition (%)									
	C	Ca	Cr	Fe	Mn	Mo	N	O	P	Ni
Bare SS felt	45.59	0.94	1.76	4.76	1.31	0.24	1.78	42.24	1.35	0.03
Oxidized SS felt	28.37	0	0	13.25	1.94	0.62	1.1	54.61	0	0.11

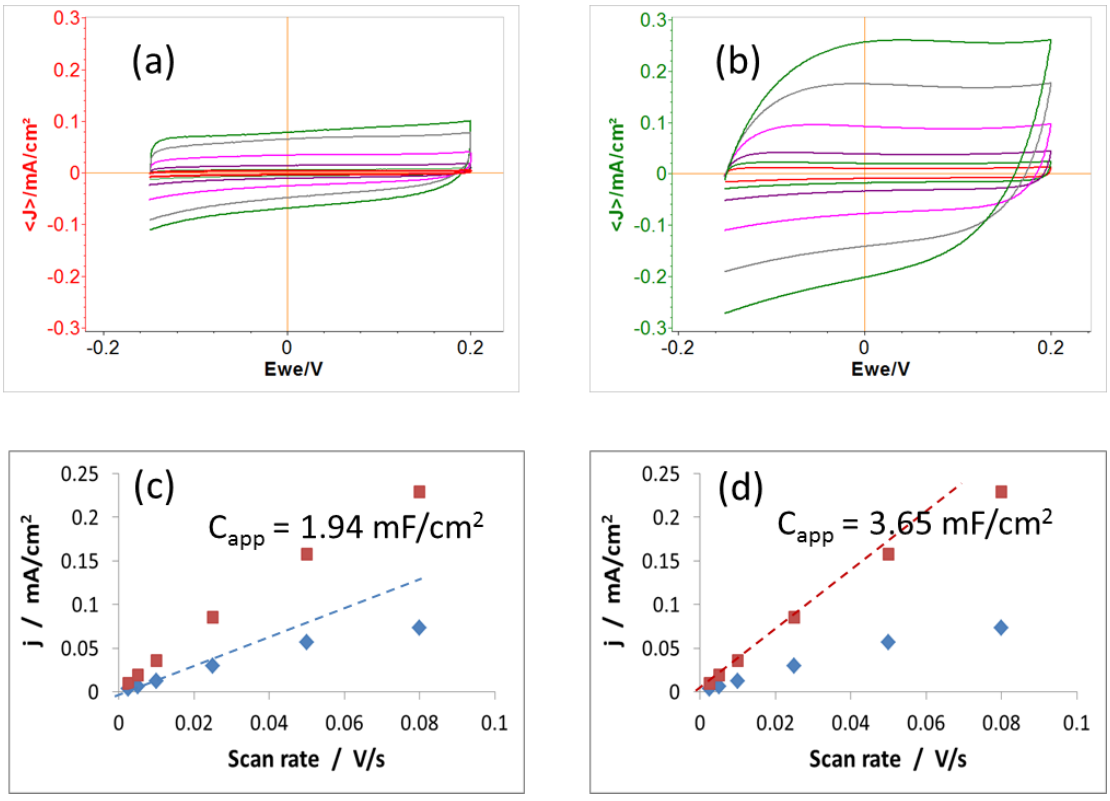

Figure S1. Capacitance capacitive current density (j_c) measurement by CVs in M9 medium at 28°C, scan rates (ν): 2.5 mV, 5 mV, 10 mV, 25 mV, 50 mV, 80 mV (a, b), Evolution of the j_c with ν (c, d) of untreated (left column) and flame oxidized (right column). Note: The relationship for j and ν would be linear for a plane electrode. Here the non-linearity translate the decrease of smaller pores ionic accessibility with the scan rate. Thus, the apparent surface capacitance (C_{app}) is therefore calculated from the slopes made by the 3 first points (dot line).

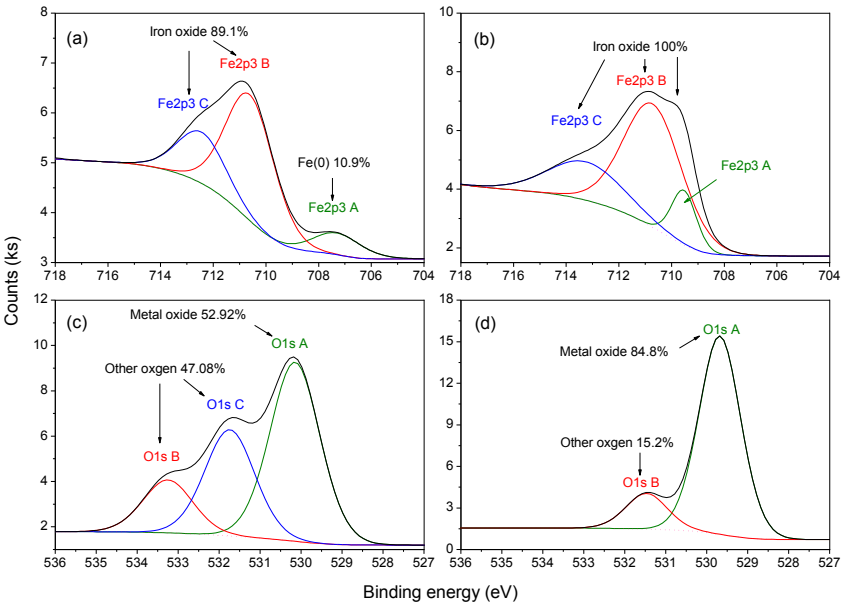

Fig. S2 Further high-resolution narrow scans and peak fitting of the iron (a, b) and oxygen (c, d) of untreated (left) and flame oxidized (right) SS felt electrodes.

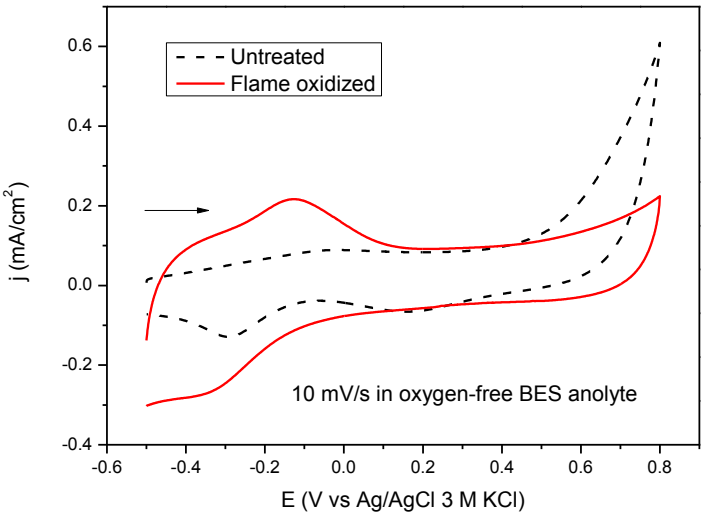

Fig. S3 CVs in higher potential range showing the corrosion behaviors of the untreated and flame oxidized SS felt electrodes.

Curriculum Vitae

PERSONAL DETAILS

Full name: Kun Guo
Gender: Male
Nationality: Chinese
Date and place of birth: November 2nd 1986, Henan
Current address: Koolkapperstraat 23B, Ghent 9000, Belgium
Phone: +3292465978 Mobile Phone: +32489642712
E-mail: kun.guo@ugent.be guokun2004@126.com

ACADEMIC BACKGROUND

2012.10 – Present PhD of Applied Biological Sciences, Laboratory of Microbial Ecology and Technology, Ghent University, Ghent, Belgium (Joint-PhD)
2011.01 – 2012.10 PhD of Chemical Engineering, Advanced Water Management Centre, The University of Queensland, Brisbane, Australia (Joint-PhD)
PhD thesis: electrode surface modifications for bioelectrochemical systems
Advisors: Prof. Korneel Rabaey, Dr. Stefano Freguia, Dr. Bogdan Donose, Prof. Jurg Keller

2010.07 – 2011.01 Research Assistant, Institute of Process Engineering, Chinese Academy of Sciences, Beijing, China
Project: Scaling up of microbial fuel cells for wastewater treatment
Supervisors: A/Prof. Haoran Li

2007.09 – 2010.07 Master of Biochemical Engineering, Institute of Process Engineering, Chinese Academy of Sciences, Beijing, China
Master thesis: Construction and optimization of microbial fuel cells and microbial electrolysis cells
Supervisors: A/Prof. Haoran Li, A/Prof. Zhuwei Du

2003.09 – 2007.07 Bachelor of Science in Biotechnology, College of Life Science, Heilongjiang University, Harbin, China
Bachelor thesis: Isolation and identification of isocarbophos-degrading strains
Supervisor: A/Prof. Chunmei Du

PUBLICATION RECORD

International Peer Reviewed Papers

1. **Kun Guo**, Bogdan C. Donose, Alexander H. Soeriyadi, Antonin Prevoteau, Sunil A.Patil, Stefano Freguia, J. Justin Gooding, Korneel Rabaey. Flame oxidation of stainless steel felt enhances anodic Bioelectrocatalysis in microbial electrochemical systems. *Environmental Science & Technology* (Under revision). 2014.

2. **Kun Guo**, Alexander H. Soeriyadi, Sunil A. Patil a, Antonin Prevoteau a, Stefano Freguia, J. Justin Gooding, Korneel Rabaey. CTAB treatment of carbon felt enhances anodic micorbial electrcatalysis in biolelectrochemical. *Electrochemistry Communication*. 2014, 39: 1-4. (IF: 4.425)

3. **Kun Guo**, Stefano Freguia, Paul G. Dennis, Xin Chen, Bogdan C. Donose, Jurg Keller, J. Justin Gooding, Korneel Rabaey. The effects of surface charge and hydrophobicity on anodic biofilm formation, community composition and current generation in bioelectrochemical systems. *Environmental Science & Technology.* 2013, 47: 7563-7570. (IF: 5.257)

4. **Kun Guo**, Xin Chen, Stefano Freguia, Bogdan Donose. Spontaneous modification of carbon surface with neutral red from its diazonium salts for bioelectrochemical systems. *Bisensors & Bioelectronics*. 2013, 47 (C):184-189. (IF: 5.437)

5. Paul G. Dennis, **Kun Guo**, Michael Imelfort, Paul Jensen, Gene W. Tyson, Korneel Rabaey. Spatial uniformity of microbial diversity in a continuous bioelectrochemical system. *Bioresource Technology.* 2013, 129: 599-605. (IF: 4.750)

6. Xinhua Tang, **Kun Guo**, Haoran Li, Zhuwei Du, Jinglei Tian. Electrochemical treatment of graphite to enhance electron transfer from bacteria to electrodes. *Bioresource Technology*. 2011, 102(3): 3558-3560. (IF: 4.980)

7. Xinhua Tang, **Kun Guo**, Haoran Li, Zhuwei Du, Jinglei Tian. Microfiltration membrane performance in two-chamber microbial fuel cells. *Biochemical Engineering Journal*. 2010, (2-3): 194-198. (IF: 2.692)

8. **Kun Guo**, Xinhua Tang, Zhuwei Du, Haoran Li. Hydrogen production from acetate in a cathode-on-top single-chamber microbial electrolysis cell with a mipor cathode. *Biochemical Engineering journal*. 2010, 51(1-2): 48-52. (IF: 2.692)

National Peer Reviewed Papers

1. **Kun Guo**, Jingjing Zhang, Haoran Li, Zhuwei Du. Progress in hydrogen production by microbial electrolysis cells. *Progress in Chemistry*. 2010, 22(4): 748-753. (IF: 0.560, In Chinese)

2. **Kun Guo**, Dingjie Li, Haoran Li, Zhuwei Du. Electricity generation of a short-arm air-cathode microbial fuel cell. *Environmental Science*. 2009, 30(10): 3082-3088. (In Chinese)

3. Chunmei Du, **Kun Guo**, Hui Yang, Shuchao Jin, Wenxiang Ping. Isolation and identification of two isocarbophos degrading strains. *Journal of Natural Science of Heilongjiang University*. 2008, 25(5): 610-613. (In Chinese)

Book Chapter

1. **Kun Guo**, Daniel J. Hassett, Tingyue Gu, "Microbial Fuel Cells: Electricity Generation from Organic Wastes by Microbes," in Microbial Biotechnology: Energy and Environment edited by R. Arora, CAB International, Oxon, United Kingdom. 2012.

Conference Presentations

1. **Kun Guo**, Stefano Freguia, Bogdan Donose, Korneel Rabaey. Detergent soaking and neutral red modification of graphite felt enhance biofilm formation and current generation of BESs. The 4th International Microbial Fuel Cell Conference, Cairns, Australia.03/09/2013. (Oral presentation)

2. **Kun Guo**, Stefano Freguia, Justin Gooding, Bogdan Donose, Jurg Keller, Korneel Rabaey. The effects of surface chemistry on biofilm formation and current generation in bioelectrochemical. The 63rd Annual Meeting of the ISE, Prague, Czech Republic.21/08/2012 (Oral presentation)

3. **Kun Guo**, Xinhua Tang, Haoran Li, Zhuwei Du. Hydrogen production from acetate in a tube-type microbial electrolysis cell. The 2nd Symposium on Microbial Fuel Cell in China, Tsinghua University, Beijing, China. 13/11/2009 (Oral presentation)

4. **Kun Guo**, Haoran Li, Juan Li, Jingjing Zhang. Hydrogen production using an upflow membrane-less microbial electrolysis cell. The 10th Chinese Hydrogen Energy Conference, Nankai University, Tianjin, China. 18/09/2009 (Oral presentation in Chinese)

Patent

1. Haoran Li, **Kun Guo**, Jingjing Zhang. A tube-type membrane-less microbial electrolysis cell. China Patent Number: 200910089440.8

HONORS & AWARDS

1. "Discovery Award for Best Scientific Paper Published in 2013", International Society of Microbial Electrochemistry and Technology, 2014

2. "Chinese Government Award for Outstanding Self-Financed Students Abroad", Chinese Scholarship Council, Ministry of Education, 2014 (6,000 USD)

3."Joint-PhD Cofunding", Ghent University, 2013-2014 (18,000 EUR)

4."IPRS and UQ Topup Scholarship", Australian Government and The University of Queensland, 2011-2014 (Covers tuition fee, living expense, and insurance)

5. "Outstanding Graduation Thesis", Institute of Process Engineering, Chinese Academy of Sciences, 2010 (10% of the students in IPE could get this honor).

6. "Excellent All-round Student Model", Graduate University of Chinese Academy of Sciences, 2009 (1% of the students in GUCAS could get this honor).

7. "Director Scholarship of IPE", Institute of Process Engineering, Chinese Academy of Sciences, 2009-2010 (10% of the students in IPE could get this honor).

8. "Excellent Cadre of Students", Graduate University of Chinese Academy of Sciences. 2008 (5% of the students in GUCAS could get this honor).

9. "Outstanding League Cadre", College of Life Science, Heilongjiang University, 2006 (10% of the students in IPE could get this honor).

10. "Excellent Undergraduate Scholarship", Heilongjiang University, 2004-2006 (5% of the students in HU could get this honor).